

博士論文

Experimental investigation into
physical aspects of quantum
joint-statistics via optical
sequential measurements

（ 光の連続測定による
量子結合統計の
物理的様相への実験的探求 ）

鈴木 佑太朗

広島大学大学院先端物質科学研究科

2016 年 9 月

目次

(Table of Contents)

1. 主論文 (Main Thesis)

Experimental investigation into physical aspects of quantum joint-statistics via optical sequential measurements

(光の連続測定による量子結合統計の物理的様相への実験的探求)

Yutaro Suzuki

2. 公表論文 (Articles)

- (1) Violation of Leggett-Garg inequalities in quantum measurements with variable resolution and back-action

Yutaro Suzuki, Masataka Iinuma, Holger F. Hofmann

New Journal of Physics **14** 103022 16pp. (2012).

3. 参考論文 (Thesis Supplements)

- (1) Experimental evaluation of nonclassical correlations between measurement outcomes and target observable in a quantum measurement

Masataka Iinuma, Yutaro Suzuki, Taiki Nii, Ryuji Kinoshita, Holger F. Hofmann

Physical Review A **93** 032104 9pp. (2016).

- (2) Weak measurement of photon polarization by back-action-induced path interference

Masataka Iinuma, Yutaro Suzuki, Gen Taguchi, Yutaka Kadoya, Holger F.

Hofmann

New Journal of Physics **13** 033041 11pp. (2011).

主 論 文
(Main Thesis)

HIROSHIMA UNIVERSITY

**Experimental investigation into physical
aspects of quantum joint-statistics via
optical sequential measurements**

by

Yutaro Suzuki

A thesis submitted in partial fulfillment for the degree of
Doctor of Philosophy

in the
Advanced Sciences of Matter

August 2016

Summary

Yutaro Suzuki

Experimental investigation into physical aspects of quantum joint-statistics via optical sequential measurements

A unique characteristic of quantum statistics is non-commutativity. The non-commutativity of two canonical observables is a mathematical foundation of quantum mechanics that the uncertainty principle is derived from and that concerns the interpretation of quantum states, which has resulted in many controversies about the details of their physical meaning. In consideration of finding a clue, we have recognized difficulty in particular to observe the expectation value of a product of non-commuting observables, since their product is no longer an observable. If we wish to find correlations between the measurement outcomes of the two observables, we need to obtain the experimental outcomes in a manner that allows us to identify the actual experimental correlations with the theoretical correlations that correspond to the mathematical formalism of quantum mechanics. Theoretically, correlations between non-commuting observables can be expressed by a quasi-probability distribution that represents a quantum state in analogy with classical phase space distributions of the non-commuting variables. Such quasi-probability distributions are given by non-positive joint probabilities, so that it is difficult to see the connection to actual experiments. However, it is possible to perform a joint measurement with errors in the measurement outcomes for the non-commuting observables.

Here, I investigate experimentally observed correlations between joint outcomes obtained from a sequential measurement of photon polarization and compare the results with a quasi-probability distribution for the initial state. Since the outcomes of two non-commuting observables are obtained in a sequence of measurements, the first measurement causes a disturbance of the state, resulting in an error of the final measurement. By using a measurement with finite measurement strength, the outcomes involve a trade-off between the measurement error due to the finite resolution and the measurement back-action caused by unavoidable influences on other non-commuting observables. The back-action effects are observed in the second measurement, where we measure an observable that does not commute with the first measurement. The statistical effects of the measurement resolution and back-action, which are conceptually known as measurement uncertainties, contribute to the experimental statistics of joint outcomes obtained with the sequential measurement. If we can evaluate these errors in the statistics, the original correlations between the non-commuting observables can be determined at any

measurement interaction strength. In a two level system, we can recover the initial statistics from the experimental probabilities of the sequential measurement outcomes using the experimental results of the statistical contrast between opposite eigenvalues observed as outcomes in the measurement apparatus.

In this thesis, I experimentally demonstrate that the original quantum statistics can be identified in the data from sequential measurements of photon polarization, so that the same result is obtained at any measurement strength. An experimental outcome of the first measurement is given by two output ports of an interferometer that realizes a diagonal (PM) polarization measurement with variable measurement strength. The following measurement of Horizontal/Vertical (HV) polarization is performed with polarizers inserted after the interferometer. Polarization rotations in paths of the interferometer can control the measurement back-action, so that we can realize PM measurements from the weak regime to the strong regime. The errors of PM resolution and the back-action effect on the outcomes of the HV measurement can be confirmed experimentally from the measurement probabilities for P- and H-polarized input photons respectively. These experimentally evaluated errors can be modelled as independent flipping probabilities of the eigenvalues. Using this assumption, I reconstruct the initial joint probability distribution from the experimental probability distribution for a photon polarization halfway between P and V polarization. Moreover, the reconstructed joint probabilities correspond to the correlation that Leggett and Garg discussed in the formulation of their inequality. Such Leggett-Garg inequalities (LGIs) indicate that non-classical correlation correspond to negative joint probability in the sequentially measured observables. The results of the reconstructed joint probabilities have the same values for different measurement strengths of the PM measurement and these values are equal to the theoretical values of the one of a quasi-probability distribution that is consistent with a description of the initial quantum state. It is called the Dirac distribution, where its negative values indicate a violations of the LGIs. Therefore, the experimental obtained statistics of the two non-commuting observables reveals the presence of non-classical correlations, which can be reconstructed as non-positive probabilities, where the quantum state statistics and the measurement errors can be separated by changing the strength of the measurement.

In the LGI measurement scenario, the reconstruction neglected the possibility of correlations between errors because the real part of the correlation product between PM and HV polarization is always zero. However, the error correlations must be included for a complete characterization of the errors of the sequential measurements of PM and HV polarization, since the four possible outcomes for the PM and the HV observables can include correlations in their joint probability. This means that complex valued joint probabilities can be reconstructed if the correlation between errors is imaginary. Indeed

the operator formalism suggests that the product of the PM and the HV observables is given by the imaginary value of the circular polarization (RL) observable. To observe this imaginary correlation in the sequential measurement, I modify the interferometric setup by introducing additional polarization rotations in the interferometer. Previously, the rotations were realized toward a direction of common diagonal P polarization and were therefore limited to linear polarization. By contrast, the polarizations in the new setup are twisted towards the RL directions while keeping the same orientation towards P polarization. This rotation effect of the new degree of freedom will appear as a back-action effect in the HV measurement. The back-action effect can be evaluated by converting the imaginary correlation into real correlation between the outcomes obtained from an R state input. As before, the same reconstructed joint probabilities can be obtained at any measurement strength and the statistics of an initial elliptical polarization has both real and imaginary parts that are both independent of measurement strength. This complete measurement of the correlations between non-commuting observables provides new insights into the physics of measurement uncertainties and into the statistics of physical properties in quantum states.

Contents

Title Page	i
Summary	i
Table of Contents	iv
List of Figures	v
1 Introduction	1
2 Quantum statistics of non-commuting observables	4
2.1 Operator statistics	4
2.2 Photon polarization	5
2.3 Dirac distribution	7
2.4 Leggett-Garg inequalities	9
3 Variable strength measurement of photon polarization	12
3.1 Measurement uncertainties	13
3.2 Experimental realization using an interferometer	14
3.3 Sequential measurement and experimental evaluation of joint-statistics . .	16
4 Results for linearly polarized input states	19
4.1 Flipping errors model of measurement outcomes	19
4.2 Confirmation of LGI violations	22
4.3 Correlations between errors	24
5 Measurement of complex joint probabilities	26
5.1 Experimental realization of imaginary measurement back-action	27
5.2 Complete characterization of correlated errors	28
5.3 Reconstruction of the Dirac distribution at variable measurement strengths	30
6 Discussion and Conclusions	35
Acknowledgements	39
Bibliography	41

List of Figures

2.1	Bloch sphere representation for polarization	7
3.1	Variable strength measurement of PM polarization	15
3.2	Experimental setup	18
4.1	Measurement resolution	20
4.2	Transmission fidelity	21
4.3	Experimental probabilities for polarization halfway angle between P and V	23
4.4	Reconstructed joint probabilities with negative values	24
5.1	Measurement resolution with correlation sensitivity	29
5.2	Transmission fidelity with correlation sensitivity	29
5.3	Correlation fidelity	30
5.4	Experimental probabilities for elliptical polarization	32
5.5	Real part of the reconstructed joint probabilities	33
5.6	Imaginary part of the reconstructed joint probabilities	34

Chapter 1

Introduction

The non-commutativity of observables expresses the mystery of quantum physics that is at the heart of quantum measurement and quantum information. Often, the wave-particle duality or the uncertainties of measurement results are identified as the associated features of quantum world. However, many controversies still remains regarding the physics of the relation between quantum states and the experimentally observable statistics of non-commuting observables [1–4]. On the other hand, non-classical statistics of quantum states can be described within the mathematical formalism by selecting a specific ordering of the observables, as shown in a number of works [5–8]. Such statistical representations of the state are called quasi-probability distributions, since they correspond to a non-positive joint probability of the non-commuting outcomes. Although this joint probability does not define a relative frequency of the joint measurement outcome, it can express correlation between the outcomes that is needed to explain the relations with other observables. Therefore, correlations between measurement outcomes of non-commuting observables may be expected to produce new insights with regard to the controversies on quantum measurements once they are observed on a well-defined procedure and method.

By performing a projective measurement of a single observable, we can obtain the average value of the physical property of a quantum state. However, experimental measurement outcomes for a single observable are insufficient to identify a quantum state. Likewise, the representation of a quantum state in a single basis is not very useful for a more detailed understanding of measurement outcomes which may include the effects of non-classical correlations in their statistics. For this reason, conventional tomography of a quantum state, where a density operator representing an initial state is only reconstructed from a sufficient set of the average values of the observables, should not be considered as a direct measurement of coherence or non-classical correlations, even if it

succeeds in defining the off-diagonal terms of the density matrix based on experimental results. Instead, the only direct way to identify correlations between two non-commuting observables with the statistics of measurement results is to analyze the measurement errors in a joint measurement. Any joint measurement on non-commuting observables cannot be performed without measurement uncertainty errors in the outcomes, so that a proper errors analysis is necessary to identify the correlations between the measurement outcomes with the original correlations between the observables. Here, a sequential measurement of non-commuting observables has the advantage of separating the effects of errors in the initial measurement outcome from back-action errors caused by changes in the value of the observable measured in the final measurement. A well-known example of such a sequential measurement is a weak measurement which is performed with the pre- and post-selected state. In the weak measurement, the interaction is weak and hence the measurement back-action is negligibly small. Therefore, non-commuting observables can be measured without error after an initial measurement with almost zero back-action [9]. Since the measurement strength is weak, it is not possible to resolve the eigenvalues of the observable measured in the initial measurement. However, we can obtain the measurement results of the non-commuting observable without error in the final measurement in exchange for the noisy statistics from the initial measurement. The error in the initial measurement can be evaluated from the statistics of repeated measurements. Thus, the joint statistics of two non-commuting observables can be found from the experimentally obtained statistics in the weak measurement [10–15].

Theoretically, the quantum statistics of two non-commuting observables have been represented by many kinds of quasi-probability distribution [16–19]. All of these quasi-probabilities are based on the analogy with classical phase space [20, 21]. In sequential measurements, the Dirac distribution emerges because its ordering of the two operators completely matches the sequence of the measurement of the two non-commuting observables [22]. Although it is represented by complex valued joint probabilities, the Dirac distribution can be observed directly in weak measurements [23, 24]. Moreover, the joint probability of the Dirac distribution can explain the violation of the limit on the set of expectation values of two spin components in a sequence of spin measurements imposed by positive joint probabilities. This limit of correlations is expressed by the Leggett-Garg inequalities (LGIs) [25]. The violation of the LGIs has also been demonstrated using weak measurements [26–29]. Thus, the Dirac distribution of an initial state can represent the non-classical correlations between non-commuting observables and can be observed in the noisy statistics of sequential measurement outcomes if we can compensate the statistical errors of the joint outcomes using the known statistics of the measurement errors caused by low resolution. However, it is difficult to understand

a measurement situation with finite back-action from the results of weak measurements, because weak measurements avoid the effects of measurement back-action.

In general, a quantum measurement of finite measurement strength results in a partially resolved result for the targeted physical property and a disturbance of the initial state, where the back-action effects can be seen in the non-commuting observables. If we perform a successive measurement with finite measurement strength as the initial measurement, the probability distribution of the outcomes will include the back-action effects in the statistics. We may identify the errors caused by the back-action effect statistically in a sequential measurement of two non-commuting observables, where the error can be evaluated in same manner as the resolution error in the weak measurement. We can then evaluate the statistical effects of the measurement resolution and back-action in the experimentally accessible statistics of joint outcomes obtained with the sequential measurement. The correlations between the non-commuting outcomes can be obtained without any limitations on the interaction strength by taking into account all of the errors [30]. The deconvolution from the experimentally observed probabilities of measurement outcomes then results in a joint probability for non-commuting physical properties.

In the following, I present the experimental results for the joint statistics of sequential measurement outcomes for non-commuting photon polarizations, where I implement back-action control of the measurement using an interferometer. The interference can be controlled by polarization rotations in each path after splitting the paths into the Horizontal (H) and Vertical (V) polarization components. The two output ports of the interferometer correspond to polarization measurements of diagonal (P and M) polarization components. Inserting the polarizers along the H/V polarization direction after these ports, we can obtain the experimental probabilities of the non-commuting polarization properties PM and HV with both resolution and back-action errors. These errors originate from the finite measurement interaction with the polarization in the interferometer, where the back-actions are produced by coherently rotating polarization. The measurement errors can be identified by using eigenvalues inputs to distinguish error-free results from errors in the outcomes. By reconstructing the joint probability distribution with the evaluated errors, I investigate the role of non-classical correlations between the initial measurement outcomes and the final measurement outcomes in the sequential measurement of non-commuting linear polarization observables.

Chapter 2

Quantum statistics of non-commuting observables

In the first chapter, I discuss the characteristic of quantum statistics described by the mathematical formalism of Hilbert space. Although quantum physics appears to be a theory of a probability, the product of two non-commuting observables cannot be described by conventional statistics of products in the operator formalism. On the other hand, correlation products are important quantities in the characterization of a physical system, and the polarization of a single photon is no exception. I introduce the representation of the initial quantum state as a joint probability distribution which includes the correlation terms of two non-commuting observables and give an example of how these correlations appear in the context of a sequence of measurements.

2.1 Operator statistics

The operators in Hilbert space are useful whenever quantum mechanics applies. We can characterize a projective measurement result of the observable \hat{A} by the expectation value of $\langle \hat{A} \rangle$. An individual value of A_a can be associated with the observable \hat{A} , since the operator \hat{A} is Hermitian (self-adjoint), so that the values A_a correspond to the eigenvalues and \hat{A} can be represented by the spectral decomposition,

$$\langle \hat{A} \rangle = \sum_a A_a \langle i|a \rangle \langle a|i \rangle = \sum_a A_a P(a), \quad (2.1)$$

where $|i\rangle$ is the initial state and $P(a) = |\langle a|i \rangle|^2$ is the probability of obtaining A_a . This also indicates that $|a\rangle$ is a basis in which $|i\rangle$ can be expressed. Another observable \hat{B} can be similarly represented by eigenvalues B_b and an eigenvector basis $|b\rangle$. The expectation

values of both $\langle \hat{A} \rangle$ and $\langle \hat{B} \rangle$ are statistical properties of the initial state. Then, I will consider the question of the relation between these operators if the operators are non-commuting $[\hat{A}\hat{B}] \neq 0$. When the relation is given by $[\hat{A}\hat{B}] = i\hat{C}$, the expectation value of the ordered product of the observables is given by

$$\langle \hat{A}\hat{B} \rangle = \frac{i}{2} \langle \hat{C} \rangle, \quad (2.2)$$

where the operator product is non-Hermitian, so that the product cannot be identified with any other observable. Consequently, there are open questions about relations between the product of non-commuting observables and their experimentally observable statistics deeply related to the cornerstones of quantum physics, which seem to be the uncertainty principle, the interpretation of the quantum state, and the quantum measurement problem. A straightforward attempt to answer these questions is to consider correlations between possible measurement outcomes. If we assume that the operator product corresponds to a joint probability distribution of the outcomes of precise measurement for the two non-commuting observables, the expectation value of the product can be expressed by

$$\langle \hat{A}\hat{B} \rangle = \sum_a \sum_b A_a B_b P(a, b), \quad (2.3)$$

where $P(a, b) = \langle i|a\rangle\langle a|b\rangle\langle b|i\rangle$ now appears as a joint probability of obtaining A_a and B_b , even though this definition of $P(a, b)$ does not satisfy the familiar conditions that apply to conventional probabilities.

2.2 Photon polarization

A photon has a physical property of polarization as a degree of freedom, which can be operated and observed. We can measure a direction of polarization by filtering into the transmitted photon statistically. The obtained probabilities can be used to evaluate the polarization observables expressed by the Stokes parameters. The observable is defined the difference between the probabilities of two orthogonal polarization. Since polarization can be considered as a two level system, all polarization observables can be written by the differences of the projection to the eigenstates in following

$$\begin{aligned} \hat{S}_{\text{HV}} &= |\text{H}\rangle\langle\text{H}| - |\text{V}\rangle\langle\text{V}|, \\ \hat{S}_{\text{PM}} &= |\text{P}\rangle\langle\text{P}| - |\text{M}\rangle\langle\text{M}|, \\ \hat{S}_{\text{RL}} &= |\text{R}\rangle\langle\text{R}| - |\text{L}\rangle\langle\text{L}|, \end{aligned} \quad (2.4)$$

where H is horizontal polarization, V is vertical polarization, and P is diagonal (plus superposition of H and V), M is anti-diagonal (minus superposition of H and V) polarization, and R is right-handed circular polarization, L is left-handed circular polarization respectively. Hence, the expectation values on each eigenstate equal to the eigenvalues. Since the eigenvalues are two values of ± 1 , these observables correspond to the Pauli matrices of a spin 1/2 particle. Note that any set of two of these has the non-commuting relation. Thus, we cannot simultaneously determine the all expectation values of the polarization observables by a projective measurement for the photon ensemble. Actually, a quantum measurement definitely destroys the initial state, so that the polarization after the measurement does not identify the original polarization before the measurement.

It is convenient for visualization of photon polarization to use a Bloch vector on the Bloch sphere. The Bloch sphere is mathematically formulated in a two dimensional Hilbert space, so that any density matrix in the two level system can be uniquely represented by the vector in it. The three axes of the Bloch sphere of polarization are the expectation values of the observables represented in equation (2.4), which are similar to the Stokes parameters showing a polarized light with the Poincare sphere. Therefore, a polarization state is characterized by the three parameters and decided by the expectation values of the Stokes parameters. The general notation of the Bloch vector is given by

$$\rho = \frac{1}{2}(\hat{I} + \sum_{i=H,V,PM,RL} v_i \hat{S}_i), \quad (2.5)$$

where v_i is a component of the Bloch vector and its magnitude corresponds to the purity of the quantum state. Any unitary operation to the state can be shown by a rotation of the Bloch vector. In general, the estimation of an unknown state by using the necessary amount of parameters, like the identification of the Bloch vector, is called the quantum state tomography. The pure state $|\Psi\rangle$ that is represented by the vector on the surface of Bloch sphere is more interesting to consider a quantum feature of photon statistics. At the pure state, ρ in equation (2.5) is expressed by $\rho = |\Psi\rangle\langle\Psi|$. The pure state of polarization $|\Psi\rangle$ is given by

$$|\Psi\rangle = \cos\left(\frac{\theta}{2}\right) |H\rangle + e^{i\phi} \sin\left(\frac{\theta}{2}\right) |V\rangle, \quad (2.6)$$

where the angles θ and ϕ represent the geometrical relations between the state vector and three axes showing the expectation values of the Stokes parameters. Figure 2.1 shows the Bloch vector $|\Psi\rangle$ on the Bloch sphere. Note that these relations as shown in equation (2.6) schematically express initial properties on the viewpoint of the single basis. Originally, the values represented on the axes in the Bloch sphere are not compatible but just combined to be the quantum state in Hilbert formalism.

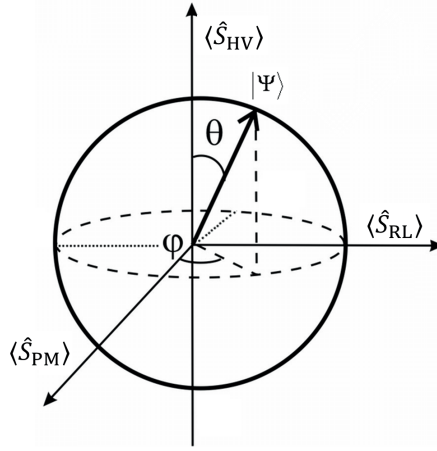


FIGURE 2.1: Any pure state for polarization is represented by a vector from the origin to the surface of the Bloch sphere. The dynamics of polarization can be visually considered as the transformation of the vector.

There is the non-commutativity between the observables of polarization. The product of the two observables is associated with the imaginary part of the other observable, for example,

$$\hat{S}_{HV}\hat{S}_{PM} = i\hat{S}_{RL}. \quad (2.7)$$

The relations indicate that the values of the non-commuting observables are not independent, so that the unique relations in the Hilbert space may be concealed into statistics of correlations between the observables of the initial state.

2.3 Dirac distribution

It is also possible to describe a quantum state by using a quasi-probability distribution of two non-commuting variables. Quasi-probability distributions are defined as an analogy of the classical phase space distribution of canonical variables [20, 21]. In this thesis, correlations between two non-commuting observables will be argued from actual measurement results. Although a quasi-probability does not satisfy all probability rules, it can be considered as a joint probability, which is natural treatment with correlations of outcomes. Since an ordering of the operators corresponds to a sequence of measurements, the Dirac distribution is suited for sequential measurement outcomes and shows a direct consequence of non-classical aspects by the statistics [22]. It had been originally considered that the Dirac distribution had no direct connection to actual experiments, since its probability can be allowed to take a complex value. However, weak measurements have recently shown an experimental method to obtain it directly from the noisy statistics of the measurement outcomes [31, 32]. In this section, the formalism of the Dirac distribution is theoretically introduced as follows.

The Dirac distribution is defined by the three non-commuting properties,

$$D_\rho(a, b|i) = \langle i|b\rangle\langle b|a\rangle\langle a|i\rangle, \quad (2.8)$$

where i represents the initial property of the system and both a and b are the different eigenvalues of the targeted non-commuting observables. In the case of photon polarization, we can write down the Dirac distribution with the specific choice of the operator ordering of \hat{S}_{PM} and \hat{S}_{HV} . Its property is represented by joint outcomes of the eigenvalues $s_{\text{PM}} = \pm 1$ and $s_{\text{HV}} = \pm 1$, so that the form is written by

$$D_\rho(s_{\text{PM}}, s_{\text{HV}}|i) = \langle i|s_{\text{HV}}\rangle\langle s_{\text{HV}}|s_{\text{PM}}\rangle\langle s_{\text{PM}}|i\rangle. \quad (2.9)$$

Generally, its value is complex and it corresponds to the component of the density matrix ρ of the initial state. For example, the diagonal term of ρ in PM basis is

$$\langle \text{P}|\rho|\text{P}\rangle = D_\rho(\text{P}, \text{H}|i) + D_\rho(\text{P}, \text{V}|i). \quad (2.10)$$

The off-diagonal term of ρ in PM basis can also be given by

$$\langle \text{P}|\rho|\text{M}\rangle = \frac{\langle \text{H}|\text{M}\rangle}{\langle \text{H}|\text{P}\rangle} D_\rho(\text{P}, \text{H}|i) + \frac{\langle \text{V}|\text{M}\rangle}{\langle \text{V}|\text{P}\rangle} D_\rho(\text{P}, \text{V}|i). \quad (2.11)$$

Mathematically, the imaginary part of the Dirac distribution corresponds to the off-diagonal term of the density matrix, because the coefficients in equation (2.11) are real. If the initial state is an elliptical polarization, the joint probability of the Dirac distribution $D_\rho(s_{\text{PM}}, s_{\text{HV}}|i)$ takes a complex value. On the other hand, the only real part of the Dirac distribution $D_\rho(s_{\text{PM}}, s_{\text{HV}}|i)$ corresponds to a linear polarization, since the joint probability is represented by \hat{S}_{PM} and \hat{S}_{HV} .

The Dirac distribution can represent measurement results for the outcomes of the projective measurement. The marginal probability of equation (2.9) is consistent with the transition probability of selecting one basis in each observable.

$$\begin{aligned} \sum_{s_{\text{PM}}} D_\rho(s_{\text{PM}}, \text{H}|i) &= |\langle \text{H}|i\rangle|^2, \\ \sum_{s_{\text{HV}}} D_\rho(\text{P}, s_{\text{HV}}|i) &= |\langle \text{P}|i\rangle|^2 \end{aligned} \quad (2.12)$$

This equation (2.12) can show the difference representing the projective result on another non-commuting basis by averaging out one property of the observables, although it is similar to the representation of the diagonal component of the density matrix by equation (2.10). As we are expected, correlations between the non-commuting properties can also

be expressed with the Dirac distribution, considering the average product of the non-commuting observables in the similar way to equation (2.3). Since the order of the operators are fixed, the expectation value of the product numerically corresponds to the expectation value multiplied by the imaginary unit, where the assigned observable is provided by the commutation relation between the non-commuting observables, that is,

$$\begin{aligned}\langle \hat{S}_{\text{HV}} \hat{S}_{\text{PM}} \rangle &= \sum_{s_{\text{PM}}, s_{\text{HV}}} s_{\text{PM}} s_{\text{HV}} D_{\rho}(s_{\text{PM}}, s_{\text{HV}} | i) \\ &= i \langle \hat{S}_{\text{RL}} \rangle = i \sum_{s_{\text{RL}}} s_{\text{RL}} P(s_{\text{RL}}),\end{aligned}\tag{2.13}$$

where imaginary value of the product appears when the initial state is an elliptical polarization because of the complex joint probabilities of the Dirac distribution. Since an elliptical polarization has the RL component, the Dirac distribution connects the product of the non-commuting properties to the property that is necessary for the complete description of the initial state with imaginary correlations corresponding the non-commuting relation between the two targeted observables. In this sense, the Dirac distribution of equation (2.9) represents the initial polarization state with the PM and the HV component and the product between them in terms of the correlation between the PM and the HV component. Note that the Dirac distribution of the initial state can be expressed by another set of the two physical properties, where imaginary correlation depends on the order of the two chosen observables.

2.4 Leggett-Garg inequalities

Leggett and Garg introduced the inequalities for the upper limit of classical correlations in a series of two measurements conditioned by the preparation of a pure state, like the analysis of Bell's inequalities [25]. If the inequalities are violated, it is judged that the targeted system is quantum because of a sign of observation for non-classical correlations. Originally, Leggett-Garg inequalities (LGIs) have been proposed to test if quantum physics can be applied to a macroscopic system using the analysis of correlations of outcomes. Hence, the inequalities should be violated in a microscopic system, which obeys the quantum physics. On the argument of correlations of outcomes, the discussion about the violation of the LGIs is smoothly related to the Dirac distribution and a sequential measurement of joint outcomes for photon polarization.

On a two level system, obtained statistics is associated with the outcomes of the eigenvalue $s = \pm 1$. Then, we assume that the initial value s_1 is fixed to +1 by the prepared pure state, and the values of the initial and final measurements result in $s_2 = \pm 1$ and

$s_3 = \pm 1$ respectively. From these statistics, correlation functions $K_{ij} = \langle s_i s_j \rangle$ are derived and the classical limit of the correlation can be given by

$$1 + K_{13} \geq K_{12} + K_{23}. \quad (2.14)$$

If the initial measurement of s_2 and the final measurement of s_3 are orthogonal in each other, real part of average product of the s_2 and the s_3 outcomes is always zero, that is $K_{23} = 0$. Then, we expect that the LGI given by equation (2.14) can be violated when a expectation value for s_2 is positive and a expectation value for s_3 is negative in the initial state with $s_1 = +1$. In the case of the initial measurement for PM polarization and the final measurement for HV polarization, the maximal violation of equation (2.14) is expected when the initial polarization is linearly directed to the halfway between P and V polarization, resulting in $\langle s_{\text{PM}} \rangle = 1/\sqrt{2}$ and $\langle s_{\text{HV}} \rangle = -1/\sqrt{2}$, where the left side value of equation (2.14) is 0.414 smaller than the right side value of one.

It is necessary for the agreement with the set of the expectation values violating the classical limit to promise a non-classical statistics between the s_{PM} and the s_{HV} . On the argument of the correlation functions, a joint probability distribution of the measurement outcomes is useful and straightforward to analyze non-classical feature of these statistics. The LGI violation can be expressed in term of the negative probability of the Dirac distribution. In details, the joint probabilities of the Dirac distribution given by equation (2.9) are related with the correlation functions K_{ij} as following,

$$\begin{aligned} D_\rho(\text{P}, \text{H}) &= \frac{1}{4} (1 + K_{13} + K_{12} + K_{23}) \\ D_\rho(\text{M}, \text{H}) &= \frac{1}{4} (1 + K_{13} - K_{12} - K_{23}) \\ D_\rho(\text{P}, \text{V}) &= \frac{1}{4} (1 - K_{13} + K_{12} - K_{23}) \\ D_\rho(\text{M}, \text{V}) &= \frac{1}{4} (1 - K_{13} - K_{12} + K_{23}), \end{aligned} \quad (2.15)$$

where $D_\rho(\text{M}, \text{H}) \geq 0$ is equivalent to the limit of the LGI represented in equation (2.14). Therefore, non-classical correlations between the s_{PM} and the s_{HV} are represented by the negative real parts of the Dirac distribution in quantum mechanics. On the above argument of the LGI, the average product of the two outcomes $\langle s_{\text{HV}} s_{\text{PM}} \rangle$ is always zero, but no positive joint probability $D_\rho(\text{M}, \text{H})$ is necessary to explain the combination of these outcomes with $\langle s_{\text{PM}} \rangle$ and $\langle s_{\text{HV}} \rangle$ observed for a maximally polarized photon.

It is difficult to observe these correlations in a sequence of an actual measurement, because measurements of non-commuting observables are limited by measurement uncertainties [33, 34]. Since the effects of the measurement uncertainties must be included

in the observed statistics, the LGI violations in a sequential measurement of two non-commuting observables may not appear unless a valid analysis for the measurement statistics is applied in these demonstration, where the identification of the statistics before measurements is more clearly required than when the observation of Bell's inequalities violations in bipartite quantum systems [\[35\]](#).

Chapter 3

Variable strength measurement of photon polarization

A quantum measurement has both aspects of obtaining the information for a targeted observable and of causing the back-action effects on the system, where the other observables will be disturbed even if we do not obtain these information. Therefore, it is not possible to observe the joint probability of the precise values on a joint measurement. In this chapter, I introduce a polarization measurement with varying the measurement interaction strength to investigate roles of the measurement and relationship to the Dirac distribution on a sequential measurement of photon polarization. The measurement uncertainties appear on the outcomes of non-commuting observables. The sequential measurement of PM and HV polarization in this thesis is composed of the initial PM measurement with variable measurement strength and the final HV measurement with fully projective measurement. The measurement uncertainties can be characterized by the sequential outcomes comparing the expectation values of the initial and the final observable respectively. Since the HV measurement is completely projective, uncertainty errors of the PM measurement with finite measurement strength can be categorized to the statistical effects of the measurement resolution and back-action. The variable strength measurement of PM polarization is realized by an interferometer. The measurement back-action can be controlled by the rotation of polarizations on the paths, where the rotation angle corresponds to measurement strength. The final measurement of HV polarization after the initial measurement of PM polarization results in obtaining each probability for four joint outcomes. By inputting the eigenvalue as the eigenstate of each observable, the uncertainty errors of the measurement resolution and back-action can be directly evaluated from the experimental probabilities of the joint outcomes.

3.1 Measurement uncertainties

Since a quantum measurement of finite measurement strength changes the initial state, we cannot obtain the identified value of the initial state at the successive measurement of the non-commuting observable. We should take into accounts of such a measurement back-action as well as insufficient resolution of the initial measurement in sequential measurement outcomes. Especially, in order to identify the intrinsic joint probability distribution of the initial state, we need to evaluate the errors of measurement uncertainties originated from both the insufficient resolution and the non-vanishing back-action of the initial PM measurement. In the following, I consider how to quantify the measurement resolution and back-action errors in sequential measurements of PM and HV polarization, where outcomes m are obtained by the PM measurement and outcomes f are obtained by the HV measurement respectively.

The measurement errors in the uncertainties can be regarded as the difference between the probabilities of a correct value and of an opposite value in a two level system. Thus, the PM measurement resolution ε is defined as the difference between the probabilities of if the outcome m is correct eigenvalue or not,

$$\varepsilon = P(m = s_{\text{PM}}) - P(m = -s_{\text{PM}}). \quad (3.1)$$

The ε can be evaluated by comparing the average value of m determined from the experimental results with the expectation value of the observable \hat{S}_{PM} on the input state,

$$\varepsilon = \frac{\langle m \rangle_{\text{exp}}}{\langle \hat{S}_{\text{PM}} \rangle_{\text{input}}}. \quad (3.2)$$

At the variable strength measurement of PM polarization, the resolution ε becomes increasing with the measurement strength. As a higher resolution is obtained, then the effects of the measurement back-action are more remarkable. Since we perform the final measurement of HV polarization, we can confirm the back-action effects on the HV outcomes. The measurement error on \hat{S}_{HV} is characterized in terms of the HV transmission τ . This back-action effect τ of the PM measurement is also defined as the difference between the probabilities when the outcome value f equals to the input value s_{HV} and is opposite to the s_{HV} ,

$$\tau = P(f = s_{\text{HV}}) - P(f = -s_{\text{HV}}). \quad (3.3)$$

Experimentally, the τ can be determined by comparing the average value of f with the expectation value of the observable \hat{S}_{HV} on the input state,

$$\tau = \frac{\langle f \rangle_{\text{exp}}}{\langle \hat{S}_{HV} \rangle_{\text{input}}}. \quad (3.4)$$

Thus, the measurement uncertainty errors originated from the initial PM measurement of finite measurement strength are experimentally parameterized by the measurement resolution of PM polarization and the transmission fidelity of HV polarization as the measurement back-action effect.

3.2 Experimental realization using an interferometer

To implement a variable strength measurement of PM polarization, I use an interferometer where interference is induced by unitary rotations of polarization associating with the paths. The polarization controls are separately done into the H and the V component of an input photon before the path interference. On the other hand, we obtain the which path information by detecting the photon in either two output ports after the interferometer. The measurement interaction can change in response to indistinguishability between the separated polarization components, which can be rotated under our operation. Thus, such an indirect and non-projective quantum measurement controls the measurement back-action. It is essential for the realization to separate two paths associating with input polarization by a polarizing beam splitter (PBS) and to rotate toward the P polarization by half wave plates (HWPs) before the paths interfere [36].

Figure 3.1 shows a Mach-Zehnder interferometer with polarization dependence, on which the PM measurements of variable strengths are implemented. On the PBS, The H component of polarization of the input photon is mapped to the transmitted path and the V component of it is mapped to the reflected path respectively. Next, the polarization components in both paths are coherently rotated to angle 2θ along the meridian of the Bloch sphere toward the P direction by opposite rotating the HWPs. The polarization component before a 50:50 non-polarizing beam splitter (BS) acquires both the H and the V components depending on the rotation angle 2θ . Then, the same component of two paths can interfere in each other on the BS, since HV distinguishability between the both paths is lost depending on the amplitude of the overlapped components on the H and the V basis. Finally, the output paths are regarded as the outcomes of m related by the PM measurement. Importantly, this interferometric measurement is controlled by the rotations of polarization. Thus, we operate the measurement back-action with the

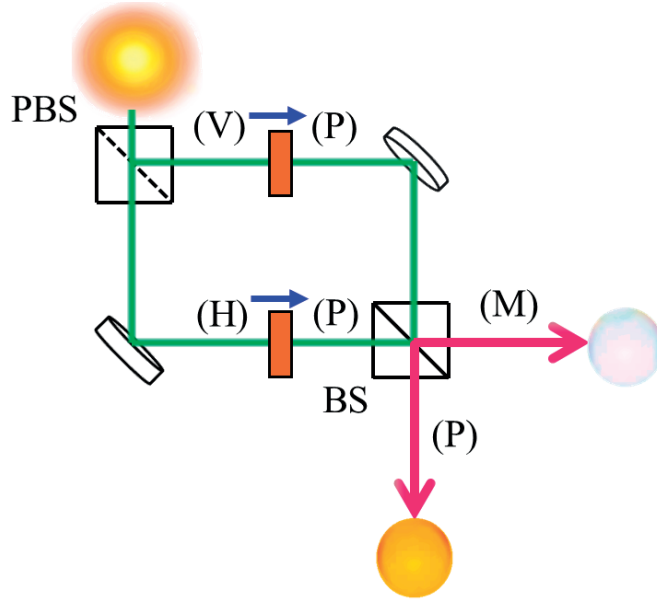


FIGURE 3.1: A basic scheme for realization of the PM measurement with controlling the measurement back-action. The motion of polarization components induces interference after the beam splitter, resulting in the outputs having PM information of the input photon.

HWPs angle θ directly connecting measurement strength and the induced interference results in the PM measurement resolution ϵ .

The above operations in the PM measurement can be described in term of following measurement operators \hat{M}_P and \hat{M}_M in the HV basis. The transmission states after the interferometer are given by,

$$\begin{aligned}
 \hat{M}_P|H\rangle &= \frac{1}{\sqrt{2}} (\cos(2\theta)|H\rangle + \sin(2\theta)|V\rangle), \\
 \hat{M}_P|V\rangle &= \frac{1}{\sqrt{2}} (\sin(2\theta)|H\rangle + \cos(2\theta)|V\rangle), \\
 \hat{M}_M|H\rangle &= \frac{1}{\sqrt{2}} (\cos(2\theta)|H\rangle - \sin(2\theta)|V\rangle), \\
 \hat{M}_M|V\rangle &= \frac{1}{\sqrt{2}} (-\sin(2\theta)|H\rangle + \cos(2\theta)|V\rangle).
 \end{aligned} \tag{3.5}$$

It is possible to represent equation (3.5) in the only measurement operators with the form of the positive operator valued measure $\hat{E}_P = \hat{M}_P^\dagger \hat{M}_P$, $\hat{E}_M = \hat{M}_M^\dagger \hat{M}_M$ as follows,

$$\begin{aligned}
 \hat{E}_P &= \frac{1}{2}(\hat{I} + \sin(4\theta)\hat{S}_{PM}), \\
 \hat{E}_M &= \frac{1}{2}(\hat{I} - \sin(4\theta)\hat{S}_{PM}),
 \end{aligned} \tag{3.6}$$

From this expression of the PM measurement, it is readily seen that the implemented

operation leaves PM polarization unchanged and plays partially projective on \hat{S}_{PM} depending on the HWPs angle of θ . The difference between the expectation values of the operators represented by equation (3.6) gives the result of the \hat{S}_{PM} measurement with resolution $\sin(4\theta)$.

$$\langle \hat{E}_{\text{P}} \rangle - \langle \hat{E}_{\text{M}} \rangle = \sin(4\theta) \langle \hat{S}_{\text{PM}} \rangle \quad (3.7)$$

3.3 Sequential measurement and experimental evaluation of joint-statistics

We can associate the interferometric PM measurement varying measurement strength θ with the characteristic of the measurement errors in term of the PM resolution ε and the HV transmission τ by performing the projective measurement to H/V polarization with the transition states after the interferometer, because the back-action effects appear on the outcome of the final measurement on the non-commuting observable. By inserting the polarizers after the outputs of the interferometer, we can perform the final HV measurement after the initial PM measurement. The polarizers are set the optical axis to H/V directions before detectors. Thus, we obtain the probabilities $P_{\text{exp}}(m, f)$ from a sequential measurement of the joint outcomes m and f . Moreover, all of the measurement errors in the variable strength measurement can be determined by the only experimentally obtained statistics.

The complete setup of the sequential measurement of photon polarization is shown in figure 3.2. Input photons are prepared by a CW titanium-sapphire laser (wavelength 830nm) and reduced by Neutral Density (ND) filters to permit the detection of single photons. Polarization is aligned by passing through a Glan-Thompson polarizer to H. Output photons are detected with single photon counting modules (SPCM-AQR-14) connecting multi-mode fibers guided by objective lens with fiber couplers. Typical count rates are 150MHz. To compensate undesirable fluctuations of the intensity of the input laser, the input beam is divided by a BS upstream of the interferometer. A lens inserted downstream of the ND filters is used to optimize the beam profile to get the path interference. Any initial polarization can be prepared by a combination of quarter wave plate (QWP) and HWP upstream of the interferometer, where rotating the HWP with fixing the optical axis of the QWP to the H direction can produce the arbitrary linear polarization. The initial PM measurement is realized by the Sagnac interferometer, which have better stability of the interference than the one of a Mach-Zehnder interferometer. The basic function of optical elements in the interferometer is similar to the explanation in section 3.2. In this deformed Sagnac interferometer however, a PBS and a BS are combined to a hybrid-coated beam splitter (HBS), where

the reflectance surface in 4 by 10 functions as a PBS for separating the input beam and the one in 6 by 10 plays as a BS for interfering the counter-propagating beams.

The measurement strength can be varied by the rotation angle θ of the HWP inside the interferometer, where a reflected beam by the PBS part of the HBS is passed through the HWP from the opposite side, so that its rotation setting the only θ angle results in the same rotations toward the P polarizations in both of the two counter-propagating beams. The θ can be set from 0° to 22.5° , where any measurement strength is realized from the weak region to the strong region. Two $\lambda/8$ wave plates (OWPs) in the interferometer is discussed later, although these are important for considering imaginary correlations between the outcomes m and f . Now the OWPs are removed from the setup (or setting the optical axes to H/V directions) and put something out of your mind for the moment. Finally, polarizers into the two output paths select H or V polarizations before the detector1 and the detector2, so that the count rates depending on the rotating angle of the HWP and the polarizers settings are identified in the joint outcomes of (P,H) and (P,V) in the detector1 and (M,H) and (M,V) in the detector2. Therefore, we can obtain the experimental joint probabilities $P_{\text{exp}}(m, f)$ into the detector1 as $P_{\text{exp}}(\text{P}, \text{H})$ or $P_{\text{exp}}(\text{P}, \text{V})$ and the detector2 as $P_{\text{exp}}(\text{M}, \text{H})$ or $P_{\text{exp}}(\text{M}, \text{V})$.

For the resolution of the PM measurement, we use a P-polarized input and evaluate the probabilities of the measurement outcomes P and M to obtain

$$\varepsilon = P(\text{P}|\text{P}) - P(\text{M}|\text{P}). \quad (3.8)$$

A similar characterization can be performed for the transmission τ . In this case, we use a H-polarized input and the HV polarization is measured in both output ports. The total transmission fidelity is then given by

$$\tau = P(\text{P}, \text{H}|\text{H}) + P(\text{M}, \text{H}|\text{H}) - P(\text{P}, \text{V}|\text{H}) - P(\text{M}, \text{V}|\text{H}). \quad (3.9)$$

In variable strength measurement, the ε increases with the measurement strength. On the other hand, the τ decreases when measurement strength increases. These relations is ideally decided by the setting of the rotation angle θ . The PM resolution ε is fixed to the angle θ at perfect interference with

$$\varepsilon_{\text{ideal}} = \sin(4\theta). \quad (3.10)$$

The HV transmission τ is controlled by the same HWP angle θ as

$$\tau_{\text{ideal}} = \cos(4\theta). \quad (3.11)$$

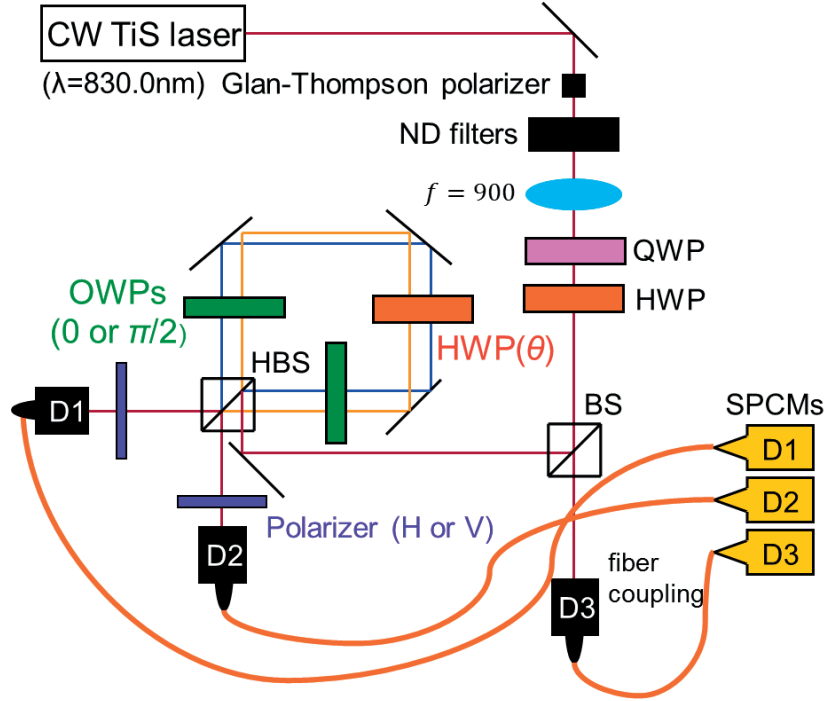


FIGURE 3.2: Experimental setup for the sequential measurement of PM and HV polarization. A Sagnac interferometer with a hybrid-coated beam splitter operating as polarizing beam splitter in the input and as polarization insensitive 50:50 beam splitter in the output is used to separate and interfere the horizontal and vertical polarization components. The measurement strength is adjusted by the rotation angle of the half-wave plate inside the interferometer, with the two $\lambda/8$ -wave plates changing the polarization rotation to induce sensitivity to the non-classical correlations between PM polarization and HV polarization in the input.

Thus, the measurement errors in the PM variable strength measurement are obtainable at any measurement strength from the experimental statistics in the sequential measurement.

Chapter 4

Results for linearly polarized input states

In this chapter, I experimentally show joint-statistics of linear polarization state before the sequential measurement. A method for reconstructing the intrinsic joint probability distribution is introduced by using evaluated measurement errors. Experimental results of the measurement errors categorized by measurement resolution and back-action effects are shown when inputting the eigenstates and the errors can be understood from flipping probabilities of the outcomes. To demonstrate the maximum violation of the Leggett-Garg inequality (LGI), I prepare a linear polarization in which the negative joint probability is predicted by the Dirac distribution. The LGI is violated at any measurement strength in the reconstructed joint probability distribution. This reconstructed joint probabilities are consistent with the value of the Dirac distribution, including the negativity, although the experimentally obtained probabilities cannot violate the correlation limit of the LGI. These results suggest that quantum effects originated from the non-commuting observables of the initial state appear in non-realistic combination of the eigenvalues and are always concealed by the unavoidable uncertainty errors in a quantum measurement. In addition, I mention that the argument for correlations between the errors themselves is necessary to complete their characterization.

4.1 Flipping errors model of measurement outcomes

We can directly evaluate ε and τ from $P_{\text{exp}}(m, f)$ for inputting the P state in equation (3.8) and the H state in equation (3.9) respectively. The experimental results obtained at various measurement strengths is shown in figures 4.1 and 4.2. The experimentally determined resolution ε in figure 4.1 depends on the measurement strength θ and can be

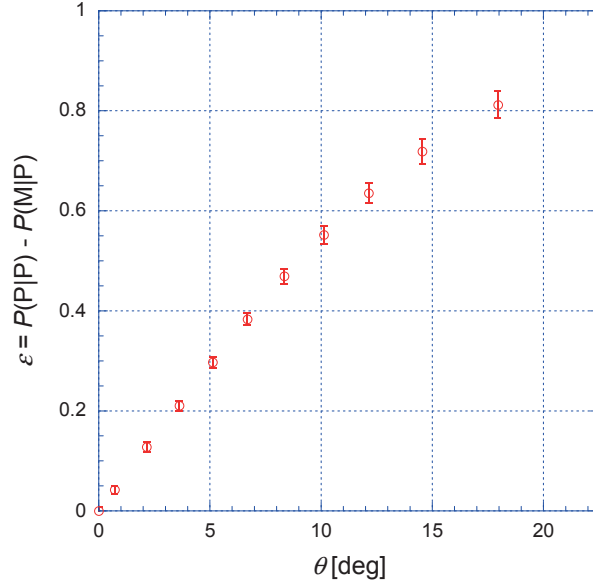


FIGURE 4.1: Experimental evaluation of measurement resolution. Data points show the difference $P(P) - P(M)$ between the probabilities of the measurement outcomes P and M for a P-polarized input state. This difference is equal to the measurement resolution ε of the PM measurement.

fitted by $\varepsilon = V_\varepsilon \sin(4\theta)$, where V_ε is obtained with an experimental visibility $V_\varepsilon = 0.853 \pm 0.010$. This value is consistent with finite visibility of the interference independently observed in the fringe on the output of the BS part of the HBS. As expected, the dependence of the back-action effect of the transmission τ in figure 4.2 is close to the ideal relation in equation (3.11). We can also parameterize a tiny decoherence effects of HV polarization with an experimental visibility V_τ , so that $\tau = V_\tau \cos(4\theta)$ with $V_\tau = 0.9997 \pm 0.0001$. This indicates that the back-action nearly equals the rotation of polarization in the interferometer on the PM measurement and the precise setting of both PM and HV measurement bases have been achieved in the experimental setup. Thus, we find the experimental evidence of controlling the measurement back-action with rotating the HWPs on variable strength measurement of PM polarization in figure 4.2.

The measurement errors characterized by ε and τ can be understood as a flipping probabilities when obtaining the measurement outcomes. In a two level system, since the measurement outcomes are two values ± 1 , the outcome is distributed to either equal value or opposite value for the input value. The input value is here fixed to the eigenvalue $+1$ in figures 4.1 and 4.2 respectively. Thus, the ε and the τ are independently related as the flipping error probability of $(1 - \varepsilon)/2$ and $(1 - \tau)/2$ from the outcome $+1$ to the outcome -1 . The mixture of both the flipping and the non-flipping statistics can explain the experimental PM resolution and HV transmission over the whole measurement strengths. Note that the present flipping errors can be only applied for the

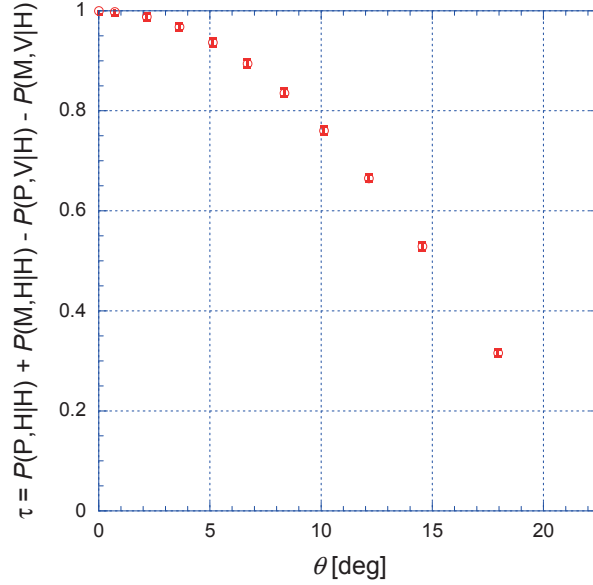


FIGURE 4.2: Experimental evaluation of measurement back-action. Data points show the difference $P(H) - P(V)$ between the probabilities of the measurement outcomes H and V for an H-polarized input state. Since this difference is reduced by the back-action of the PM measurement, its value is equal to the HV transmission τ .

linear polarized input states, because we consider the LGI scenario, where the maximum violation is assumed on $\langle s_{\text{PM}} s_{\text{HV}} \rangle = 0$. Thus, we just check the error characteristic as independent flips of the two PM and HV outcomes from the experimental data in figures 4.1 and 4.2. Since the expectation value of the product between the outcomes is fixed, this flipping errors model may be valid for describing each outcome of correlated joint-statistics from \hat{S}_{PM} and \hat{S}_{HV} . In this scenario, we can reconstruct the joint probabilities $\rho(s_{\text{PM}}, s_{\text{HV}})$ of any linear polarized input state from the experimentally obtained probability distribution $P_{\text{exp}}(m, f)$ for the joint outcomes of m and f . For example, the experimental joint probability of assigned outcome (P,H) consists of a mixture of the intrinsic joint probabilities of the joint outcomes (P,H), (M,H), (P,V) and (M,V) depending on conditional probabilities determined by the flipping error probability of $(1 - \varepsilon)/2$ and $(1 - \tau)/2$. This relation is given by

$$\begin{aligned}
P_{\text{exp}}(m, f) &= \left(\frac{1 + \varepsilon}{2}\right) \left(\frac{1 + \tau}{2}\right) \rho(s_{\text{PM}} = m, s_{\text{HV}} = f) \\
&+ \left(\frac{1 - \varepsilon}{2}\right) \left(\frac{1 + \tau}{2}\right) \rho(s_{\text{PM}} = -m, s_{\text{HV}} = f) \\
&+ \left(\frac{1 + \varepsilon}{2}\right) \left(\frac{1 - \tau}{2}\right) \rho(s_{\text{PM}} = m, s_{\text{HV}} = -f) \\
&+ \left(\frac{1 - \varepsilon}{2}\right) \left(\frac{1 - \tau}{2}\right) \rho(s_{\text{PM}} = -m, s_{\text{HV}} = -f). \tag{4.1}
\end{aligned}$$

Inverting this map, the intrinsic joint probabilities can be reconstructed from the experimental data,

$$\begin{aligned}
\rho(s_{\text{PM}}, s_{\text{HV}}) &= \frac{(1+\varepsilon)(1+\tau)}{4\varepsilon\tau} P_{\text{exp}}(m = s_{\text{PM}}, f = s_{\text{HV}}) \\
&\quad - \frac{(1-\varepsilon)(1+\tau)}{4\varepsilon\tau} P_{\text{exp}}(m = -s_{\text{PM}}, f = s_{\text{HV}}) \\
&\quad - \frac{(1+\varepsilon)(1-\tau)}{4\varepsilon\tau} P_{\text{exp}}(m = s_{\text{PM}}, f = -s_{\text{HV}}) \\
&\quad + \frac{(1-\varepsilon)(1-\tau)}{4\varepsilon\tau} P_{\text{exp}}(m = -s_{\text{PM}}, f = -s_{\text{HV}}). \tag{4.2}
\end{aligned}$$

Therefore, the joint probability distribution $\rho(s_{\text{PM}}, s_{\text{HV}})$ before the measurements can be observed in the sequential measurement of PM polarization and HV polarization with any combination of the measurement errors characterized by PM resolution and HV transmission. Note that this deconvolution with the flipping errors model is entirely based on the direct observable properties without quantum theory and only require the description of the initial state as a joint probability distribution without a choice of specific distribution function of quantum physics, of course, Dirac distribution is also not assumed.

4.2 Confirmation of LGI violations

To observe the expected maximum violation of the LGI, I prepare the input polarization halfway between P and V as the eigenstate of $s_1 = +1$. Figure 4.3 shows the experimental data obtained from the sequential measurement of PM and HV polarization with different measurement strength θ . The experimentally obtained joint probabilities $P_{\text{exp}}(m, f)$ have a tendency to obey the expectation values for the input state and a dependence of the measurement strength θ . In figure 4.3, it is always confirmed that $P_{\text{exp}}(\text{P}, \text{V})$ keeps highest probability and $P_{\text{exp}}(\text{M}, \text{H})$ is lowest one, corresponding to the input state. However, the average values of $m = s_{\text{PM}}$ and $f = s_{\text{HV}}$ obtained from the $P_{\text{exp}}(m, f)$ distribution are totally different from the expectation values of $\langle \hat{S}_{\text{PM}} \rangle = 1\sqrt{2}$ and $\langle \hat{S}_{\text{HV}} \rangle = -1\sqrt{2}$ predicted with the input state. Furthermore, this experimental probability distribution never violates the classical limit of the correlation argued in the LGI. The experimental obtained correlation is close to the limit near $\theta = 12.5^\circ$, where $P_{\text{exp}}(\text{M}, \text{H})$ is also close to zero. At this middle measurement strength, the trade-off relation between the measurement resolution and back-action is optimized in terms of obtaining the information of the joint outcomes. Nevertheless, we cannot confirm the LGI violation expressed by the negative joint probability because the measurement uncertainties restrict the observation of the non-classical correlated values of $\langle s_{\text{PM}} \rangle$ and $\langle s_{\text{HV}} \rangle$.

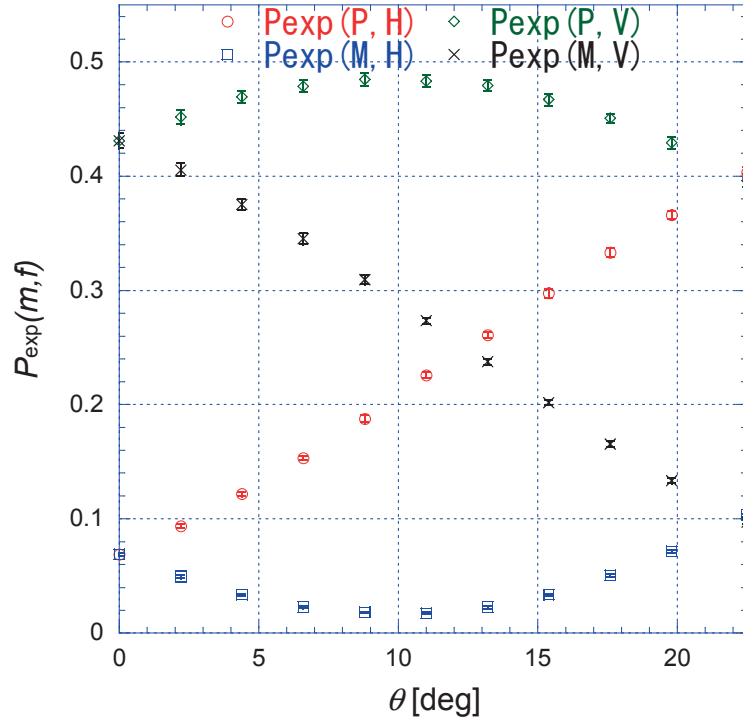


FIGURE 4.3: Experimental joint probabilities for an input polarization halfway between P and V polarization obtained at different measurement strengths θ .

On the other hand, we can apply the flipping model for the errors to reconstruct the intrinsic joint probability distribution using the evaluated resolution ε and transmission τ at any measurement strength in figures 4.1 and 4.2 in equation (4.2). The reconstructed joint probabilities $\rho(s_{PM}, s_{HV})$ at various measurement strength are shown in figure 4.4. It is readily seen that the $\rho(s_{PM}, s_{HV})$ is independent of the measurement strength. Moreover, $\rho(M, H)$ shows the negative valued probability, corresponding to the violation of the LGI. The errors bars in figure 4.4 include statistical errors from the experimental counts rate in figure 4.3 and the estimated errors of V_ε and V_τ determined by the experimental data in figures 4.1 and 4.2. In the measurement of both weak and strong limits, the statistical errors increase because the outcome m is never influenced by the initial property s_{PM} when ε equals zero and f is not reflected to s_{HV} at all on $\tau = 0$. The theoretical values of the Dirac distribution $D_\rho(s_{PM}, s_{HV})$ are also shown in figure 4.4 as dashed lines. The reconstructed joint probabilities are good agreement with the Dirac distribution over the whole measurement strengths. Therefore, the non-classical correlations between $\langle s_{PM} \rangle$ and $\langle s_{HV} \rangle$ can be demonstrated as a measurement independent property of the initial state and reflect the non-commutativity between \hat{S}_{PM} and \hat{S}_{HV} with the description of the joint probability distribution of the measurement outcomes. It is also important that the unavoidable measurement errors including the back-action can be completely removed by the simple flipping model of the outcomes

without the assumption of any quantum theory.

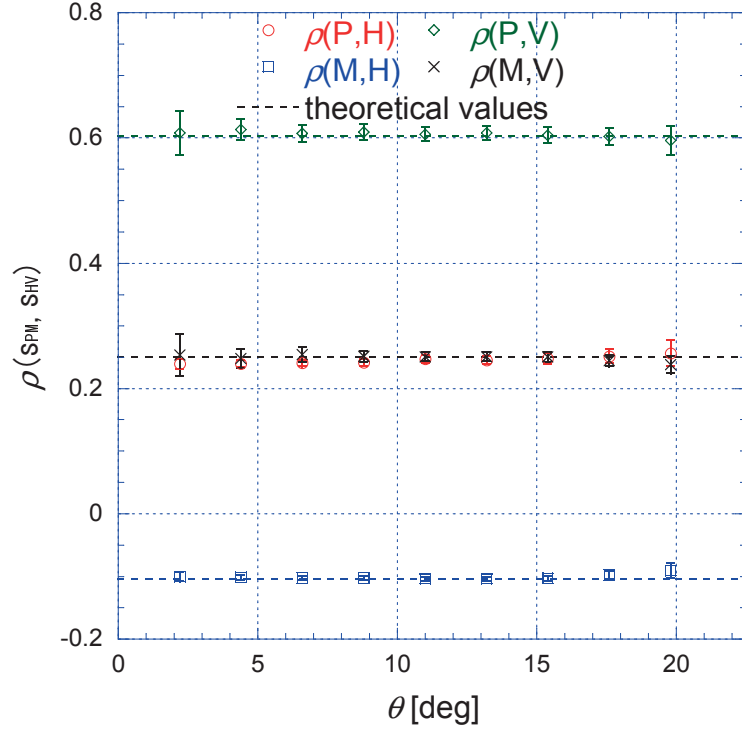


FIGURE 4.4: Intrinsic joint probabilities reconstructed using the experimentally determined values of resolution ε and transmission τ at the respective measurement strength θ . Dashed lines indicate the values theoretically predicted for the input state : Dirac distribution.

4.3 Correlations between errors

In the LGIs scenario, the measurement errors are regarded as independent and correlations between them are not taken into account. However, the error correlations are necessary to decide a general form of the errors statistics when we attempt a reconstruction of any polarization state. The reason can be seen in the following convolution of the joint probability distribution,

$$P_{\text{exp}}(m, f) = \sum_{s_{\text{PM}}, s_{\text{HV}}} P_M(m, f | s_{\text{PM}}, s_{\text{HV}}) \rho(s_{\text{PM}}, s_{\text{HV}}). \quad (4.3)$$

The experimentally obtained probabilities $P_{\text{exp}}(m, f)$ of the joint outcomes are related to the intrinsic joint probabilities $\rho(s_{\text{PM}}, s_{\text{HV}})$ of the combination of the eigenvalues with a conditional probabilities $P_M(m, f | s_{\text{PM}}, s_{\text{HV}})$ representing the errors. This equation (4.3) is similar to the flipping errors model in equation (4.1) without assuming $\langle s_{\text{HV}} s_{\text{PM}} \rangle = 0$,

where correlations between the errors have no effect on the reconstructed joint probability distribution. However, the expectation value of the product between the observables \hat{S}_{PM} and \hat{S}_{HV} is expected to be imaginary from the operator formalism, if we prepare an elliptical polarization state. Moreover, the analysis of the error statistics of joint measurements using the input having the known correlations shows the necessity of an imaginary part in the conditional error probabilities $P_M(m, f|s_{\text{PM}}, s_{\text{HV}})$, so that the errors correlate non-classically to themselves reflected in the initially correlated physical properties [37]. Thus, the reconstructed joint probabilities $\rho(s_{\text{PM}}, s_{\text{HV}})$ with complex values are expected from the complex error probabilities $P_M(m, f|s_{\text{PM}}, s_{\text{HV}})$ and result in positive probabilities $P_{\text{exp}}(m, f)$ as relative frequency obtained from the actual counts rate.

The sequential measurements have information about the correlations represented as the average product of the outcomes $\langle fm \rangle$. The correlation fidelity γ can be defined as the difference between the probabilities of the products of the outcomes fm ,

$$\gamma = P(fm = s_{\text{HV}}s_{\text{PM}}) - P(fm = -s_{\text{HV}}s_{\text{PM}}). \quad (4.4)$$

Similar to the resolution ε and the transmission τ , the correlation fidelity γ can be evaluated by comparing the average value of the product fm with the expectation value $\langle \hat{S}_{\text{PM}}\hat{S}_{\text{HV}} \rangle$ of the input state,

$$\gamma = \frac{\langle fm \rangle_{\text{exp}}}{\langle \hat{S}_{\text{HV}}\hat{S}_{\text{PM}} \rangle_{\text{input}}}. \quad (4.5)$$

The problem of this evaluation is that any input state having the simultaneous eigenvalue of \hat{S}_{PM} and \hat{S}_{HV} cannot exist, so that reliable references of the product value is out of a reality. However, we can make use of the operator algebra in equation (2.7) to relate the quantum correlation between \hat{S}_{PM} and \hat{S}_{HV} to the circular polarization of the input, which results in the assignment of an imaginary value to the correlation fidelity γ ,

$$\nu = i\gamma = \frac{\langle fm \rangle_{\text{exp}}}{\langle \hat{S}_{\text{RL}} \rangle_{\text{input}}}. \quad (4.6)$$

The statistical effect on the measurement of the imaginary correlation $\gamma = -i\nu$ can be determined by comparing the actually observed correlation between the outcome m of the PM measurement and the outcome f of the HV measurement with inputting the R polarization. Therefore, the correlation fidelity ν is given by using the R-polarized input and obtaining the correlations between the actual outcome m and f as follows,

$$\nu = P(P, H|R) + P(M, V|R) - P(P, V|R) - P(M, H|R). \quad (4.7)$$

Chapter 5

Measurement of complex joint probabilities

Quantum joint-statistics of photon polarization is demonstrated by violating the classical limit of the correlation between the average values of PM polarization and HV polarization as discussed in chapter 4. In this chapter, I take care of correlations between the initial outcomes in the PM measurement and the final outcomes in the HV measurement. Since these correlations can be related to the product of the non-commuting operators, these are identified to the imaginary correlation between two linear polarization properties associated with the circular polarization of the input. By modifying the rotation of polarization in the interferometric setup to convert imaginary correlations to real correlations, the experimentally observable correlations can be found in the measurement back-action effect on the HV measurement. To demonstrate the complex joint probability distribution of the initial state, I prepare an elliptical polarization and obtain the joint outcomes in the sequential measurement sensitive to the imaginary correlation. The reconstruction of the complex Dirac distribution is possible at any measurement strength if the all measurement errors including the correlation fidelity are evaluated. Thus, the average values of the product of PM polarization and HV polarization show the pure imaginary correlation, which is necessary for the complete characterization of the initial quantum statistics.

5.1 Experimental realization of imaginary measurement back-action

To obtain a sensitivity for the error correlation, the sequential measurement of PM and HV polarization need to be modified from the condition of $\langle fm \rangle = 0$. Here, we can introduce a brand-new degree of freedom of a polarization operation to modify the initial PM measurement of the finite measurement strength, in which the trade-off relation between the PM resolution and the HV transmission is reformed. The degree of the operation for the RL direction only remains unused and we need to obtain the sensitivity to the circular polarization input on a PM measurement. Then, we modify the rotation of the polarizations to be an elliptical polarizations with the same major axis of polarization but opposite circular polarization, so that such twist rotations towards opposite circular polarizations in the interferometer keep same HV information as much as the previous rotations towards the common P direction at each measurement strength θ . This effect reduces the PM resolution, since the indistinguishability achieved by rotating the exactly P direction is lost. On the other hand, this effect keeps HV transmission in the initial PM measurement, although it can be seen only after the final HV measurement. Hence, the correlation fidelity γ produced by the twist rotations of polarization in the interferometer appears in additional back-action effect. It actually changes the observed correlations between the joint outcomes of the sequential measurement, converting the sensitivity to non-classical correlations between PM and HV polarization. The experimental realization of the twist of polarization is given by the $\lambda/8$ wave plates (OWPs) in figure 3.2. Two OWPs located on both sides of the half wave plate (HWP) change the direction of the polarization rotated by the HWP towards elliptical polarizations halfway between PM and RL polarization, setting the fast axis of one OWP to the H direction and one of another OWP to the V direction. Generally, an additional angle ϕ corresponding to the rotation angle around the HV axis of the Bloch sphere can be used in describing the measurement operators. Since the coherent transition expressed with the HV basis of the initial state in equation (3.5) are modified with the additional phase ϕ , the new measurement operators are given by

$$\begin{aligned}\hat{M}_{P\phi} &= \frac{1}{\sqrt{2}} \left(\cos(2\theta) \hat{I} + e^{i\phi} \sin(2\theta) \hat{S}_{PM} \right) \\ \hat{M}_{M\phi} &= \frac{1}{\sqrt{2}} \left(\cos(2\theta) \hat{I} - e^{i\phi} \sin(2\theta) \hat{S}_{PM} \right).\end{aligned}\tag{5.1}$$

Note that the angle ϕ is ideally fixed at $\pi/4$ using the OWPs, which provides the middle balance between the measurement resolution and the sensitivity to the imaginary correlations.

Similar to the previous description of the ideally measurement performance in equations (3.10) and (3.11), the setting θ and ϕ can decide a trade-off relation under our perfect control. The transmission fidelity τ still depends on the only HWP angle θ as,

$$\tau_{\text{ideal}} = \cos(4\theta). \quad (5.2)$$

The measurement resolution ε depends on the both angles of the HWP θ and the ϕ of the polarization rotation around the HV axis with

$$\varepsilon_{\text{ideal}} = \cos(\phi) \sin(4\theta). \quad (5.3)$$

Note that this ideal value is only obtained for optimal visibility of the interferometer. In the same manner, the interference is necessary to observe the correlation fidelity $\nu = i\gamma$. The value for perfect interference is

$$\nu_{\text{ideal}} = -\sin(\phi) \sin(4\theta). \quad (5.4)$$

Thus, the twist angle ϕ provides the sensitivity to imaginary error correlation with additional back-action effect instead of the reduction for the measurement resolution.

5.2 Complete characterization of correlated errors

On the sequential measurement with finite correlation sensitivity, we can also evaluate the all measurement errors separately with optimal eigenstates as input represented in equations (3.2), (3.4) and (4.6). Figure 5.1 shows the experimental result for different measurement strength with the input of P polarization. The maximum value of the resolution ε decreases comparing the experimental result for no sensitivity to imaginary correlation in figure 4.1 as expected. The data are fitted with $\varepsilon = V_\varepsilon \sin(4\theta)$ of the experimental visibility $V_\varepsilon = 0.408 \pm 0.004$. The transmission τ obtained the experimental data with the H state as input is shown by figure 5.2. The results are similar to the previous sequential measurement in figure 4.2 and close to the ideal values given by equation (5.2). On the other hand, a high visibility of HV transmission $\tau(0) = 0.98 \pm 0.04$ is achieved at $\theta = 0$, but a difference between the H and the V probabilities is non-vanishing at maximum measurement strength of $\theta = 22.5^\circ$. It is difficult to characterize this effect to the experimental visibility V_τ of $\tau = V_\tau \cos(4\theta)$. The data suggests that the control of linear polarization is not matched precisely in each other path at strong region of the measurement strength θ . The reason may be affected by the operation of the twist rotations of polarization.

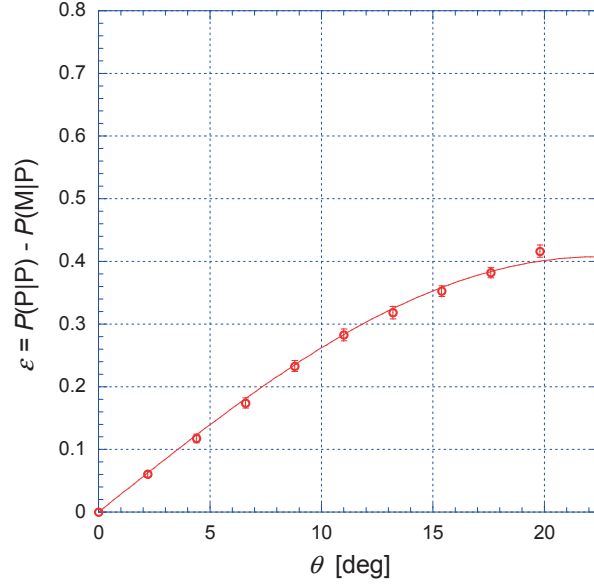


FIGURE 5.1: Experimental evaluation of measurement resolution ε using P-polarized input photons. The measurement strength θ is given by the degrees of rotation for the half-wave plate in the interferometer.

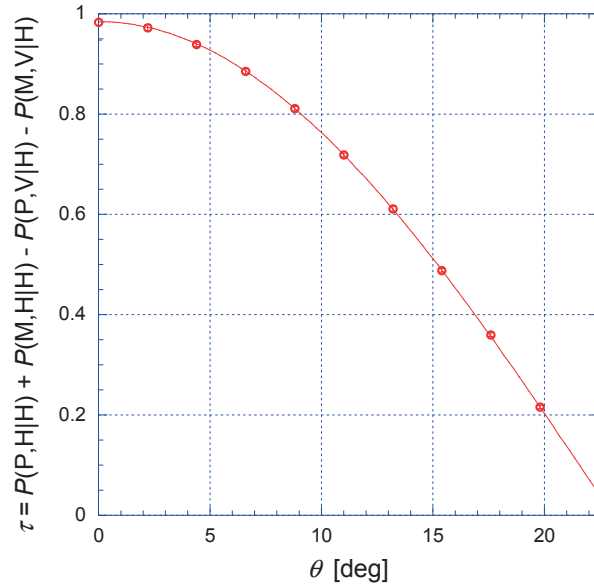


FIGURE 5.2: Experimental evaluation of transmission τ as a function of measurement strength θ using H-polarized input photons.

The remaining measurement error is the correlation fidelity $\nu = i\gamma$, which is the most important element of the error statistics to reconstruct the complex joint probability distribution. In the previous measurements, the correlations between the outcomes are always zero, so that $\nu = 0$ is satisfied at any measurement strength by the experimentally observable statistics. On the other hand, the finite values of $\nu = i\gamma$ can be evaluated in the modified operations, since the angle ϕ makes the outcomes correlated. The correlation fidelity is directly determined by inputting the R-polarized state, shown in figure

5.3. The experimental results have a dependence of measurement strength described by

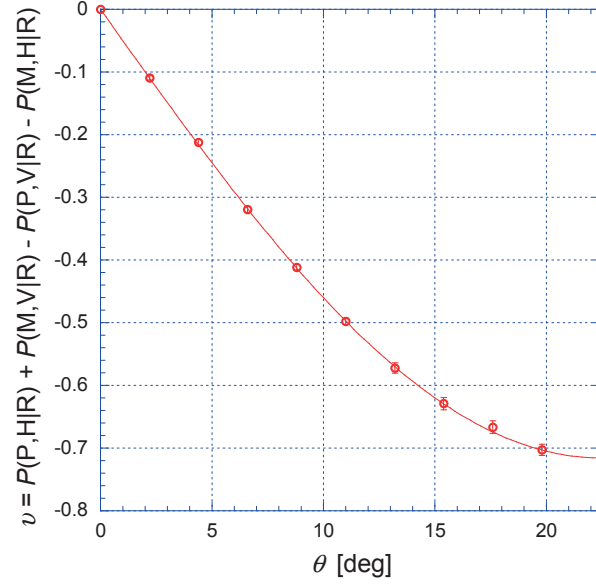


FIGURE 5.3: Experimental evaluation of correlation fidelity $\nu = i\gamma$ as a function of measurement strength θ using R-polarized input photons. The negative sign indicates that a positive imaginary correlation appears as an anti-correlation between the sequential outcomes in the experimental measurement statistics.

a sine function as expected. The negative values of ν are derived from the direction of the polarization rotations with anti-correlation between the measurement outcomes for the input of the positive imaginary correlations given by R polarization. We can fit the data with $\nu = -V_\nu \sin(4\theta)$, where the experimental visibility $V_\nu = 0.716 \pm 0.003$ is obtained. On actual interference at the beam splitter, both resolution ε and correlation ν depend on the fringe of the visibility. This is confirmed from the total visibility given by $\sqrt{V_\varepsilon^2 + V_\nu^2} = 0.824 \pm 0.003$, which is consistent with the visibility of 0.82 observed in the fringe at the output ports. The difference between the values of ε and ν indicates that the actual rotation angle ϕ is 60.3° , although two visibilities are expected to be the same for $\phi = 45^\circ$. This experimental characterization shows that the birefringent phase shift in the interferometer of our setup is actually larger than the expected angle of 45° given by the use of the OWPs.

5.3 Reconstruction of the Dirac distribution at variable measurement strengths

By completely characterizing the correlated measurement errors using the experimental data, we can observe the non-classical correlation between the non-commuting observables \hat{S}_{PM} and \hat{S}_{HV} from the joint outcomes obtained in the sequential measurement

converting unobservable imaginary correlations to obtainable real correlations. The error probability $P_M(m, f|s_{\text{PM}}, s_{\text{HV}})$ in equation (4.3) can be expressed by the experimentally evaluated errors, i.e. the resolution ε in figure 5.1, the transmission τ in figure 5.2, and the imaginary correlation $\gamma = -i\nu$ in figure 5.3,

$$\begin{aligned} P_{\text{exp}}(m, f) &= \frac{1 + \varepsilon + \tau - i\nu}{4} \rho(s_{\text{PM}} = m, s_{\text{HV}} = f) \\ &+ \frac{1 - \varepsilon + \tau + i\nu}{4} \rho(s_{\text{PM}} = -m, s_{\text{HV}} = f) \\ &+ \frac{1 + \varepsilon - \tau + i\nu}{4} \rho(s_{\text{PM}} = m, s_{\text{HV}} = -f) \\ &+ \frac{1 - \varepsilon - \tau - i\nu}{4} \rho(s_{\text{PM}} = -m, s_{\text{HV}} = -f). \end{aligned} \quad (5.5)$$

The complex joint probability distribution $\rho(s_{\text{PM}}, s_{\text{HV}})$ can be reconstructed from the experimental data by inverting this map,

$$\begin{aligned} \rho(s_{\text{PM}}, s_{\text{HV}}) &= \left(\frac{1}{4} + \frac{1}{4\varepsilon} + \frac{1}{4\tau} + \frac{i}{4\nu} \right) P_{\text{exp}}(m = s_{\text{PM}}, f = s_{\text{HV}}) \\ &+ \left(\frac{1}{4} - \frac{1}{4\varepsilon} + \frac{1}{4\tau} - \frac{i}{4\nu} \right) P_{\text{exp}}(m = -s_{\text{PM}}, f = s_{\text{HV}}) \\ &+ \left(\frac{1}{4} + \frac{1}{4\varepsilon} - \frac{1}{4\tau} - \frac{i}{4\nu} \right) P_{\text{exp}}(m = s_{\text{PM}}, f = -s_{\text{HV}}) \\ &+ \left(\frac{1}{4} - \frac{1}{4\varepsilon} - \frac{1}{4\tau} + \frac{i}{4\nu} \right) P_{\text{exp}}(m = -s_{\text{PM}}, f = -s_{\text{HV}}). \end{aligned} \quad (5.6)$$

This reconstructed distribution is expected to agree with the Dirac distribution in quantum mechanics. Note that this reconstruction has no assumption of any specific form of quasi-probability distribution, just assuming that an initial state can be described as a joint probability distribution and the expectation value of the operator product can be assigned to the imaginary value.

We expect that an arbitrary input state of polarization, where a state for an elliptical polarization can be described by the Dirac distribution having imaginary values, can be reconstructed from the experimental probabilities of the joint outcomes obtained in the sequential measurements of two non-commuting observables. Here, I demonstrate the reconstruction at any measurement strength by choosing a right circulating elliptically polarized input state with half ellipticity and the major axis of the ellipse pointing halfway angle between P and H polarization. The experimental results for the probabilities of the four joint outcomes at various measurement strength are shown in figure 5.4. The results of figures 5.4 and 4.3 have the only common tendency that the lowest probability of the joint outcomes has the reverse preference for the most likely outcomes of the input state over the whole measurement strengths. The others are totally different for the preference of the outcomes. Especially, the effect of correlation sensitivity

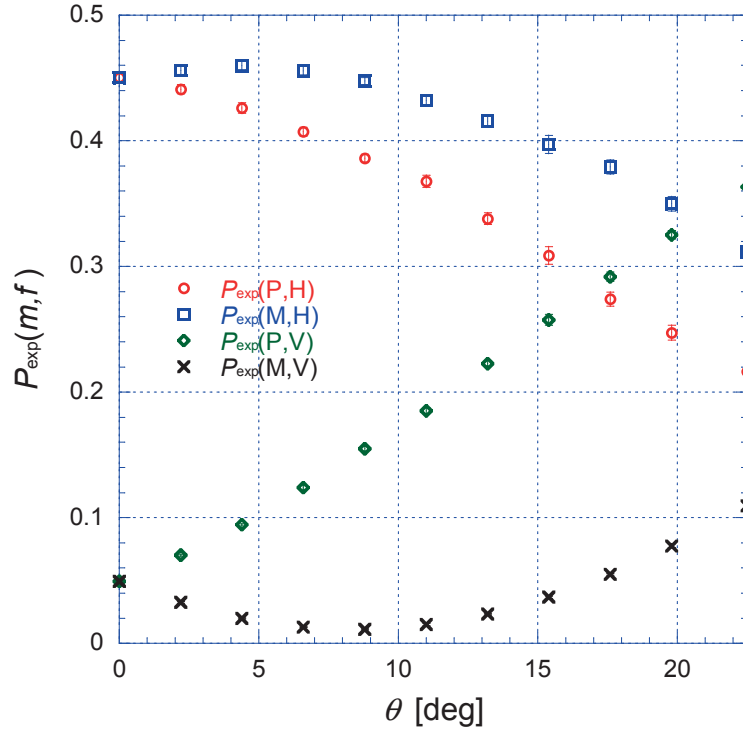


FIGURE 5.4: Experimental joint probabilities for an elliptically polarized input state at different measurement strengths θ

can be seen in figure 5.4 taking notice of the product of the outcomes. The present results in figure 5.4 tend to more observe the two outcomes with $fm = -1$ than the two outcomes with $fm = +1$ at any measurement strength expect for no measurement with $\theta = 0^\circ$. As measurement strength increases, the average value of m is expected with increasing, due to the positive expectation value of \hat{S}_{PM} predicted by P-biased polarization of the input state. However, the $\langle m \rangle$ is not monotonic increasing but taking the negative value. Moreover, the probabilities of (M,H) is always higher than the probabilities of (P,H), which is expected to be the highest probability because of the input state. In the strong regions, the other probability of (P,V) is also more likely than the most expected probability of (P,H) for the input state. This reason can be explained from the characteristic of our realized measurements. As shown in figures 5.1 and 5.3, the resolution of the correlation product of the outcomes is stronger than the resolution of PM polarization due to the large angle ϕ , so that the tendency to negative correlations between two measurement outcomes strongly appears in the observed results. Here, the average value of fm is negative for the eigenvalue $s_{\text{RL}} = +1$ when inputting the right circular polarization.

By applying the evaluated errors with the separate measurements to equation (5.6), we can reconstruct the complex valued joint probability distribution, expected to the

correspondence with the Dirac distribution. The experimental data in figure 5.4 is deconvoluted by using the measurement data shown in figures 5.1, 5.2, and 5.3. The real part of the reconstructed joint probabilities is shown in figure 5.5. The error bars show the statistical errors which combine the experimental data in figure 5.4 with statistical errors in the evaluated values of ε and τ . The later statistical errors increase in both the weak and the strong limit of measurement strength, since it is difficult to determine the very small values close to zero for the resolution ε and the transmission τ by finite statistics. The reconstructed results originally obtained at different measurement

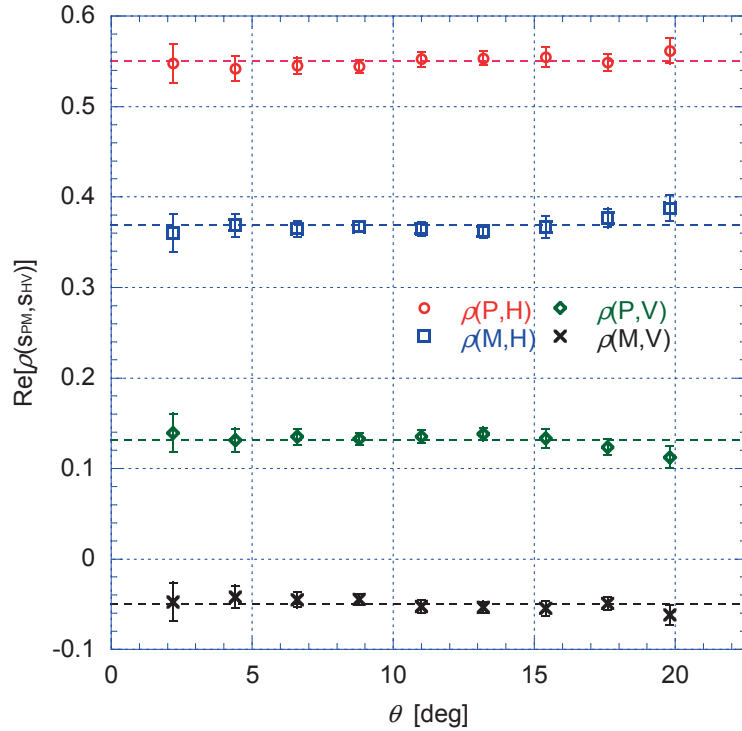


FIGURE 5.5: Real part of the complex joint probability distribution obtained from the experimental probabilities at different measurement strengths. As indicated by the dashed lines, the results obtained at different measurement strengths are all explained by the same input state statistics.

strength reproduce the same joint probability distribution $\rho(s_{\text{PM}}, s_{\text{HV}})$ in figure 5.5 as indicated by the dashed lines. This average results correspond to two expectation values of $\langle \hat{S}_{\text{PM}} \rangle = 0.36$ and $\langle \hat{S}_{\text{HV}} \rangle = 0.84$. This shows that the reconstructed joint probabilities have same preference to the input state with much biased H polarization than P polarization. As indicated by figure 5.5, the real part of the correlations $\langle s_{\text{HV}} s_{\text{PM}} \rangle$ is always zero, even if we measure the finite correlations between the measurement outcomes. The reason derives from the model of the reconstruction in equation (5.5), especially assigning the correlation product to imaginary value. Thus, the reconstructed joint probabilities $\rho(s_{\text{PM}}, s_{\text{HV}})$ have same characteristic for the Dirac distribution $D_\rho(s_{\text{PM}}, s_{\text{HV}})$, where the real part of the correlation product is not only zero but also the imaginary part of one

has a meaningful value depending on the state. We expect that the average product value between the PM polarization and the HV polarization appears in the imaginary part of the reconstructed joint probability distribution.

Figure 5.6 shows the results for the imaginary part of the reconstructed distribution using the experimental values of the correlation fidelity ν . The error bars are large only in the weak regions, since the ν reduces to zero in the weak limit. The results confirm that the same intrinsic statistics is observed at all measurement strengths θ . The average

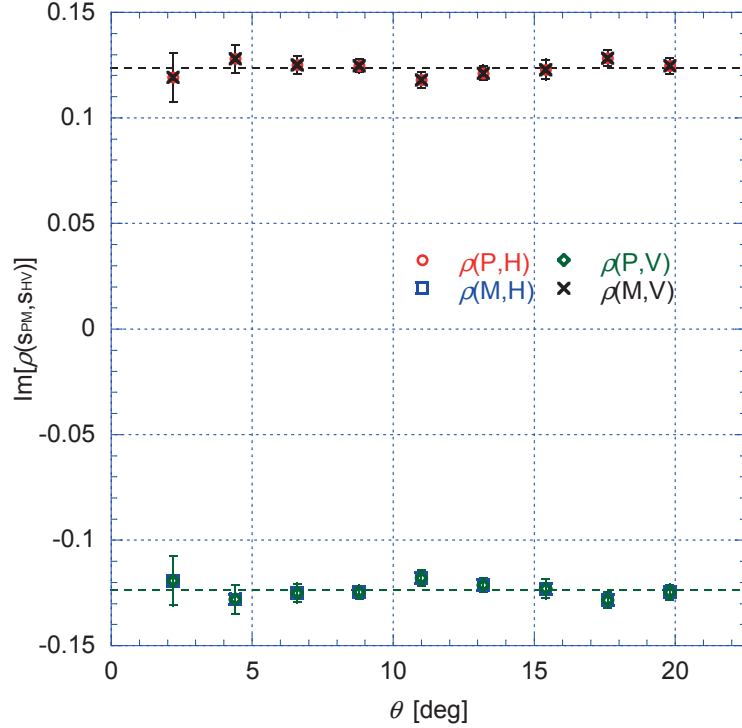


FIGURE 5.6: Imaginary part of the complex joint probability distribution obtained from the experimental probabilities at different measurement strengths. Since marginal probabilities must be real, $\text{Im}[\rho(P, H)] = -\text{Im}[\rho(M, H)] = -\text{Im}[\rho(P, V)] = \text{Im}[\rho(M, V)]$.

products of the imaginary joint probabilities reconstructed from the experimental data correspond to an expectation value of $\langle \hat{S}_{HV} \hat{S}_{PM} \rangle = i0.50$, which is imaginary correlation of the input with right circulated elliptical polarization.

Chapter 6

Discussion and Conclusions

In summary of this thesis, I investigate photon polarization statistics including the non-commuting observables with the sequential measurements of PM and HV polarization, where the outcomes are affected by the unavoidable measurement errors as a result of the initial measurement with a finite measurement strength. However, the measurement errors characterized by the resolution and the back-action can be evaluated directly with the experimental probabilities obtained from the joint outcomes conditioned by inputting the eigenstates, where the eigenvalues work reliable references considering the well established relation between the value of the measurement outcome and the corresponding state. By grasping the modification of the measured statistics, we can observe the non-classical correlations between the initial physical properties including the average value of the product between them by reconstructing the intrinsic joint probability distribution from the experimental data at any measurement strength independent of quantum theory. The description of the correlations between PM and HV polarization property is certainly valid for providing a statistical evidence with concrete physics of the measurement beyond the “algorithmic” management using a state and observables.

The sequential measurements are performed with the variable strength measurement of the PM observable and successively projective measurement of the HV observable. The experimental setup consists of the interferometer that make PM polarization partially projective measurement and the polarizers inserted after the interferometer for the fully projective measurement of H/V polarization. The PM measurement is controlled by the precise rotations of polarizations on the two paths of the interferometer toward the P-polarized directions. Since the operations work as the measurement back-action, the interference on the output beam splitter results in the measurement resolution. The various measurements of different measurement strength are performed to vary the rotation angle and we obtain the experimental probabilities of the PM and the HV measurement

outcomes with the complementary measurement errors. The actual nonzero correlations between them can be obtained in the modified control of the polarization rotations adding the twist to R/L directions. Note that this correlation sensitivity is produced by the back-action in the interferometric PM measurement and its effects can be seen after the final HV measurement. The measurement errors including the back-action in the initial PM measurement can be considered as accidental flipping of the outcomes. Since the flipping errors probabilities can be considered in both the resolution and the back-action errors, all measurement errors in the PM measurement of a finite measurement strength can be evaluated from the experimental data and applied to arbitrary input of quantum superposition state. By using the flipping errors model thus, we can reconstruct the intrinsic joint probability distribution before the measurement at any measurement strength.

The reconstructed results from the experimental data reveal a role of correlations between the non-commuting PM and HV observables in quantum statistics. The violation of the Leggett-Garg inequality, corresponding to the negativity of the Dirac distribution shows that the combination of the average value of s_{PM} and s_{HV} exceed the classical limit of the correlation when the average product $\langle s_{\text{HV}} s_{\text{PM}} \rangle$ is always zero. In this scenario, the maximum violation of the inequality is expected by inputting the linear polarization state that is non-biased between PM polarization and HV polarization. We observe the expected maximum violation as reconstructed negative joint probability from noisy statistics of the measurement outcomes independent of measurement strength. On the other hand, the operator algebra shows that the expectation value of the product of the non-commuting PM and HV observables is pure imaginary when preparing a elliptical polarization state. Therefore, it is reasonably possible that the correlation product of the physical properties of photon polarization generally has imaginary part. We demonstrate the reconstruction of the complex joint probability distribution converting imaginary correlations to real correlations by the twist control of polarization in the interferometric setup. According to the successful reconstruction with agreement to the Dirac distribution at any measurement strength, we can observe the imaginary correlation between the PM and the HV outcomes. The statistical preference of the joint outcomes in reconstructed data certainly explains the more detail characteristic of quantum statistics than conventional representation in a tomography of the initial state, showing the effect of the non-classical correlations between non-commuting observables in the initial state. I wish the contents argued in this thesis can promote comprehensive treatment of the quantum measurement and the quantum statistics.

Returning to the Dirac distribution as being a quasi-probability, its negative or complex valued probability tells us not to be reconciled with any joint reality of the two assigned eigenvalues. On the other hand, the reconstructed statistics corresponding to the Dirac

distribution is originated from the joint outcomes in our sequential measurement with the finite resolution and back-action errors. The full analysis of the measurement errors may suggest that the physical properties of photon polarization represented by the eigenvalues have a non-realistic relation between their combination, that is, the single eigenvalue never exists, but the non-classically correlative relation between the eigenvalues reproduces the average value of the physical property that is consistent with the expectation value of the single projective measurement. Therefore, the non-probabilistic values of the Dirac distribution represent a unique characteristic of quantum statistics, which is out of the meaning of the relative frequency rather than it is temporary called as a joint “probability”. To relate the above argument about the value of the Dirac distribution, I also mention usage of a initial state. The Dirac distribution includes the assignment of the two measured observables and their order in the representation of the initial state. In the expression of the Dirac distribution therefore, it is nonsense to consider the initial state as a totally prior information, but the physical properties of the initial state can be argued if we take into account of the measurement context. A quasi-probability distribution mathematically corresponds to a quantum state. However, the statistical connection between experimentally observed statistics and quantum statistics predicted by quantum formalism is still unclear included in the other distributions of a quasi-probability. The most popular distribution is the Wigner function. If we can find a difference in a proper reconstruction of the Wigner function that has no imaginary value, it may be deeply understood that the quantum statistics is completely different from the concept of the wave-particle duality.

In the context of the measurement uncertainties on a sequential measurement, we can argue about a qualitative value of the initial state. In this thesis, the measurement errors referred with the eigenvalues of the observables are evaluated by looking the measurement back-action. Thus, all values of the outcomes are assigned to the eigenvalues and the error probability means the rate of the opposite value against a correct eigenvalue. However, we can also consider a possibility of a value except for the eigenvalue, which might connect a weak value formulated by the two state vector formalism [38]. Unfortunately, the qualitative argument in the measurement outcome has just started in the field of quantum measurements [39, 40]. A positive probability distribution of the most likely values estimated from minimizing the measurement errors [39] might be similar to the Dirac distribution of the pair of the eigenvalues reconstructed in this thesis. Moreover, it is expected that a complex value of the targeted observable includes correlations of the physical properties of the initial state. When developing researches, a possibility that fluctuations of the initial properties are not existed in quantum world might be experimentally investigated.

Finally, I indicate that the analysis is basically applicable to any two level system. By applied to the other systems except for photon polarization, we will expect to observe a unexploited correlation by realizing a brand-new control of a quantum measurement in much complex systems, such as operations of an atom by a photon, an ion by a photon and an electron by a photon. Especially, spin statistics might be rediscovered in a experimental evidence, connecting statistical mechanics with quantum physics. Note that the method cannot be directly used in a three or more multi level system, because the analysis of the back-action becomes complicated. A solution for the complexity would give a more rich picture of quantum statistics and a guide for easy control on the quantum system.

Acknowledgements

Overviewing my period of the doctor course, I strongly feel an importance of self-help efforts for my future life. Nevertheless, I was being helped by many peoples, especially movements of my familiar guys, which were necessary for fulfilling my Ph. D. thesis.

I would like to express my very great appreciation to Hofmann-sensei (Holger F. Hofmann) and Iinuma-sensei (Masataka Iinuma) for long term encouragement. Holger F. Hofmann, who is a theorist for physics, strongly motivated to understand the experimental phenomena has both vitality and insight into asking the essence of physics. He scientifically supported my study with his ideas and gave the directions of the research. Masataka Iinuma, who is a experimentalist for physics, having a large area of the physical experience is sociable for any person and caring for all related students around him. Many discussions with him about physics also gave me scientific supports and he was the closest mentor in positive and negative meanings.

I would also like to offer my special thanks to Takahashi-sensei (Tohru Takahashi) and his laboratory for spending freewheeling days of my research. In this lab, Shin-ichi Kawada and Ryuta Tanaka, who are room mates in same generation were a bit eccentric persons, but they seriously tackled their researches, which approach totally different topics respectively. Their attitude sometimes encouraged me.

My special thanks are extended to Kadoya-sensei (Yutaka Kadoya) and Prof. Geoff (Geoff Pryde) for freely using experimental equipments in Hiroshima University and Griffith University respectively. Especially, some equipments had been suddenly broken in my use. For their cares, I had continued the experiments without big interruption. My special thanks goes to staffs in Hiroshima University and the place as promoting academic researches.

I am grateful for the support and good times given by colleagues of the writing center in Hiroshima University, where I made new friends in my doctor course. I was interested to miscellaneous topic of science and various background guys with unique personalities, so that I could enjoy fresh discussions with them.

To my family, I am grateful for long time watching affectionately.

I am extremely grateful to the student loan in Japan Student Services Organization (JASSO) and the research fellowship for young scientists in Japan Society for the Promotion of Science (JSPS) for these financial supports. Without these funds, none of my Ph. D. thesis would have been fulfilled.

Finally, I appreciate former achievements and gratis something around the research given by great known and unknown guys, who I have not seen and contacted yet. To readers, I hope this thesis would make a curious encounter as a case of human relationship.

Bibliography

- [1] Masanao Ozawa. “Universally valid reformulation of the heisenberg uncertainty principle on noise and disturbance in measurement”. *Physical Review A*, **67**(4): 042105, 2003.
- [2] Yu Watanabe, Takahiro Sagawa, and Masahito Ueda. “Uncertainty relation revisited from quantum estimation theory”. *Physical Review A*, **84**(4):042121, 2011.
- [3] Paul Busch, Pekka Lahti, and Reinhard F. Werner. “Proof of heisenberg ’ s error-disturbance relation”. *Physical Review Letters*, **111**(16):160405, 2013.
- [4] Justin Dressel and Franco Nori. “Certainty in heisenberg’s uncertainty principle: Revisiting definitions for estimation errors and disturbance”. *Physical Review A*, **89**(2):022106, 2014.
- [5] Neal H. McCoy. “On the function in quantum mechanics which corresponds to a given function in classical mechanics”. *Proceedings of the National Academy of Sciences of the United States of America*, pages 674–676, 1932.
- [6] John G. Kirkwood. “Quantum statistics of almost classical assemblies”. *Physical Review*, **44**(1):31–37, 1933.
- [7] Paul AM. Dirac. “On the analogy between classical and quantum mechanics”. *Reviews of Modern Physics*, **17**(2-3):195–199, 1945.
- [8] Lars M. Johansen. “Quantum theory of successive projective measurements”. *Physical Review A*, **76**(1):012119, 2007.
- [9] Yakir Aharonov, David Z Albert, and Lev Vaidman. “How the result of a measurement of a component of the spin of a spin-1/2 particle can turn out to be 100”. *Physical review letters*, **60**(14):1351–1354, 1988.
- [10] Reza Mir, Jeff S. Lundeen, Morgan W. Mitchell, Aephraim M. Steinberg, Josh L Garretson, and Howard M. Wiseman. “A double-slit ‘ which-way ’ experiment on

- the complementarity–uncertainty debate”. *New Journal of Physics*, **9**(8):287, 2007.
- [11] Kazuhiro Yokota, Takashi Yamamoto, Masato Koashi, and Nobuyuki Imoto. “Direct observation of hardy’s paradox by joint weak measurement with an entangled photon pair”. *New Journal of Physics*, **11**(3):033011, 2009.
- [12] Jeff S. Lundeen and Aephraim M. Steinberg. “Experimental joint weak measurement on a photon pair as a probe of hardy ’ s paradox”. *Physical Review Letters*, **102**(2):020404, 2009.
- [13] Alessandro Fedrizzi, Marcelo P. Almeida, Matthew A. Broome, Andrew G. White, and Marco Barbieri. “Hardy ’ s paradox and violation of a state-independent bell inequality in time”. *Physical review letters*, **106**(20):200402, 2011.
- [14] Tobias Denkmayr, Hermann Geppert, Stephan Sponar, Hartmut Lemmel, Alexandre Matzkin, Jeff Tollaksen, and Yuji Hasegawa. “Observation of a quantum cheshire cat in a matter-wave interferometer experiment”. *Nature communications*, **5**, 2014.
- [15] Brendon L. Higgins, Matthew S. Palsson, Guoyong Xiang, Howard M. Wiseman, and Geoff J. Pryde. “Using weak values to experimentally determine “ negative probabilities ” in a two-photon state with bell correlations”. *Physical Review A*, **91**(1):012113, 2015.
- [16] Eugene Wigner. “On the quantum correction for thermodynamic equilibrium”. *Physical review*, **40**(5):749–759, 1932.
- [17] Roy J. Glauber. “Coherent and incoherent states of the radiation field”. *Physical Review*, **131**(6):2766–2788, 1963.
- [18] Ennackal CG. Sudarshan. “Equivalence of semiclassical and quantum mechanical descriptions of statistical light beams”. *Physical Review Letters*, **10**(7):277, 1963.
- [19] Lars M. Johansen and Pier A. Mello. “Quantum mechanics of successive measurements with arbitrary meter coupling”. *Physics Letters A*, **372**(36): 5760–5764, 2008.
- [20] Girish S. Agarwal and Emil Wolf. “Calculus for functions of noncommuting operators and general phase-space methods in quantum mechanics. ii. quantum mechanics in phase space”. *Physical Review D*, **2**(10):2187–2205, 1970.
- [21] Girish S. Agarwal and Emil Wolf. “Calculus for functions of noncommuting operators and general phase-space methods in quantum mechanics. i. mapping

- theorems and ordering of functions of noncommuting operators". *Physical Review D*, **2**(10):2161–2186, 1970.
- [22] Holger F. Hofmann. "Derivation of quantum mechanics from a single fundamental modification of the relations between physical properties". *Physical Review A*, **89**(4):042115, 2014.
- [23] Holger F. Hofmann. "On the role of complex phases in the quantum statistics of weak measurements". *New Journal of Physics*, **13**(10):103009, 2011.
- [24] Jeff S. Lundeen and Charles Bamber. "Procedure for direct measurement of general quantum states using weak measurement". *Physical review letters*, **108**(7):070402, 2012.
- [25] Anthony J. Leggett and Anupam Garg. "Quantum mechanics versus macroscopic realism: Is the flux there when nobody looks?". *Physical Review Letters*, **54**(9):857–860, 1985.
- [26] Nathan S. Williams and Andrew N. Jordan. "Weak values and the leggett-garg inequality in solid-state qubits". *Physical review letters*, **100**(2):026804, 2008.
- [27] Agustin Palacios-Laloy, François Mallet, François Nguyen, Patrice Bertet, Denis Vion, Daniel Esteve, and Alexander N. Korotkov. "Experimental violation of a bell's inequality in time with weak measurement". *Nature Physics*, **6**(6):442–447, 2010.
- [28] Justin Dressel, Curtis J. Broadbent, John C. Howell, and Andrew N. Jordan. "Experimental violation of two-party leggett-garg inequalities with semiweak measurements". *Physical Review Letters*, **106**(4):040402, 2011.
- [29] George C. Knee, Stephanie Simmons, Erik M. Gauger, John JL. Morton, Helge Riemann, Nikolai V. Abrosimov, Peter Becker, Hans-Joachim Pohl, Kohei M. Itoh, Mike LW. Thewalt, George AD. Briggs, and Simon C. Benjamin. "Violation of a leggett-garg inequality with ideal non-invasive measurements". *Nature communications*, **3**:606, 2012.
- [30] Holger F. Hofmann. "Sequential measurements of non-commuting observables with quantum controlled interactions". *New Journal of Physics*, **16**(6):063056, 2014.
- [31] Charles Bamber and Jeff S. Lundeen. "Observing dirac 's classical phase space analog to the quantum state". *Physical review letters*, **112**(7):070405, 2014.

- [32] Jeff Z. Salvail, Megan Agnew, Allan S. Johnson, Eliot Bolduc, Jonathan Leach, and Robert W. Boyd. “Full characterization of polarization states of light via direct measurement”. *Nature Photonics*, **7**(4):316–321, 2013.
- [33] Johannes Kofler and Časlav Brukner. “Classical world arising out of quantum physics under the restriction of coarse-grained measurements”. *Physical Review Letters*, **99**(18):180403, 2007.
- [34] Johannes Kofler and Časlav Brukner. “Conditions for quantum violation of macroscopic realism”. *Physical review letters*, **101**(9):090403, 2008.
- [35] Adam Bednorz, Wolfgang Belzig, and Abraham Nitzan. “Nonclassical time correlation functions in continuous quantum measurement”. *New Journal of Physics*, **14**(1):013009, 2012.
- [36] Masataka Inuma, Yutaro Suzuki, Gen Taguchi, Yutaka Kadoya, and Holger F Hofmann. “Weak measurement of photon polarization by back-action-induced path interference”. *New Journal of Physics*, **13**(3):033041, 2011.
- [37] Shota Kino, Taiki Nii, and Holger F. Hofmann. “Characterization of measurement uncertainties using the correlations between local outcomes obtained from maximally entangled pairs”. *Physical Review A*, **92**(4):042113, 2015.
- [38] Yakir Aharonov and Lev Vaidman. “Properties of a quantum system during the time interval between two measurements”. *Physical Review A*, **41**(1):11, 1990.
- [39] Masataka Inuma, Yutaro Suzuki, Taiki Nii, Ryuji Kinoshita, and Holger F. Hofmann. “Experimental evaluation of nonclassical correlations between measurement outcomes and target observable in a quantum measurement”. *Physical Review A*, **93**(3):032104, 2016.
- [40] Taiki Nii, Masataka Inuma, and Holger F. Hofmann. “On the relation between measurement outcomes and physical properties”. *arXiv preprint arXiv:1603.06291*, 2016.

公表論文 (Articles)

- (1) Violation of Leggett-Garg inequalities in quantum measurements with variable resolution and back-action
Yutaro Suzuki, Masataka Iinuma, Holger F. Hofmann
New Journal of Physics **14** 103022 16pp. (2012).

Violation of Leggett–Garg inequalities in quantum measurements with variable resolution and back-action

Yutaro Suzuki^{1,3}, Masataka Inuma¹ and Holger F Hofmann^{1,2}

¹ Graduate School of Advanced Sciences of Matter, Hiroshima University,
1-3-1 Kagamiyama, Higashi-Hiroshima 739-8530, Japan

² JST, Crest, Sanbancho 5, Chiyoda-ku, Tokyo 102-0075, Japan

E-mail: yutaro-s@huhep.org

New Journal of Physics **14** (2012) 103022 (16pp)

Received 28 June 2012

Published 16 October 2012

Online at <http://www.njp.org/>

doi:10.1088/1367-2630/14/10/103022

Abstract. Quantum mechanics violates Leggett–Garg inequalities because the operator formalism predicts correlations between different spin components that would correspond to negative joint probabilities for the outcomes of joint measurements. However, the uncertainty principle ensures that such joint measurements cannot be implemented without errors. In a sequential measurement of the spin components, the resolution and back-action errors of the intermediate measurement can be described by random spin flips acting on an intrinsic joint probability. If the error rates are known, the intrinsic joint probability can be reconstructed from the noisy statistics of the actual measurement outcomes. In this paper, we use the spin-flip model of measurement errors to analyze experimental data on photon polarization obtained with an interferometric setup that allows us to vary the measurement strength and hence the balance between resolution and back-action errors. We confirm that the intrinsic joint probability obtained from the experimental data is independent of measurement strength, and show that the same violation of the Leggett–Garg inequality can be obtained for any combination of measurement resolution and back-action.

³ Author to whom any correspondence should be addressed.



Content from this work may be used under the terms of the [Creative Commons Attribution-NonCommercial-ShareAlike 3.0 licence](https://creativecommons.org/licenses/by-nc-sa/3.0/). Any further distribution of this work must maintain attribution to the author(s) and the title of the work, journal citation and DOI.

Contents

1. Introduction	2
2. Leggett–Garg inequalities for sequential measurements	3
3. Spin-flip model for measurement resolution and back-action	5
4. Experimental realization of a sequential photon polarization measurement	7
5. Experimental values of resolution and back-action	9
6. Joint probabilities for an input polarization halfway between V and P polarization	10
7. Effects of resolution and back-action	13
8. Conclusion	14
Acknowledgments	15
References	15

1. Introduction

In quantum mechanics, it is not possible to make a joint measurement of two non-commuting observables. In a sequential measurement, the initial measurement interaction must therefore cause an unavoidable back-action on the system, so that the result of the final measurement cannot be identified with the value that the corresponding observable had before the initial measurement was made. Nevertheless, Leggett and Garg argued that the fundamental quantum statistics observed in separate measurements might still be interpreted in terms of a single joint probability distribution in order to establish a realist interpretation of quantum mechanics. They then showed that such joint statistics should satisfy the Leggett–Garg inequality (LGI) and pointed out that the predictions of quantum theory appear to violate this limit [1].

Recently, several experimental tests of LGIs were implemented, all of which confirm the predicted violation in accordance with the fundamental laws of quantum mechanics [2–9]. Most of these experiments were weak measurements, where the effects of the measurement back-action in the sequential measurement were minimized and the joint statistics were reconstructed using the weak values of the intermediate measurements [10]. Although this approach can also be used at non-negligible back-action, doing so reduces the observed violation of LGIs [6]. Alternatively, it is possible to reconstruct the correlations between observables by using an appropriate set of parallel measurements [2]. Conceptually, this reconstruction of undisturbed pre-measurement statistics is similar to the approach recently used to evaluate measurement back-action and resolution in the context of Ozawa’s uncertainty limits [11], where the implicit assumption is that the operator formalism provides a correct description of the statistical relations between measurements that cannot be carried out at the same time. Importantly, the results obtained from the operator statistics are fully consistent with the results obtained in weak measurements [12], suggesting that the strange statistics observed in weak measurements is a fundamental feature of quantum mechanics.

Since the violation of LGIs appears to be a direct consequence of the operator formalism, it is reasonable to expect that it should not depend on the measurement strategy used to verify it. In particular, the negative joint probabilities observed in weak measurements should be an intrinsic statistical property of the initial quantum state [13–17], and not just an artifact of the measurement that disappears as the interaction strength is increased, as suggested by the analysis

of weak values at finite measurement strength [6]. In the following, we therefore analyze the roles of measurement resolution and back-action in a variable strength measurement and show that the same intrinsic joint probability of two orthogonal spin components can be derived from the statistics of sequential measurements at any measurement strength.

The experiment was realized using our recently introduced interferometric setup for variable strength measurements of photon polarization [18]. The input state defined an initial polarization represented by the spin direction s_1 , the variable strength measurement partially resolved the diagonal polarizations, corresponding to a spin direction s_2 , and the final measurement distinguished the horizontal and vertical polarizations, corresponding to a spin direction s_3 . The joint probabilities of s_2 and s_3 include resolution errors in the results for s_2 and back-action errors in the results for s_3 . Since there are only two possible measurement outcomes for each measurement, the measurement errors can be described in terms of spin-flip probabilities, defined as the probability of obtaining a spin value opposite to the initial value. We determined the spin-flip probabilities of our experiments from the output statistics of s_2 and s_3 for known inputs and used the result to reconstruct the intrinsic joint probabilities of the quantum state polarized along s_1 . Although the experimentally observed joint probabilities of the measurement outcomes depend strongly on measurement strength, the results for the reconstructed joint probabilities are independent of measurement strength and reproduce the joint probabilities theoretically predicted from the operator statistics of the input state. In particular, the LGI violation is represented by a single negative probability consistently obtained for the outcome with experimental probabilities close to zero. We thus verify the predicted LGI violation at all measurement strengths, and show how measurement resolution and back-action combine to convert the negative joint probabilities associated with the LGI violation into experimentally observable positive probabilities.

The rest of the paper is organized as follows. In section 2, we discuss the relation between LGIs and joint probability distributions in sequential measurements. In section 3, we show how the effects of resolution and back-action modify an intrinsic probability distribution if the errors are represented by random spin flips. In section 4, we describe the experimental setup. In section 5, we characterize our realization of a sequential quantum measurement in terms of the experimental values of measurement resolution and back-action at various measurement strengths. In section 6, the intrinsic joint probabilities are reconstructed and the LGI violation is confirmed. In section 7, the effects of resolution and back-action are analyzed separately and the relation between quantum state statistics and measurement statistics is considered. Section 8 summarizes the results and concludes the paper.

2. Leggett–Garg inequalities for sequential measurements

LGIs essentially impose a limit on the possible correlations between the spin components of a two-level system observed at different measurement times, based on the assumption that the measurement outcome of each measurement should not depend on whether the previous measurements were made or not. In the following, we consider a sequential measurement of the spin components as shown schematically in figure 1. In the quantum formalism, the initial state and the two measurement results are represented by Hilbert space vectors. However, the actual measurement results associated with each state vector are represented by outcomes of $s_i = \pm 1$

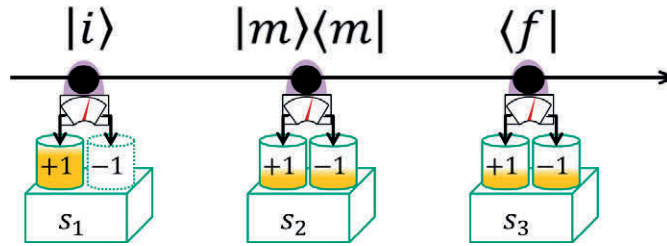


Figure 1. Schematic view of a sequential measurement on a single two-level system. The initial state is represented by a ket-vector, the intermediate measurement is represented by a projector and the final measurement is represented by a bra-vector. Below the arrow indicating the measurement sequence, the same measurement outcomes are described in terms of the actual measurement results obtained for the corresponding spin directions.

for the respective spin component. Hence, state preparation can be identified with a spin value of $s_1 = +1$ for the initial spin orientation s_1 , and the intermediate and final measurements result in spin values of $s_2, s_3 = \pm 1$ for the spin orientations s_2 and s_3 .

In the case of a back-action-free measurement, the outcome of the final measurement of s_3 should not depend on whether the measurement of s_2 was carried out or not. The measurement statistics could then be explained in terms of spin averages observed in the initial state, regardless of the measurement sequence. As Leggett and Garg argued, these spin statistics can then be expressed in terms of intrinsic spin correlations, $K_{ij} = \langle s_i s_j \rangle$. Since these correlations can be determined in separate and independent measurements, it is possible to test whether quantum theory allows a realistic description of back-action-free measurements by formulating limits for the spin correlations that must be valid for any statistical description of the independent spins s_i . In close analogy to Bell's inequalities, one of these statistical limits is given by

$$1 + K_{13} \geq K_{12} + K_{23}. \quad (1)$$

The violation of this LGI can be confirmed by considering the fundamental quantum statistics of spins. In particular, separate measurements can be used to obtain K_{13} , K_{12} and K_{23} [2]. For orthogonal spins, anti-commutation results in $K_{23} = 0$, so a violation of the LGI given by equation (1) can occur if the eigenstate with $s_1 = +1$ has a negative expectation value for s_3 and a positive expectation value for s_2 . Under these conditions, the maximal violation is obtained when $\langle s_2 \rangle = 1/\sqrt{2}$ and $\langle s_3 \rangle = -1/\sqrt{2}$, where the left side of the LGI is $1 - 1/\sqrt{2}$, which is 0.414 smaller than the right side value of $1/\sqrt{2}$.

The reason why the spin correlations can violate the LGI is that they are actually obtained in separate measurements. Realism and non-invasive measurability would require that the same correlations could be observed directly by carrying out the non-invasive measurement of s_2 and the measurement of s_3 in sequence. The statistics of the measurement outcomes of a precise back-action-free measurement of s_2 followed by a measurement of s_3 would then be described by the intrinsic joint probability $P_\psi(s_2, s_3)$ of the spin directions s_2 and s_3 in the initial eigenstate

of s_1 . Specifically, the joint probabilities associated with the spin correlations K_{ij} are given by

$$\begin{aligned} P_\psi(+1, +1) &= \frac{1}{4}(1 + K_{13} + K_{12} + K_{23}), \\ P_\psi(-1, +1) &= \frac{1}{4}(1 + K_{13} - K_{12} - K_{23}), \\ P_\psi(+1, -1) &= \frac{1}{4}(1 - K_{13} + K_{12} - K_{23}), \\ P_\psi(-1, -1) &= \frac{1}{4}(1 - K_{13} - K_{12} + K_{23}). \end{aligned} \quad (2)$$

In a realist interpretation of the quantum statistics describing the outcomes of non-invasive sequential measurements, each of these joint probabilities should be positive. This requirement results in the LGIs. Specifically, the LGI given by equation (1) simply describes the requirement that the probability $P_\psi(-1, +1)$ for the measurement outcomes $s_2 = -1$ and $s_3 = +1$ should be positive. Interestingly, fundamental quantum mechanics seems to suggest that these joint probabilities—if they can be defined at all—may be negative.

The violation of LGIs by negative joint probabilities has been confirmed in a number of experiments based on weak measurements [3–9]. In weak measurements, a low-resolution measurement with negligible back-action is used to determine the average value of an observable equally defined by the initial state and a final measurement outcome. If such weak values are obtained for projection operators $|m\rangle\langle m|$, they provide a definition of joint probabilities for the intermediate measurement outcome m and the final measurement outcome f . Significantly, the predictions of weak measurements correspond to the correlations K_{ij} obtained in separate measurements of s_2 and s_3 . This correspondence of the weak measurement results with the results obtained from separate measurements of spin correlations and with fundamental predictions of quantum theory suggests that the non-positive joint probabilities observed in weak measurements are an intrinsic feature of the initial quantum state, and do not depend on the circumstances of the measurement by which they are obtained.

In previous works, it has been pointed out that a direct observation of LGI violations in actual measurement sequences is generally prevented by the limited measurement resolution associated with measurement uncertainties [19–22]. In the weak measurement limit, the LGI violation is obtained by reconstructing the intrinsic statistics of the quantum state from the noisy detection signal [22]. Here, we apply a corresponding procedure to the case of non-vanishing measurement back-action by reconstructing an intrinsic joint probability based on a simple statistical model. Specifically, we assume that the measurement results originate from the actual values of the spins s_2 and s_3 in the initial state, with random errors caused by finite resolution and back-action. We can then explain the correlations observed in the experimental data in terms of an intrinsic joint probability $P_\psi(s_2, s_3)$ that characterizes the fundamental spin correlations of the input state before the measurement errors took effect. The fact that we can obtain the same values of $P_\psi(s_2, s_3)$ at different measurement strengths confirms the assumption that the correlations between s_2 and s_3 are an intrinsic property of the quantum state and are not just an artifact of the measurement procedure. At the same time, the consistent observation of a negative joint probability indicates the failure of the realist model and highlights the paradoxical nature of quantum statistics.

3. Spin-flip model for measurement resolution and back-action

In general, the final measurement outcome in a series of measurements is affected by the measurement back-action of the intermediate measurement. Therefore, the joint probabilities

$P_{\text{exp}}(s_2, s_3)$ that are directly obtained in a sequential measurement of s_2 and s_3 are different from the intrinsic joint probabilities $P_{\psi}(s_2, s_3)$ of the initial quantum state. Specifically, the experimental probabilities will depend not only on the initial quantum state, but also on the errors introduced by a finite measurement resolution and the disturbance of the state by the measurement back-action. In the following, we will evaluate the effects of these measurement uncertainties and show how the experimentally observed probabilities $P_{\text{exp}}(s_2, s_3)$ relate to the intrinsic joint probabilities $P_{\psi}(s_2, s_3)$ that characterize the initial quantum state.

The measurement resolution describes how well the two possible values of s_2 can be distinguished in the measurement. In the present case, we consider a measurement with two possible outcomes. Therefore, the measurement value is either equal or opposite to the correct value, and the resolution is given by the difference between the measurement and a random guess. We can model this by assuming that sometimes the measurement result accidentally flips. If the spin-flip probability is $1/2$, the measurement outcome is completely random and the measurement resolution ε is zero. As the spin-flip probability decreases, the measurement resolution increases. For a linear relation between measurement resolution ε and spin-flip probability, the probability of a spin-flip error is given by $(1 - \varepsilon)/2$. Since the spin flips mix the outcomes of $s_2 = +1$ and -1 , the average value of s_2 observed in the measurement is reduced in proportion to the measurement resolution ε . In general, the measurement resolution ε can then be defined as the ratio of the average measurement value determined from the experimental probability distribution $P_{\text{exp}}(s_2, s_3)$ and the expectation value $\langle \hat{S}_2 \rangle_{\text{input}}$ of the original input state,

$$\varepsilon = \frac{\sum_{s_2, s_3} s_2 P_{\text{exp}}(s_2, s_3)}{\langle \hat{S}_2 \rangle_{\text{input}}}, \quad (3)$$

where the same value of ε should be obtained for all possible input states and their corresponding measurement probabilities $P_{\text{exp}}(s_2, s_3)$. Experimentally, this value can be determined directly from the difference between the probabilities for $s_2 = +1$ and -1 for an input state with an eigenvalue of $s_2 = +1$.

One advantage of the spin-flip model is that it applies the same logic to measurement errors and to the back-action. Specifically, the back-action on s_3 caused by a measurement of s_2 is described by the probability of a spin flip in s_3 . Since a spin-flip probability of $1/2$ corresponds to complete randomization, we define this limit as a back-action of $\eta = 1$, so that the spin-flip probability associated with a back-action of η is equal to $\eta/2$. The measurement back-action η can then be defined as the relative reduction in the expectation value of s_3 after the measurement of s_2 . In terms of the joint probability $P_{\text{exp}}(s_2, s_3)$,

$$\eta = 1 - \frac{\sum_{s_2, s_3} s_3 P_{\text{exp}}(s_2, s_3)}{\langle \hat{S}_3 \rangle_{\text{input}}}. \quad (4)$$

Experimentally, this value can be directly obtained from the difference between the probabilities for $s_3 = +1$ and -1 for an input state with an eigenvalue of $s_3 = +1$.

It should be noted that neither the spin-flip model nor the definition of resolution and back-action requires any concepts from quantum theory. The only requirement is that reliable reference measurements for s_2 and s_3 can be carried out to obtain the correct expectation values for a specific input. In optics, such precise measurements of polarization can be realized by using polarization filters, and the experimentally confirmed resolution of these measurements is

close enough to 100% to neglect the effects of technical imperfections. The resolution ε and the back-action η are therefore empirically defined properties of our measurement setup.

From a classical viewpoint, all combinations of values would be permitted, and our model does not impose any restrictions on the measurement uncertainties. However, the uncertainty principle requires that sequential measurements of non-commuting spin components cannot achieve a resolution of $\varepsilon = 1$ at zero back-action. For orthogonal spin components, the quantitative limit can be expressed in terms of the uncertainty relation [18, 23]

$$\varepsilon^2 + (1 - \eta)^2 \leq 1. \quad (5)$$

It is therefore impossible to construct a setup that can measure the intrinsic joint probabilities $P_\psi(s_2, s_3)$ directly. However, the spin-flip model allows us to reconstruct this joint probability from the experimentally observed distribution of sequential outcomes, $P_{\text{exp}}(s_2, s_3)$. Due to the spin-flip errors, each measurement outcome (s_2, s_3) can also originate from different spin values, with probabilities determined by the spin-flip probabilities of $(1 - \varepsilon)/2$ and $\eta/2$. The relation between the experimental probabilities and the intrinsic probabilities is then given by

$$\begin{aligned} P_{\text{exp}}(s_2, s_3) = & \left(\frac{1 + \varepsilon}{2}\right) \left(1 - \frac{\eta}{2}\right) P_\psi(s_2, s_3) + \left(\frac{1 - \varepsilon}{2}\right) \left(1 - \frac{\eta}{2}\right) P_\psi(-s_2, s_3) \\ & + \left(\frac{1 + \varepsilon}{2}\right) \left(\frac{\eta}{2}\right) P_\psi(s_2, -s_3) + \left(\frac{1 - \varepsilon}{2}\right) \left(\frac{\eta}{2}\right) P_\psi(-s_2, -s_3). \end{aligned} \quad (6)$$

This linear map can be inverted to reconstruct the intrinsic joint probabilities $P_\psi(s_2, s_3)$ from the experimentally observed joint probabilities $P_{\text{exp}}(s_2, s_3)$. If the measurement resolution and the back-action are known, the same joint probabilities $P_\psi(s_2, s_3)$ should be obtained at any measurement strength. The relations that describe the reconstruction of intrinsic joint probabilities from the measurement data are given by

$$\begin{aligned} P_\psi(s_2, s_3) = & \frac{(1 + \varepsilon)(2 - \eta)}{4\varepsilon(1 - \eta)} P_{\text{exp}}(s_2, s_3) - \frac{(1 - \varepsilon)(2 - \eta)}{4\varepsilon(1 - \eta)} P_{\text{exp}}(-s_2, s_3) \\ & - \frac{(1 + \varepsilon)\eta}{4\varepsilon(1 - \eta)} P_{\text{exp}}(s_2, -s_3) + \frac{(1 - \varepsilon)\eta}{4\varepsilon(1 - \eta)} P_{\text{exp}}(-s_2, -s_3). \end{aligned} \quad (7)$$

Note that the spin-flip model used to reconstruct the intrinsic joint probabilities of the quantum state does not require any assumptions from quantum theory and is based entirely on the experimentally observable spin-flip rates $(1 - \varepsilon)/2$ and $\eta/2$. Its essential assumptions are that the measurement results for s_2 and s_3 originate from the physical properties s_2 and s_3 of the input system, and that the errors in the two measurements are independent and random.

4. Experimental realization of a sequential photon polarization measurement

To investigate the role of measurement resolution and back-action experimentally, we use an interferometric measurement of photon polarization, where the diagonal polarizations can be measured by path interference between the horizontal (H) and vertical (V) polarization components [18]. Specifically, one output port of the interferometer corresponds to the positive superposition of H and V (P polarization) and the other port corresponds to the negative superposition (M polarization). The strength of the measurement is controlled by the measurement back-action that rotates the H and V polarizations towards each other, so that the polarizations in the path are not orthogonal anymore and can interfere with each other.

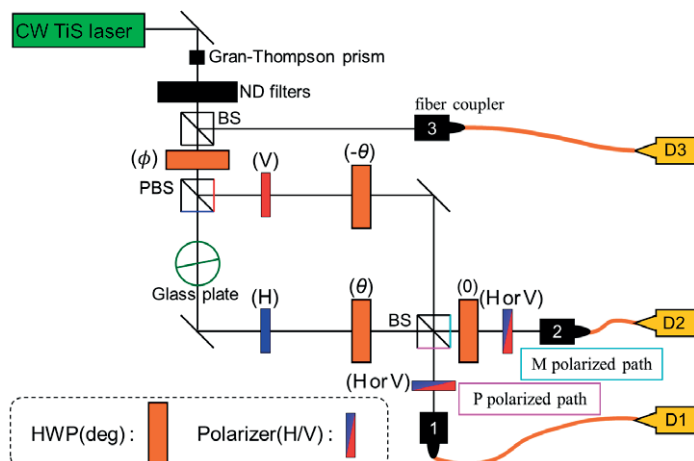


Figure 2. Experimental setup for the sequential measurement of PM and HV polarization. The measurement strength of the interferometric PM measurement is controlled by the rotation angles θ of the HWPs. HV polarization is detected by using polarization filters in the output.

The experimental setup is shown in figure 2. The photon path is initially split into H- and V-polarized paths by a polarizing beam splitter (PBS). Next, the polarization in each path is rotated in opposite directions by half-wave plates (HWPs). Finally, the two polarization components interfere at a beam splitter (BS). Input photons were prepared by a CW titanium-sapphire laser (wavelength 828.7 nm, output power 600 mW) and passed through a Glan–Thompson prism to ensure that the photons were H polarized. Neutral density filters were used to reduce the intensity to a few-photon level for the single photon counting modules (SPCM-AQR-14) used in output detection. Typical count rates were around 1 MHz. To monitor the intensity fluctuation of the input photons, the input beam was divided by a BS upstream of the interferometer and the number of photons was counted with a counting module coupled to the path by using a multi-mode optical fiber and a fiber coupler. A glass plate in one of the paths was used to compensate for phase differences between the two paths of the interferometer.

The initial linear polarization state $|i\rangle$ was prepared by rotating an HWP upstream of the PBS at the input port of the interferometer. The measurement strength was controlled by the rotation angle θ of the HWPs inside the interferometer, which was varied between 0° and 22.5° to cover the complete range from weak measurements to maximally resolved projective measurements. The rotation of the polarizations in the two paths causes the polarization states to overlap, resulting in interference at the output BS. Ideally, the interference between H and V then increases or decreases the probabilities of finding the photon in detector 1 or 2 depending on whether the photon is P or M polarized. However, we found that even a slight imbalance in the ratio between transmittivity and reflectivity of the BS can result in a significant systematic error. To compensate for this effect, we obtained half of the data by rotating the HWPs in the positive direction, and half by rotating them in the opposite direction, effectively exchanging the P-polarized output path and the M-polarized output path with each other. By taking the average of both settings, the unwanted sensitivity of the P- and M-polarized output paths to the HV polarization of the input cancels out and the remaining difference in the count rates of the two detectors corresponds to the PM polarization of the state.

In the final stage of the measurement, we inserted polarizers into the output paths to select only the H- or V-polarized components for the final measurement. Depending on polarizer settings and the rotation direction of the HWPs, the count rates obtained in the two detectors can then be identified with the joint measurement outcomes of (P, H) and (P, V) in one of the detectors, and (M, H) or (M, V) in the other detector.

A detailed description of our measurement in terms of appropriate measurement operators is given in our previous work [18]. Here, it is sufficient to note that the theoretical prediction for the measurement resolution is $\varepsilon = \sin(4\theta)$ and the corresponding value for the measurement back-action is $\eta = 1 - \cos(4\theta)$, where θ is the rotation angle of the HWPs. Note that these values achieve the uncertainty limit given by equation (5) at all rotation angles. In the actual experiment, the measurement resolution is further limited by the visibility of the path interference, resulting in a slight increase of measurement uncertainties. Importantly, the following analysis depends neither on the quantum theory of the measurement nor on an achievement of the uncertainty bound. Instead, all the necessary information can be obtained from the joint probabilities of PM and HV obtained from the count rates of the detectors 1 and 2, with H or V polarization filters inserted.

5. Experimental values of resolution and back-action

Our experimental setup makes a sequential measurement of PM and HV polarization, resulting in two separate outcomes for the non-commuting observables $\hat{S}_2 = \hat{S}_{\text{PM}}$ and $\hat{S}_3 = \hat{S}_{\text{HV}}$. As explained in section 3, such a sequential measurement is characterized by a resolution ε and a back-action η , defined in terms of the measurement errors for PM and HV polarization, respectively. To determine the experimental values of resolution and back-action at different measurement strengths, we made separate measurements to determine the rate of errors in the PM measurement and the rate of errors in the HV measurement. Specifically, the measurement resolution ε is equal to the difference between the probabilities for the measurement outcomes of P and M for an input polarization of P, and the back-action η is equal to the difference between the probabilities of H and V for an input polarization of H. The results of our measurements at different HWP angles θ are shown in figure 3.

As mentioned in section 4, the theoretical expectations for the dependence of resolution ε and back-action η on the measurement strength θ are given by $\varepsilon = \sin(4\theta)$ and $1 - \eta = \cos(4\theta)$. The measurement results show very good qualitative agreement with this θ -dependence, but the resolution is consistently lower than the theoretical value by a constant factor of about 0.85. This reduction in the measurement resolution can be explained by the finite visibility of the interference at the output BS. The actual resolution can be given by $\varepsilon = V_{\text{PM}}\sin(4\theta)$, with an experimentally obtained visibility $V_{\text{PM}} = 0.853 \pm 0.010$. The dependence of back-action η on the HWP angle θ is very close to the theoretically expected relation. However, small decoherence effects can also be modeled by a visibility V_{HV} , so that $\eta = 1 - V_{\text{HV}}\cos(4\theta)$. An optimal fit to the experimental data is obtained with $V_{\text{HV}} = 0.9997 \pm 0.0001$, confirming that the back-action is dominated by the rotation of polarization due to the HWPs in the H- and V-polarized paths of the interferometer.

In the absence of experimental imperfections, the relation between resolution and back-action would satisfy the uncertainty limit given by equation (5). In our actual setup, the relation

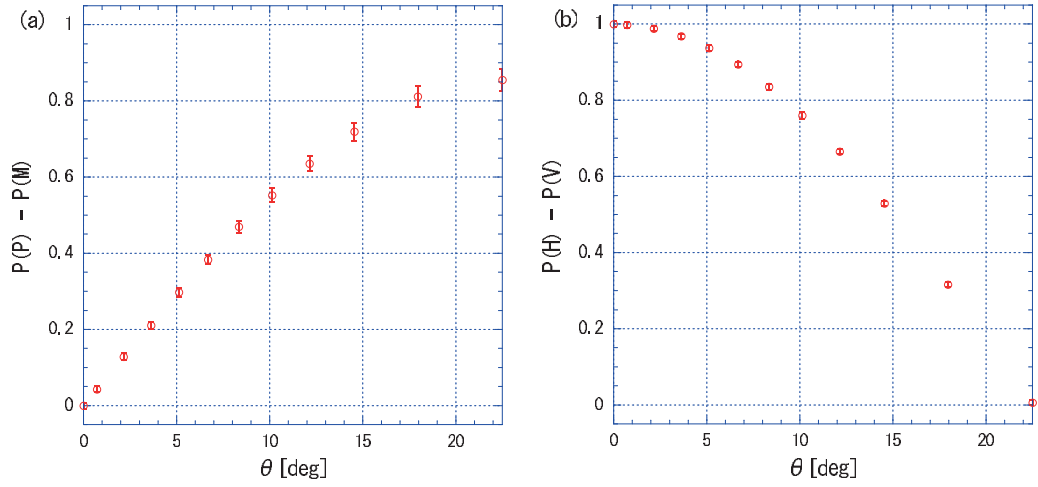


Figure 3. Experimental characterization of measurement resolution and back-action. (a) The difference $P(P) - P(M)$ between the probabilities of the measurement outcomes P and M for a P-polarized input state is shown. This difference is equal to the measurement resolution ε of the PM measurement. (b) The difference $P(H) - P(V)$ between the probabilities of the measurement outcomes H and V for an H-polarized input state is shown. Since this difference is reduced by the back-action η , its value is equal to $1 - \eta$.

is modified by the visibilities and now reads

$$\frac{\varepsilon^2}{V_{PM}^2} + \frac{(1 - \eta)^2}{V_{HV}^2} = 1. \quad (8)$$

This relation is shown in figure 4. Note the very good agreement between the theoretical prediction of equation (8) and the experimental results at different measurement strengths. The experimental results obtained from P- and H-polarized inputs therefore allow us to determine the resolution ε and the back-action η of our experimental setup at all available measurement strengths.

6. Joint probabilities for an input polarization halfway between V and P polarization

To obtain the LGI violation, we need to use an input polarization s_1 that does not commute with the polarizations of s_2 and s_3 . We therefore chose an input polarization halfway between V and P polarization, with a polarization angle of $\phi = 22.496^\circ$ from the vertical direction. We then performed the sequential measurements of PM and HV polarization at various HWP rotation angles θ and obtained the joint probabilities $P_{\text{exp}}(s_2, s_3)$ from the count rates observed in the output. Figure 5 shows the experimental results as a function of HWP angle θ .

Since the input state has expectation values of $\langle \hat{S}_{PM} \rangle = 1/\sqrt{2}$ and $\langle \hat{S}_{HV} \rangle = -1/\sqrt{2}$, the highest probabilities are obtained for $P_{\text{exp}}(+1, -1)$ and the lowest probabilities are obtained for $P_{\text{exp}}(-1, +1)$. In the limit of weak measurements, the final result is most reliable, so $P_{\text{exp}}(-1, -1)$ is larger than $P_{\text{exp}}(+1, +1)$. In the opposite limit, the high resolution of the intermediate measurement ensures that the initial result is most reliable, while the back-action randomizes the final result. Therefore, $P_{\text{exp}}(+1, +1)$ becomes larger than $P_{\text{exp}}(-1, -1)$.

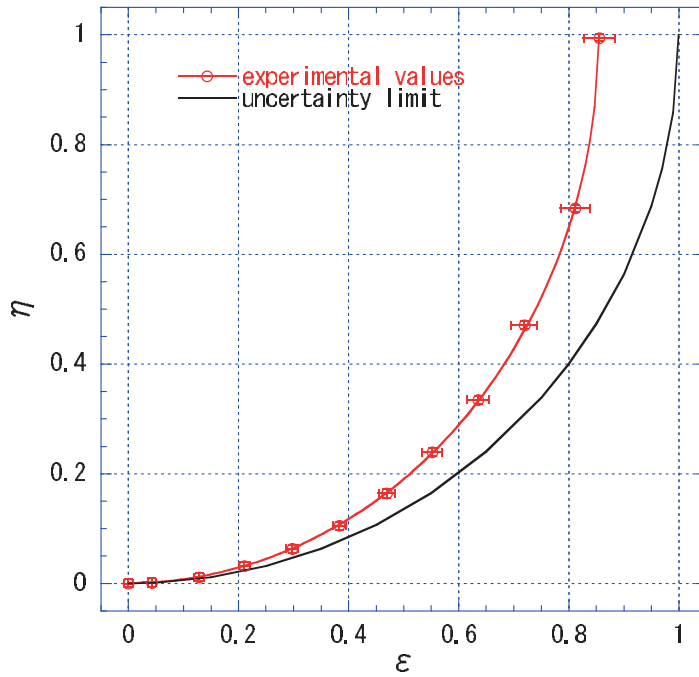


Figure 4. Measurement resolution ε and back-action η at different HWP angles. The red line shows the theoretical curve expected for visibilities of $V_{\text{PM}} = 0.853$ and $V_{\text{HV}} = 0.9997$. The black line shows the uncertainty limit that would be achieved with visibilities of 1.

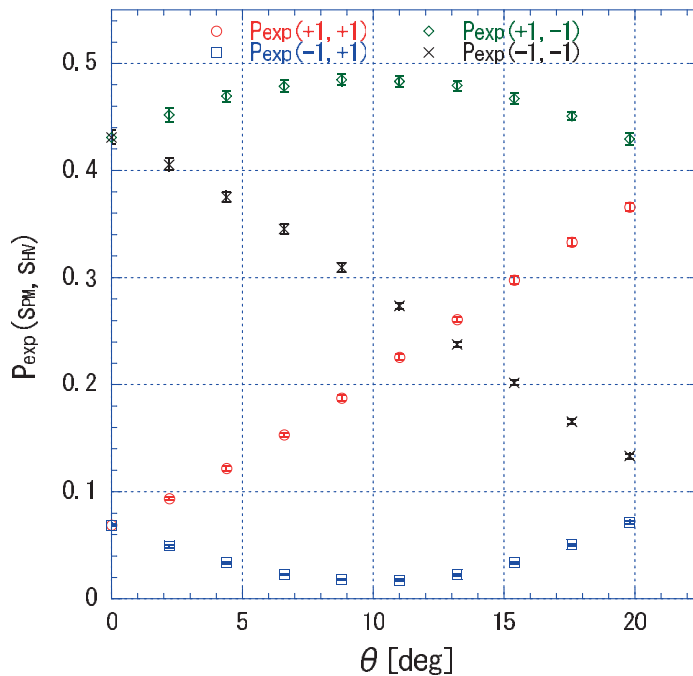


Figure 5. Experimental joint probabilities for an input polarization halfway between V and P polarization obtained at different measurement strengths θ .

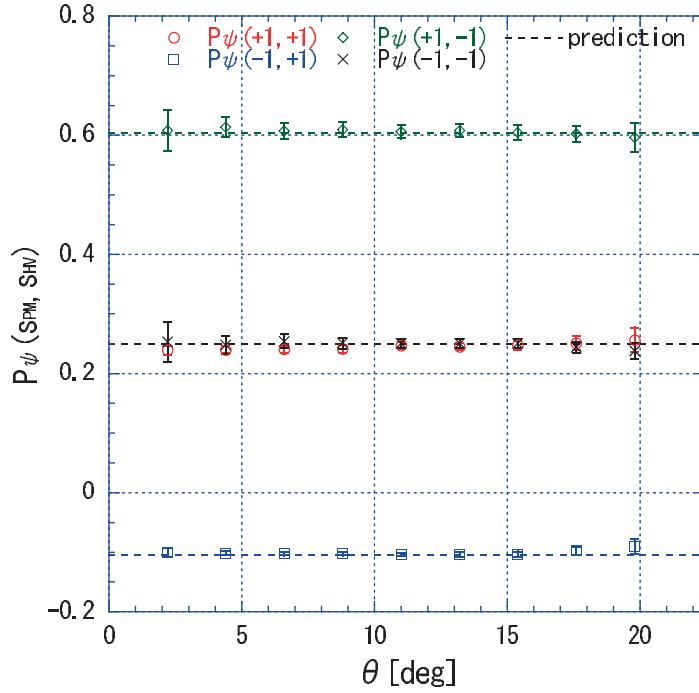


Figure 6. Intrinsic joint probabilities reconstructed using the experimentally determined values of resolution ε and back-action η at the respective measurement strength θ . Dashed lines indicate the values theoretically predicted for the input state.

as measurement strength increases, with a crossover near $\theta = 12.5^\circ$ that marks the point where measurement back-action and measurement resolution result in exactly the same amount of measurement errors.

According to the spin-flip model, the results for $P_{\text{exp}}(s_{\text{PM}}, s_{\text{HV}})$ obtained at different measurement strengths θ originate from the same intrinsic joint probability $P_\psi(s_{\text{PM}}, s_{\text{HV}})$. The differences between the experimental probabilities observed at different measurement strengths are due to the different statistical errors caused by the limited measurement resolution ε and the non-vanishing back-action η . The intrinsic joint probability $P_\psi(s_{\text{PM}}, s_{\text{HV}})$ of the quantum state can be reconstructed from the experimental results in figure 5 by using equation (7), where the values of ε and η are the experimental values for the specific HWP angle θ used in that set of experiments. Figure 6 shows the results of $P_\psi(s_{\text{PM}}, s_{\text{HV}})$ reconstructed at various measurement strengths. As predicted, the same intrinsic probabilities are obtained at all measurement strengths, even though the experimental count rates shown in figure 5 are quite different. Note that the error bars in figure 6 include both statistical errors and the estimated errors of V_{HV} and V_{PM} used in the determination of ε and η . In the weak measurement limit, the statistical errors increase because P and M results are difficult to distinguish as ε goes to zero. In the strong measurement limit, they increase because H and V are difficult to distinguish as η goes to one. Consequently, the statistical errors are minimal in the region around $\theta = 12.5^\circ$, where ε and $1 - \eta$ are nearly equal.

The results shown in figure 6 clearly demonstrate that the intrinsic joint probabilities obtained in the weak measurement limit are also obtained at all other measurement strengths

if both measurement resolution and back-action are taken into account. The results are also consistent with the theoretical values obtained from equation (2) using the correlations between spin directions observed in separate quantum measurements. The negative value of $P_\psi(-1, +1)$ responsible for the LGI violation is therefore not an artifact of a specific measurement procedure, but represents a context-independent property of the fundamental quantum correlations in the input state.

We can conclude that the violation of LGI is a result of the correlations between non-commuting physical properties predicted by fundamental quantum mechanics. These correlations can be characterized in terms of non-positive joint probabilities that can be obtained experimentally from a large variety of different measurement strategies. In each actual measurement, the negative joint probability $P_\psi(-1, +1)$ never results in a negative experimental probability, because the errors in measurement resolution and back-action required by the uncertainty principle guarantee that $P_{\text{exp}}(-1, +1)$ will always remain positive.

7. Effects of resolution and back-action

The results presented in the previous section show how the combined effects of measurement resolution and back-action change the non-positive intrinsic joint probability $P_\psi(s_2, s_3)$ into the positive experimentally observed probability $P_{\text{exp}}(s_2, s_3)$. However, the relative significance of the two error sources depends strongly on measurement strength. In [6], the analysis inspired by the weak measurement limit was applied to measurements of variable strength, resulting in LGI violations that depended on measurement strength, with no violation observed for sufficiently strong measurements. As our detailed analysis shows, this dependence of LGI violations on measurement strength was observed because the effects of measurement back-action were not taken into account in the reconstruction of the intrinsic joint probabilities.

In the weak measurement limit, measurement back-action is negligible and the intrinsic probability can be obtained by compensating only for the errors caused by the limited measurement resolution ε . However, the reconstructed probability $P_\eta(s_2, s_3)$ still includes back-action errors, and deviates from the intrinsic probability $P_\psi(s_2, s_3)$ as the measurement strength increases. Likewise, the measurement resolution is nearly perfect in the strong measurement limit, so it is sufficient to compensate for only the errors caused by the back-action η in order to obtain the intrinsic joint probability. However, the reconstructed probability $P_\varepsilon(s_2, s_3)$ still includes resolution errors, and deviates from the intrinsic probability $P_\psi(s_2, s_3)$ as the measurement strength decreases. To see which errors are responsible for keeping the experimental joint probabilities positive, we can determine $P_\eta(-1, +1)$ or $P_\varepsilon(-1, +1)$ from equation (7) with the correct value of ε and $\eta = 0$ or the correct value of η and $\varepsilon = 1$, respectively. The results are shown in figure 7, together with the experimental probability $P_{\text{exp}}(-1, +1)$ and the intrinsic probability $P_\psi(-1, +1)$.

For weak measurements, all errors originate from the low measurement resolution ε , so $P_\eta(-1, +1)$ is close to the intrinsic probability $P_\psi(-1, +1)$, and $P_\varepsilon(-1, +1)$ is close to the experimental probability $P_{\text{exp}}(-1, +1)$. As the measurement strength increases, the effects of back-action can be observed in the increase of $P_\eta(-1, +1)$ until this probability becomes positive at around $\theta = 16^\circ$. On the other hand, resolution errors decrease and $P_\varepsilon(-1, +1)$ drops until it becomes negative at around $\theta = 7^\circ$. We can therefore conclude that uncompensated back-action errors prevent observation of LGI violations above $\theta = 16^\circ$, and uncompensated resolution errors prevent observation of LGI violations below $\theta = 7^\circ$. In the interval between

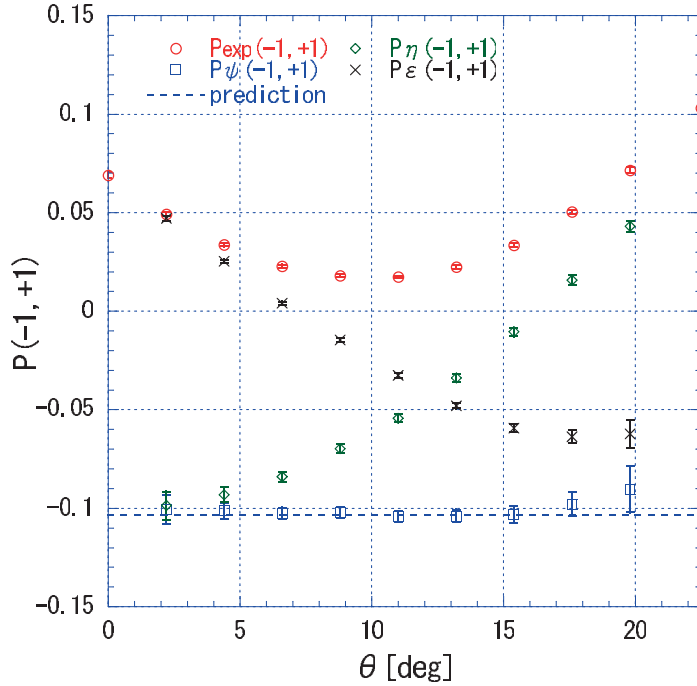


Figure 7. $P_{\varepsilon}(-1, +1)$ and $P_{\eta}(-1, +1)$ as a function of the measurement strength θ together with $P_{\text{exp}}(-1, +1)$ and $P_{\psi}(-1, +1)$. They are obtained by reconstruction with only η or only ε , respectively.

these two measurement strengths, compensating for either one of the two errors results in a negative joint probability, and hence in a violation of LGI.

In our experiment, the limit of a strong measurement with a perfect resolution of $\varepsilon = 1$ cannot be achieved because of the limited visibility V_{PM} . Nevertheless, it is easy to see that $P_{\varepsilon}(-1, +1)$ approaches $P_{\psi}(-1, +1)$, and $P_{\eta}(-1, +1)$ approaches $P_{\text{exp}}(-1, +1)$ in the limit of strong measurements. Thus, the transition from weak measurement to strong measurement merely reverses the roles of measurement resolution and back-action. Ultimately, both should be taken into account when interpreting the measurement outcomes in terms of the initial properties of the quantum system. The dependence of LGI violation on measurement strength reported in [6] is a result of the data analysis used, which failed to account for the effects of back-action. Likewise, a data analysis that compensated for the effects of back-action but neglected the errors associated with a finite measurement resolution would conclude that LGI violations could only be observed in sufficiently strong measurements. In fact, LGI violations are an intrinsic property of fundamental quantum statistics, and their observation simply depends on the proper analysis of the statistical errors in the data.

8. Conclusion

LGI violations originate from fundamental spin correlations that correspond to a negative joint probability for a specific combination of spin values. However, quantum mechanics does not allow error-free joint measurements of non-commuting spin components. In a sequential measurement, the back-action of the intermediate measurement changes the result of the final

measurement at a rate related to the measurement resolution of the intermediate measurement. These measurement errors prevent a direct observation of the paradoxical quantum statistics that violate LGIs. However, a proper analysis of the measurement errors allows a systematic reconstruction of the joint probabilities for non-commuting spin components from which the noisy statistics observed in the experiment originate.

To prove the consistency of our statistical approach to measurement uncertainties, we have carried out a sequential measurement of photon polarization using an intermediate measurement with variable measurement strength. The measurement errors of the setup were evaluated experimentally, and the results were used to obtain the error-free joint probability of the non-commuting polarization components before the intermediate measurement. The experimental results show that this joint probability is independent of the measurement strength, indicating that it is an intrinsic feature of the initial quantum state. The violation of LGI by the negative joint probability $P_{\psi}(-1, +1)$ is therefore a fundamental property of the quantum statistics in the initial state, and not just an artifact of the measurement procedure used to confirm the LGI violation.

The results presented in this paper indicate that a proper understanding of paradoxical quantum statistics requires a more thorough investigation of the statistical effects that characterize the physics of quantum measurements. It is important to remember that measurement errors are needed to ensure that the negative joint probability $P_{\psi}(-1, +1)$ can never be observed directly. The uncertainty principle is therefore necessary to avoid the unresolvable contradictions that would arise if negative probabilities were associated with actual measurement outcomes. On the other hand, it may be equally important to recognize that negative joint probabilities provide a consistent description of measurement statistics once uncertainty errors are included in the description of the actual experiments. The present analysis thus shows how close quantum mechanics is to classical statistics once the specific relations between experimentally observed results and the intrinsic statistics of the quantum state are taken into account.

Acknowledgments

We thank A J Leggett for helpful remarks. This work was supported by JSPS through KAKENHI grant numbers 24540428, 24540427 and 21540409.

References

- [1] Leggett A J and Garg A 1985 *Phys. Rev. Lett.* **54** 857–60
- [2] Knee G C *et al* 2012 *Nature Commun.* **3** 606
- [3] Jordan A N, Korotkov A N and Buttiker M 2006 *Phys. Rev. Lett.* **97** 026805
- [4] Williams N S and Jordan A N 2008 *Phys. Rev. Lett.* **100** 026804
- [5] Palacios-Laloy A, Mallet F, Nguyen F, Bertet P, Vion D, Esteve D and Korotkov A N 2010 *Nature Phys.* **6** 442–7
- [6] Goggin M E, Almeida M P, Barbieri M, Lanyon B P, O’Brien J L, White A G and Pryde G J 2011 *Proc. Natl Acad. Sci. USA* **108** 1256–62
- [7] Fedrizzi A, Almeida M P, Broome M A, White A G and Barbieri M 2011 *Phys. Rev. Lett.* **106** 200402
- [8] Dressel J, Broadbent C J, Howell J C and Jordan A N 2011 *Phys. Rev. Lett.* **106** 040402
- [9] Xu J-S, Li C-F, Zou X-B and Guo G-C 2011 *Sci. Rep.* **1** 101

- [10] Aharonov Y, Albert D Z and Vaidman L 1988 *Phys. Rev. Lett.* **60** 1351–4
- [11] Erhart J, Sponar S, Sulyok G, Badurek G, Ozawa M and Hasegawa Y 2012 *Nature Phys.* **8** 185–9
- [12] Lund A P and Wiseman H M 2010 *New J. Phys.* **12** 093011
- [13] Johansen L M 2007 *Phys. Rev. A* **76** 012119
- [14] Lundeen J S, Sutherland B, Patel A, Stewart C and Bamber C 2011 *Nature* **474** 188–91
- [15] Lundeen J S and Bamber C 2012 *Phys. Rev. Lett.* **108** 070402
- [16] Hofmann H F 2012 *New J. Phys.* **14** 043031
- [17] Hofmann H F 2011 *Phys. Rev. Lett.* **109** 020408
- [18] Inuma M, Suzuki Y, Taguchi G, Kadoya Y and Hofmann H F 2011 *New J. Phys.* **13** 033041
- [19] Calarco T, Cini M and Onofrio R 1999 *Europhys. Lett.* **47** 407–13
- [20] Kofler J and Brukner C 2007 *Phys. Rev. Lett.* **99** 180403
- [21] Kofler J and Brukner C 2008 *Phys. Rev. Lett.* **101** 090403
- [22] Bednorz A, Belzig W and Nitzan A 2012 *New J. Phys.* **14** 013009
- [23] Englert E-G 1996 *Phys. Rev. Lett.* **77** 2154–7

参 考 論 文

(Thesis Supplements)

- (1) Experimental evaluation of nonclassical correlations between measurement outcomes and target observable in a quantum measurement
Masataka Inuma, Yutaro Suzuki, Taiki Nii, Ryuji Kinoshita, Holger F. Hofmann
Physical Review A **93** 032104 9pp. (2016).
- (2) Weak measurement of photon polarization by back-action-induced path interference
Masataka Inuma, Yutaro Suzuki, Gen Taguchi, Yutaka Kadoya, Holger F. Hofmann
New Journal of Physics **13** 033041 11pp. (2011).

Experimental evaluation of nonclassical correlations between measurement outcomes and target observable in a quantum measurement

Masataka Iinuma,^{*} Yutaro Suzuki, Taiki Nii, Ryuji Kinoshita, and Holger F. Hofmann*Graduate School of Advanced Sciences of Matter, Hiroshima University 1-3-1 Kagamiyama, Higashi-Hiroshima, 739-8530, Japan*

(Received 15 October 2015; published 2 March 2016)

In general, it is difficult to evaluate measurement errors when the initial and final conditions of the measurement make it impossible to identify the correct value of the target observable. Ozawa proposed a solution based on the operator algebra of observables which has recently been used in experiments investigating the error-disturbance trade-off of quantum measurements. Importantly, this solution makes surprisingly detailed statements about the relations between measurement outcomes and the unknown target observable. In the present paper, we investigate this relation by performing a sequence of two measurements on the polarization of a photon, so that the first measurement commutes with the target observable and the second measurement is sensitive to a complementary observable. While the initial measurement can be evaluated using classical statistics, the second measurement introduces the effects of quantum correlations between the noncommuting physical properties. By varying the resolution of the initial measurement, we can change the relative contribution of the nonclassical correlations and identify their role in the evaluation of the quantum measurement. It is shown that the most striking deviation from classical expectations is obtained at the transition between weak and strong measurements, where the competition between different statistical effects results in measurement values well outside the range of possible eigenvalues.

DOI: [10.1103/PhysRevA.93.032104](https://doi.org/10.1103/PhysRevA.93.032104)

I. INTRODUCTION

Although the uncertainty principle is usually considered to be a fundamental principle of quantum mechanics, its precise theoretical formulation is not always clear. A breakthrough in the investigation of measurement uncertainties was achieved when Ozawa demonstrated in 2003 that the uncertainty trade-off between measurement error and disturbance may be much lower than the uncertainty trade-off between noncommuting properties in a quantum state [1]. Recently, the definitions of measurement uncertainties introduced by Ozawa have been evaluated experimentally using two-level systems such as neutron spins [2] and photon polarizations [3,4]. These experimental tests have confirmed the lower uncertainty limits predicted by Ozawa and resulted in the formulation and confirmation of even tighter bounds [5–8]. However, there has also been some controversy concerning the role of the initial state in this definition of measurement uncertainties [9–11]. It may therefore be useful to take a closer look at the definition of measurement errors and their experimental evaluation.

In principle, it is natural to define the error of a measurement as the statistical average of the squared difference between the measurement outcome and the actual value of the target observable. However, quantum theory makes it difficult to assign a value to an observable when neither the initial state nor the final measurement is represented by an eigenstate of the observable. Nevertheless, the operator formalism defines correlations between the measurement outcome and the operator \hat{A} that represents the target observable, and this correlation between operators can be evaluated by weak measurements [12] or by statistical reconstruction using variations of the input state [13]. Essentially, the experimental evaluations of Ozawa uncertainties is therefore based on an evaluation of

nonclassical correlations between the measurement outcome and the target observable in the initial quantum state $|\psi\rangle$.

In the following, we investigate the role of nonclassical correlations in quantum measurements by applying a sequential measurement to the polarization of a single photon, such that the initial measurement commutes with the target polarization, while the final measurement selects a complementary polarization. In this scenario, the initial measurement can be described by classical error statistics, and the evaluation of the measurement errors corresponds to conventional statistical methods. However, the final measurement introduces nonclassical correlations that provide additional information on the target observable. By varying the strength of the initial measurement, we can control the balance between classical and nonclassical effects in the correlations. In addition, we obtain two separate measurement outcomes, one of which refers directly to the target observable, and another one which can relate only to the target observable via correlations in the input state. Our measurement results thus provide a detailed characterization of nonclassical effects in the relation between measurement outcomes and target observable. In particular, our results show that the initial measurement outcome modifies the nonclassical correlations between the final outcome and the target observable, which can result in a counterintuitive assignment of measurement values, where the initial measurement outcome and the estimates values seem to be anticorrelated. Our results thus illustrate that the combination of classical and nonclassical correlations can be highly nontrivial and should be investigated in detail to achieve a more complete understanding of the experimental analysis of quantum systems.

The rest of the paper is organized as follows. In Sec. II, we point out the role of nonclassical correlations in the definition of measurement errors and discuss the experimental evaluation using variations of the input state. In Sec. III, we derive the evaluation procedure for two-level systems and discuss the evaluation of the experimental data. In Sec. IV, we introduce

^{*}iinuma@hiroshima-u.ac.jp; <http://home.hiroshima-u.ac.jp/qfg/qfg/index.html>

the experimental setup and discuss the sequential measurement of two noncommuting polarization components. In Sec. V, we discuss the measurement results obtained at different measurement strengths and analyze the role of nonclassical correlations in the different measurement regimes. In Sec. VI, we discuss the effects of nonclassical correlations on the statistical error of the measurement. In Sec. VII, we conclude the paper by summarizing the insights gained from our detailed study of the nonclassical aspects of measurement statistics.

II. MEASUREMENT ERRORS AND NONCLASSICAL CORRELATIONS

Measurement errors can be quantified by taking the average of the squared difference between the measurement outcomes $A_{\text{out}}(m)$ and the target observable \hat{A} . As shown by Ozawa [1], this definition of errors can be applied directly to the operator statistics of quantum theory, even if the observable \hat{A} does not commute with the measurement outcomes m . If the probability of the measurement outcome m is represented by the positive valued operator \hat{E}_m , the measurement error for an input state $|\psi\rangle$ is given by

$$\begin{aligned}\varepsilon^2(A) &= \sum_m \langle \psi | (A_m - \hat{A}) \hat{E}_m (A_m - \hat{A}) | \psi \rangle \\ &= \langle \psi | \hat{A}^2 | \psi \rangle + \sum_m A_m^2 \langle \psi | \hat{E}_m | \psi \rangle \\ &\quad - 2 \sum_m A_m \text{Re}[\langle \psi | \hat{E}_m \hat{A} | \psi \rangle].\end{aligned}\quad (1)$$

The last term in Eq. (1) evaluates the correlation between the target observable \hat{A} and the measurement outcome A_m .

If the operator \hat{A} and all of the measurement operators \hat{E}_m commute with each other, the correlation in Eq. (1) can be explained in terms of the joint measurement statistics of the outcomes m and the eigenstate projections a , where the eigenvalues of \hat{E}_m determine the conditional probabilities $P(m|a)$ of obtaining the result m for an eigenstate input of a . However, the situation is not so simple if \hat{A} and \hat{E}_m do not commute. In this case, an experimental evaluation of the measurement error $\varepsilon(A)^2$ requires the reconstruction of a genuine quantum correlation represented by operator products. Perhaps the most direct method of obtaining the appropriate data is to vary the input state [13]. To obtain the correlation between the measurement outcome m and the observable \hat{A} , it is sufficient to use two superposition states as input,

$$\begin{aligned}|+\rangle &= \frac{1}{\sqrt{1 + 2\lambda\langle\hat{A}\rangle + \lambda^2\langle\hat{A}^2\rangle}}(1 + \lambda\hat{A})|\psi\rangle, \\ |-\rangle &= \frac{1}{\sqrt{1 - 2\lambda\langle\hat{A}\rangle + \lambda^2\langle\hat{A}^2\rangle}}(1 - \lambda\hat{A})|\psi\rangle,\end{aligned}\quad (2)$$

where the expectation values in the normalization factors refer to the statistics of the original state $|\psi\rangle$. Note that λ is a completely arbitrary real number, which means that the new input states can be quite different from the original state $|\psi\rangle$. It is now possible to determine the correlation between the measurement outcome and the target observable from the weighted difference between the probabilities $P(m|+)$ and $P(m|-)$ obtained with these two superposition states,

specifically,

$$\begin{aligned}\text{Re}[\langle \psi | \hat{E}_m \hat{A} | \psi \rangle] &= \frac{1}{4\lambda} [(1 + 2\lambda\langle\hat{A}\rangle + \lambda^2\langle\hat{A}^2\rangle)P(m|+) \\ &\quad - (1 - 2\lambda\langle\hat{A}\rangle + \lambda^2\langle\hat{A}^2\rangle)P(m|-)].\end{aligned}\quad (3)$$

For $\lambda \ll 1$, the two states correspond to the outputs of a weak measurement with a two-level probe state [14]. The variation of input states is therefore closely related to the alternative method of evaluating measurement errors using weak measurements [12].

Since the operator \hat{E}_m represents the probability of the outcome m and the operator \hat{A} represents the value of a physical property, it is possible to express the correlation that is evaluated in Eq. (3) as a conditional expectation value of \hat{A} by dividing the expectation value of the product of \hat{E}_m and \hat{A} by the probability of m . As can be seen from Eq. (2), this conditional average is also equal to the value of A_m that minimizes the error $\varepsilon^2(A)$. In terms of the error measure $\varepsilon^2(A)$, the optimal estimate of A_m for an outcome of m is therefore given by

$$A_{\text{opt}}(m) = \frac{\text{Re}[\langle \psi | \hat{E}_m \hat{A} | \psi \rangle]}{\langle \psi | \hat{E}_m | \psi \rangle}.\quad (4)$$

As pointed out by Hall, this optimal estimate is equal to the real part of the weak value conditioned by the post-selection of the measurement outcome m [15]. In the present context, these weak values provide a quantitative description of the nonclassical correlation between a physical property \hat{A} and a measurement outcome m represented by an operator \hat{E}_m that does not commute with \hat{A} .

If the nonclassical correlation in Eq. (1) is expressed using the conditional average in Eq. (4), the result reads

$$\begin{aligned}\varepsilon^2(A) &= \langle \hat{A}^2 \rangle - \sum_m (A_{\text{opt}}(m))^2 P(m|\psi) \\ &\quad + \sum_m [A_m - A_{\text{opt}}(m)]^2 P(m|\psi).\end{aligned}\quad (5)$$

It is then obvious that the minimal error $\varepsilon_{\text{opt}}^2(A)$ is obtained for $A_m = A_{\text{opt}}(m)$ and that this minimal error is given by the difference between the original variance of \hat{A} in the quantum state ψ and the variance of the conditional averages $A_{\text{opt}}(m)$,

$$\varepsilon_{\text{opt}}^2(A) = \langle \hat{A}^2 \rangle - \sum_m [A_{\text{opt}}(m)]^2 P(m|\psi).\quad (6)$$

Importantly, all of the necessary information can be obtained experimentally using the superposition input states $|+\rangle$ and $|-\rangle$. As will be shown in the following, this means that for two-level systems, the nonclassical correlations can actually be derived from measurements performed on eigenstates of \hat{A} .

The most interesting aspect of the measurement errors is their dependence on correlations between noncommuting operators. To explore this dependence in more detail, it is useful to consider a measurement outcome $\mathbf{m} = (m_1, m_2)$ that is composed of two separate measurements performed in sequence. Note that m in the discussion above can always be replaced by such an array of outcomes, since none of the preceding discussion depends on the classification scheme used to distinguish the different outcomes. The only difference

between a single-valued outcome and a multivalued outcome is that we can separate the outcomes and the associated measurement operators. The complete description of the measurement is given by the operators \hat{E}_{m_1, m_2} . However, it is also possible to consider only the initial measurement m_1 , which is represented by the operator sum

$$\hat{E}_{m_1} = \sum_{m_2} \hat{E}_{m_1, m_2}. \quad (7)$$

Since the operators \hat{E}_{m_1, m_2} do not usually commute with each other, the eigenstates of \hat{E}_{m_1} can be completely different from the eigenstates of \hat{E}_{m_1, m_2} . In the following, we consider a sequential measurement, where the initial measurement is sensitive only to the target observable \hat{A} and is therefore represented by operators \hat{E}_{m_1} that commute with \hat{A} . The eigestates of \hat{A} are then eigenstates of \hat{E}_{m_1} , and the eigenvalues of \hat{E}_{m_1} are equal to the conditional probabilities $P(m_1|a)$ of obtaining the outcome m_1 if the input is the eigenstate $|a\rangle$ of \hat{A} . As will be discussed in the following, classical Bayesian statistics apply to this case, and $A_{\text{opt}}(m_1)$ satisfies all of the properties of a classical conditional average. Nevertheless, it would be wrong to interpret this result in terms of classical statistics, since the second measurement m_2 results in noncommutativity. As a result of this noncommutativity between the final measurement and the target observable \hat{A} , the more precise estimates $A_{\text{opt}}(m_1, m_2)$ obtained by individually optimizing the estimates for each joint outcome (m_1, m_2) can result in values that are quite different from the initial estimates $A_{\text{opt}}(m_1)$ and can even lie outside of the eigenvalue spectrum of \hat{A} , distinguishing them from classical conditional averages.

III. EVALUATION OF TWO-LEVEL SYSTEMS

In a two-level system, all physical properties can be expressed in terms of operators with eigenvalues of ± 1 . This results in a significant simplification of the formalism. In particular, it is possible to define the input states $|+\rangle$ and $|-\rangle$ used for the experimental evaluation of nonclassical correlations in the measurement errors by setting $\lambda = 1$ in Eq. (2). They are then defined by a projection onto eigenstates of \hat{A} , so that $|+\rangle$ and $|-\rangle$ are independent of the original input state $|\psi\rangle$. Moreover, it is possible to express the expectation value of \hat{A} in Eq. (3) in terms of the probabilities $P(+|\psi)$ and $P(-|\psi)$ obtained from precise measurements of \hat{A} , since the outcomes $+$ and $-$ correspond to eigenstates of the target observable \hat{A} with eigenvalues of $+1$ and -1 , respectively. Surprisingly, this means that the nonclassical correlations between measurement outcomes and target observables can be evaluated without applying the measurement of m to the actual input state $|\psi\rangle$, since only the measurement results for direct projective measurements of \hat{A} enter into the experimental evaluation of the nonclassical correlation. According to Eq. (3), the relation for the two-level system with eigenvalues of $A_a = \pm 1$ and $\lambda = 1$ is

$$\text{Re}[\langle\psi|\hat{E}_m\hat{A}|\psi\rangle] = P(m|+)P(+|\psi) - P(m|-)P(-|\psi). \quad (8)$$

Note that this looks like a fully projective measurement sequence, where a measurement of \hat{A} is followed by a measurement of m . However, such a projective measurement

of \hat{A} actually changes the probabilities of the final outcomes m . It is therefore quite strange that the correlation between an undetected observable \hat{A} and the measurement result m obtained from an initial state $|\psi\rangle$ can be derived from a sequential projective measurement, as if the measurement disturbance of a projective measurement of \hat{A} had no effect on the final probabilities of m .

The nonclassical features of the correlation in Eq. (8) emerge when the conditional average is determined according to Eq. (4):

$$A_{\text{opt}}(m) = \frac{P(m|+)P(+|\psi) - P(m|-)P(-|\psi)}{P(m|\psi)}. \quad (9)$$

Although this equation looks almost like a classical conditional average, it is important to note that the probabilities are actually obtained from two different measurements. As a result, the denominator is not given by the sum of the probabilities in the numerator. In fact, it is quite possible that $P(m|\psi)$ is much lower than the sum of $P(m|+)P(+|\psi)$ and $P(m|-)P(-|\psi)$, so that the conditional average $A_{\text{opt}}(m)$ is much larger than $+1$ (or much lower than -1). In fact, we should expect such anomalous enhancements of the conditional average, since Eq. (4) shows that $A_{\text{opt}}(m)$ is equal to the weak value of \hat{A} conditioned by ψ and m .

It may seem confusing that the combination of statistical results obtained in two perfectly normal experiments results in the definition of a seemingly paradoxical conditional average. However, this is precisely why quantum statistics have no classical explanation. In fact, the present two-level paradox is simply a reformulation of the violation of Leggett-Garg inequalities [16–18], where it is shown that it is impossible to explain the probabilities $P(m|\psi)$, $P(m|\pm)$, and $P(\pm|\psi)$ as marginal probabilities of the same positive valued joint probability $P(m, \pm|\psi)$. Effectively, the evaluation of measurement errors proposed by Ozawa [13] and applied in the first experimental demonstration [2] is identical to the verification of Leggett-Garg inequality violation by parallel measurements proposed in Ref. [16] and applied in Ref. [17].

We can now look at the evaluation of the measurement errors in more detail. Using the previous results to express Eq. (1) in terms of experimental probabilities, the measurement error is given by

$$\begin{aligned} \varepsilon^2(A) = & 1 + \sum_m A_m^2 P(m|\psi) \\ & - 2 \sum_m A_m [P(m|+)P(+|\psi) - P(m|-)P(-|\psi)]. \end{aligned} \quad (10)$$

Although this is already a great simplification, it is interesting to note that the evaluation used in the first experimental demonstration [2] is even more simple. This is because of an additional assumption: if we allow only an assignment of $A_m = \pm 1$, so that m can be given by $+$ or $-$ and $A_m^2 = 1$:

$$\begin{aligned} \varepsilon^2(A) = & 2 - 2[P(+|+)P(+|\psi) + P(-|-)P(-|\psi) \\ & - P(+|-)P(-|\psi) - P(-|+)P(+|\psi)]. \end{aligned} \quad (11)$$

In many cases, errors are symmetric, so that $P(+|+) = P(-|-) = 1 - P_{\text{error}}$ and $P(+|-) = P(-|+) = P_{\text{error}}$. If this

assumption is used, the evaluation of measurement errors is completely independent of the input state, since the probabilities of $A_+ = +1$ and of $A_- = -1$ add up to one, and the error is simply given by the error observed for eigenstate inputs:

$$\varepsilon^2(A) = 4P_{\text{error}}. \quad (12)$$

Importantly, this result is just a special case where the measurement error appears to be state independent because of a specific choice of A_m for the evaluation of the measurement. In the following, we will consider a setup that explores the optimization of A_m and the role of the nonclassical correlations between measurement outcomes and target observable using the evaluation of experimental data developed above.

As explained in the previous section, all of these results can be applied directly to a sequential measurement, where the specific outcome m is given by an array of two separate outcomes, (m_1, m_2) . However, the assignment of $A_m = \pm 1$ would reduce the number of different results to only two. In the following, we will therefore focus on the more general estimate A_{m_1, m_2} and its optimized values. Specifically, we can use Eq. (9) directly to obtain experimental values for the optimal estimates $A_{\text{opt}}(m_1)$ and $A_{\text{opt}}(m_1, m_2)$ from the same set of data obtained in sequential measurements of m_1 and m_2 .

IV. SEQUENTIAL MEASUREMENT OF PHOTON POLARIZATION

As mentioned in the previous section, the anomalous values of the conditional averages $A_{\text{opt}}(m)$ that also provide the optimal assignments of measurement outcomes A_m originate from the same experimental statistics that are used to violate Leggett-Garg inequalities. We are therefore particularly interested in the correlations between Bloch vector components in the equatorial plane of the Bloch sphere. In the case of photon polarization, these are the linear polarizations, where the horizontal (H) and vertical (V) polarizations define one axis and the diagonal polarizations corresponding to positive (P) and negative (M) superposition of H and V define the orthogonal axis. In terms of operators with eigenvalues of $+1$ and -1 , these polarizations can be expressed by \hat{S}_{HV} and \hat{S}_{PM} .

If our target observable is $\hat{A} = \hat{S}_{PM}$, any measurement that commutes with \hat{S}_{PM} can be explained in terms of classical statistics. We therefore use a setup that implements a variable strength measurement of diagonal polarization similar to the one we previously used to study Leggett-Garg inequality violations and weak measurements [18,19]. In the output, we then perform a measurement of HV polarization, so that the total measurement does not commute with the target observable. By dividing the measurement into two parts, we can vary the strength of the nonclassical effects and study the transition between classical correlations and quantum correlations in detail.

The experimental setup is shown in Fig. 1. As explained in Ref. [19], a variable strength measurement is implemented by separating the horizontal and vertical polarizations at a polarization beam splitter (PBS), rotating the polarizations towards each other using a half-wave plate (HWP) and interfering them at a beam splitter (BS). Essentially, the polarization beam splitter transfers a controllable fraction of the horizontal and

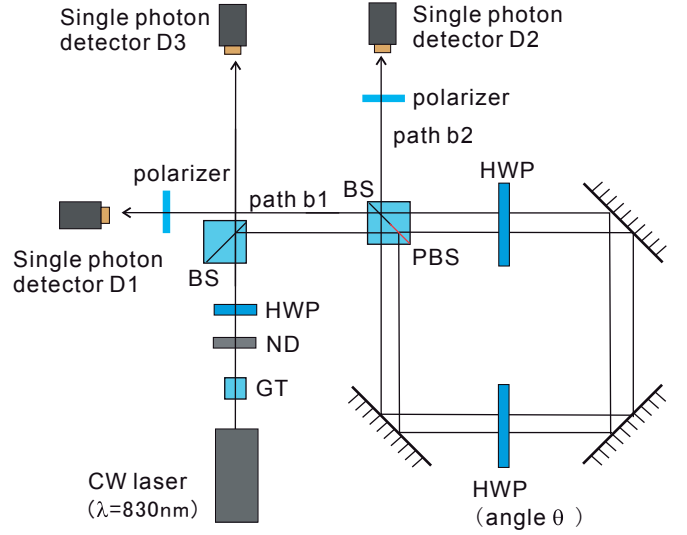


FIG. 1. Experimental setup of the sequential measurement of \hat{S}_{PM} followed by the projective measurement of \hat{S}_{HV} . This interferometer was realized by using a hybrid cube of a polarizing beam splitter (PBS) and a beam splitter (BS), where the input beam is split by the PBS part and the outputs interfere at the BS part of the cube. The variable strength measurement of the positive (P) and negative (M) superposition of horizontal (H) and vertical (V) polarizations is realized by path interference between the H and the V polarized component. The measurement strength of the PM measurement is controlled by the angle θ of the half-wave plate (HWP) inside the interferometer, which can be changed from zero for no measurement to 22.5° for a fully projective measurement.

vertical polarization components to the paths inside a two-path interferometer, so that the output ports of the interferometer can distinguish between the P polarization and M polarization, since the phase difference between the paths originates from the phase differences between the horizontal and the vertical polarization components in the input. The visibility of this interference effect, and hence the strength of the measurement, is controlled by the rotation angle of the HWP, where the angle θ can be changed from zero for no measurement to 22.5° for a fully projective measurement. As shown in Fig. 1, the interferometer is a Sagnac type, where the difference between input and output beam splitter is implemented by using a hybrid cube that acts as either a PBS or a BS, depending on the part of the cube on which the beam is incident. Input states were prepared using another HWP located just before the hybrid cube and a weak coherent light emitted by a CW Ti:S laser ($\lambda = 830$ nm). The output photon numbers in the output paths $b1$ (measurement outcome P or $m_1 = +1$) and in the path $b2$ (measurement outcome M or $m_1 = -1$) are counted by using the single photon detectors D1 and D2, respectively. Polarizers were inserted to realize the final measurement of \hat{S}_{HV} , corresponding to $m_2 = +1$ for H polarization and $m_2 = -1$ for V polarization. The number of input photons in the initial state was monitored with the single photon detector D3 in order to compensate fluctuations of intensity in the weak coherent light used as input. In the actual setup, we also detected a systematic difference between the reflectivity and the transmissivity of the final BS resulting in a slight change of

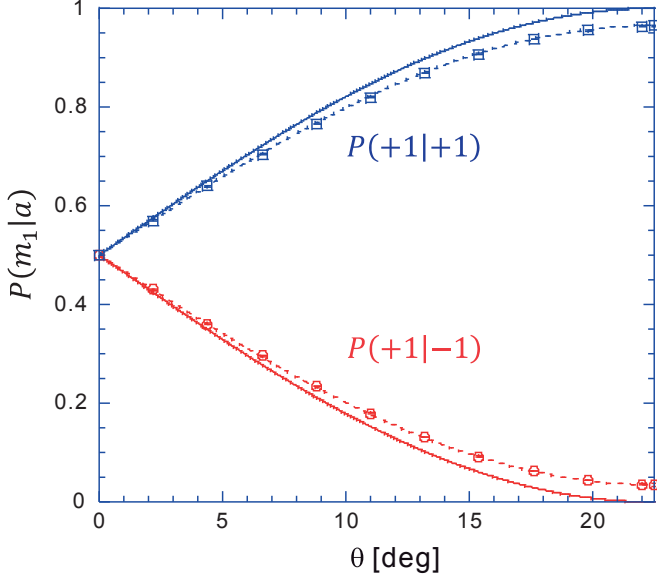


FIG. 2. Experimental probabilities $P(m_1|a)$ of the PM measurement obtained with P polarization ($a = +1$) as the initial state. The solid lines indicate the theoretically expected result for $V_{PM} = 1$ and the broken line shows the theoretical expectation for $V_{PM} = 0.93$.

the orientation of the measurement basis from the directions of PM polarization. The cancellation of this systematic effect is achieved by exchanging the roles of path b1 and path b2 using the settings of the HWP, which effectively restores the proper alignment of the polarization axes with the measurement [18].

The measurement has four outcomes $m = (m_1, m_2)$ given by the combinations of \hat{S}_{PM} eigenvalues ($m_1 = \pm 1$) and \hat{S}_{HV} eigenvalues ($m_2 = \pm 1$). In the absence of experimental errors, the measurement outcomes can be described by pure state projections:

$$\begin{aligned}
 | +1, +1 \rangle &= \frac{1}{\sqrt{2}} [\cos(2\theta)|H\rangle + \sin(2\theta)|V\rangle], \\
 | +1, -1 \rangle &= \frac{1}{\sqrt{2}} [\sin(2\theta)|H\rangle + \cos(2\theta)|V\rangle], \\
 | -1, +1 \rangle &= \frac{1}{\sqrt{2}} [\cos(2\theta)|H\rangle - \sin(2\theta)|V\rangle], \\
 | -1, -1 \rangle &= \frac{1}{\sqrt{2}} [\sin(2\theta)|H\rangle - \cos(2\theta)|V\rangle]. \quad (13)
 \end{aligned}$$

The actual measurement is limited by the visibility of the interferometer, which was independently evaluated as $V_{PM} = 0.93$ at $\theta = 22.5^\circ$. It is possible to characterize the measurement error of the PM measurement by preparing P-polarized and M-polarized input photons. If $A_m = +1$ is assigned to the $m_1 = +1$ outcomes, and $A_m = -1$ is assigned to the $m_1 = -1$ outcomes, this corresponds to a measurement of the error probability P_{error} in Eq. (12):

$$P_{\text{error}} = P(m_1 = -a|a) = \frac{1}{2} [1 - V_{PM} \sin(4\theta)]. \quad (14)$$

Figure 2 shows the experimental results obtained with our setup. Note that this figure also provides all of the data needed to determine the probabilities $P(m_1, m_2|a)$ for the analysis of

the conditional averages $A_{\text{opt}}(m)$ in the following section, since $P(m_1, m_2|a) = P(m_1|a)/2$.

For completeness, we have also evaluated the experimental errors in the final measurement of HV polarization. We obtain a visibility of $V_{HV} = 0.9976$ for the corresponding eigenstate inputs. With this set of data, we can fully characterize the performance of the measurement setup, as shown in the analysis of the following experimental results.

V. EXPERIMENTAL EVALUATION OF NONCLASSICAL CORRELATIONS

To obtain nonclassical correlations between \hat{S}_{PM} and \hat{S}_{HV} , we chose an input state $|\psi\rangle$ with a linear polarization at 67.5° , halfway between the P polarization and the V polarization. For this state, the initial expectation value of the target observable is

$$\langle \hat{S}_{PM} \rangle = \frac{1}{\sqrt{2}}. \quad (15)$$

We can now start the analysis of measurement errors by considering only the outcome m_1 , in which case the measurement operators \hat{E}_m commute with the target observable and the problem could also be analyzed using classical statistics. Specifically, commutativity means that the probability $P(m_1|\psi)$ is unchanged if a projective measurement of \hat{S}_{PM} is performed before the measurement of m_1 . It is therefore possible to determine $P(m_1|\psi)$ from the conditional probabilities $P(m_1|a)$ and $P(a|\psi)$, which results in a classical conditional average for $\hat{A} = \hat{S}_{PM}$ given by

$$\begin{aligned}
 A_{\text{opt}}(m_1) &= \frac{P(m_1|+)P(+|\psi) - P(m_1|-)P(-|\psi)}{P(m_1|+)P(+|\psi) + P(m_1|-)P(-|\psi)} \\
 &= \frac{(1 - 2P_{\text{error}})m_1 + \langle \hat{S}_{PM} \rangle}{m_1 + (1 - 2P_{\text{error}})\langle \hat{S}_{PM} \rangle} m_1. \quad (16)
 \end{aligned}$$

Equation (16) shows that the conditional averages are found somewhere between the original expectation value of $\langle \hat{S}_{PM} \rangle$ for $P_{\text{error}} = 1/2$ and the measurement result m_1 for $P_{\text{error}} = 0$. In the experiment, the error probability is controlled by the measurement strength θ as shown in Fig. 2. The corresponding dependence of $A_{\text{opt}}(m_1)$ on θ is shown in Fig. 3.

It should be noted that the result does not change if it is based on the joint probabilities $P(m_1, m_2|\psi)$ shown in Fig. 4, since the marginal probabilities $P(m_1|\psi)$ of this joint probability distribution are equal to the sums of the sequential measurement probabilities $P(m_1|a)P(a|\psi)$. This is an important fact, since the actual value of a is fundamentally inaccessible once the final measurement of m_2 is performed, regardless whether the data obtained from m_2 are used or not. Even though the correlation between \hat{S}_{PM} and m_1 can be explained using classical statistics, this possibility does not imply that we can safely assign a physical reality a to the observable. The distinction between classical and nonclassical correlations is therefore more subtle than the choice of measurement strategy.

Up to now, the analysis does not include any nonclassical correlations, since the measurement is only sensitive to the target observable $\langle \hat{S}_{PM} \rangle$. This situation changes if we include the outcome m_2 of the final HV measurement in the evaluation of the experimental data. Importantly, we intend to use the

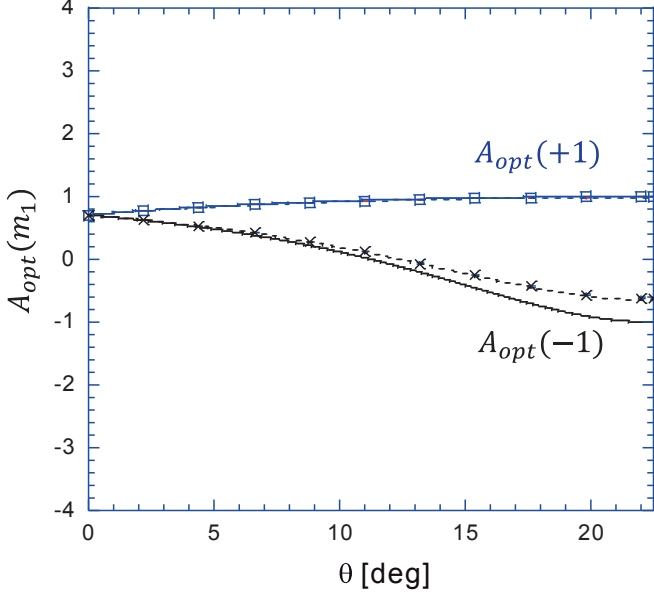


FIG. 3. Conditional average $A_{\text{opt}}(m_1)$ of the PM polarization \hat{S}_{PM} obtained after a measurement of $m_1 = +1$ (P polarization) or $m_1 = -1$ (M polarization) at different measurement strengths θ . At $\theta = 0$, the measurement outcome is random ($P_{\text{error}} = 1/2$) and the conditional average is simply given by the original expectation value of the input state. As the likelihood of measurement errors decreases, the conditional average approaches the value given by the measurement outcome m_1 .

information gained from the outcome of the HV measurement to update and improve our estimate of the PM polarization in the input. For that purpose, we need to evaluate the nonclassical correlations between $\langle \hat{S}_{PM} \rangle$ and $\langle \hat{S}_{HV} \rangle$, which can be done using the method developed in Sec. III. In addition to the

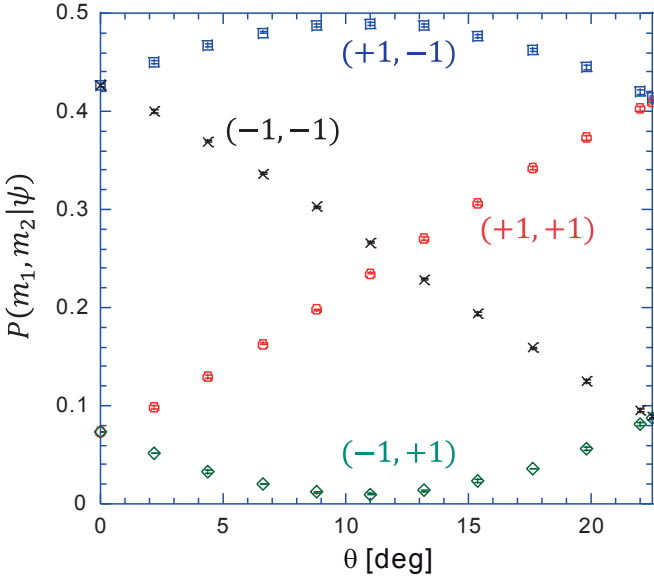


FIG. 4. Probabilities $P(m_1, m_2 | \psi)$ for the outcomes of the sequential measurement of m_1 (PM polarization) and m_2 (HV polarization) on an input state polarized at 67.5° , halfway between P and V.

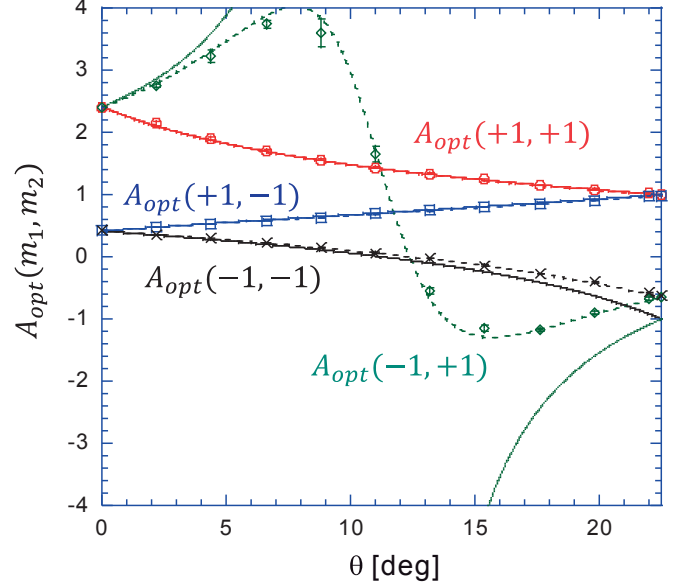


FIG. 5. Conditional averages $A_{\text{opt}}(m_1, m_2)$ as a function of measurement strength θ . The solid curve represents the theoretical prediction for a measurement without experimental imperfections, the broken line was calculated for an interferometer visibility of $V_{PM} = 0.93$.

known probabilities $P(a|\psi)$ and $P(m_1, m_2|a)$, we now need to include the measurement outcomes $P(m_1, m_2|\psi)$ which provide the essential information on the nonclassical correlations. The experimental results for $P(m_1, m_2|\psi)$ obtained at variable measurement strengths θ are shown in Fig. 4. The question is how the final result m_2 changes our estimate of \hat{S}_{PM} . According to Eq. (9), we can find the answer by dividing the difference between the probabilities of a measurement sequence of a followed by (m_1, m_2) by the probabilities obtained by directly measuring (m_1, m_2) :

$$\begin{aligned} A_{\text{opt}}(m_1, m_2) &= \frac{P(m_1, m_2|+)P(+|\psi) - P(m_1, m_2|-)P(-|\psi)}{P(m_1, m_2|\psi)} \\ &= \frac{m_1(1 - 2P_{\text{error}}) + \langle \hat{S}_{PM} \rangle}{4P(m_1, m_2|\psi)}. \end{aligned} \quad (17)$$

Note that the simplification of this relation is possible because the result m_2 of the HV measurement is completely random when the input states are eigenstates of PM polarization, so that $P(m_1, m_2|\pm) = P(m_1|\pm)/2$. Thus the m_2 dependence of the conditional average only appears in the denominator. Specifically, the difference in the probability of finding H polarization ($m_2 = +1$) or V polarization ($m_2 = -1$) in the final measurement translates directly into a difference in the conditional probabilities, where a lower probability of m_2 enhances the estimated value $A_{\text{opt}}(m_1, m_2)$.

Figure 5 shows the dependence of the conditional averages of \hat{S}_{PM} on the measurement strength θ . Significantly, the low probabilities of finding H polarization ($m_2 = +1$) result in estimates of $A_{\text{opt}}(m_1, m_2)$ that lie outside of the range of eigenvalues. The difference between $A_{\text{opt}}(+1, +1)$ and $A_{\text{opt}}(+1, -1)$ corresponds to the contribution of the nonclassical correlation between \hat{S}_{PM} and m_2 , whereas the difference

between $A_{\text{opt}}(+1, -1)$ and $A_{\text{opt}}(-1, -1)$ corresponds to the contribution of the correlation between \hat{S}_{PM} and m_1 , which is closely related to the classical correlation that determines the behavior of $A_{\text{opt}}(m_1)$ in Fig. 3. As the measurement strength increases, the correlation between \hat{S}_{PM} and m_2 drops towards zero and the correlation between \hat{S}_{PM} and m_1 increases, approaching the ideal identification of the measurement outcome m_1 with the eigenvalue of \hat{S}_{PM} . For intermediate measurement strengths, it is important to consider the correlations between the measurement outcomes as well, indicating that the nonclassical correlations associated with m_2 are modified by the results of m_1 and vice versa. The adjustment of measurement strength is therefore a powerful tool for the analysis of measurement statistics that may give us important new insights into the way that classical and nonclassical correlations complement each other.

The conditional average $A_{\text{opt}}(m_1, m_2)$ is obtained from the correlations between \hat{S}_{PM} and the two measurement results m_1 and m_2 that originate from the statistics of the initial state ψ . Specifically, the estimate is obtained by updating the initial statistics of ψ based on the outcomes m_1 and m_2 , where the measurement strength controls the relative statistical weights of the information obtained from m_1 and m_2 . At a maximal measurement strength of $\theta = 22.5^\circ$, the PM measurement completely randomizes the HV polarization, so that the conditional average $A_{\text{opt}}(m_1, m_2)$ is independent of m_2 and the estimation procedure is based on the classical correlations between m_1 and \hat{S}_{PM} . As the measurement strength is weakend, a small contribution of nonclassical correlations emerges as the conditional averages for $m_2 = +1$ and for $m_2 = -1$ split, with the estimates for the more likely m_2 outcomes dropping towards zero and the estimates for the less likely m_2 outcomes diverging to values greater than $+1$ for $m_1 = +1$ and more negative than -1 for $m_1 = -1$. Even small contributions of nonclassical correlations therefore result in estimates that cannot be reproduced by classical statistics. Due to experimental imperfections, the anomalous values of $A_{\text{opt}}(+1, +1) > 1$ are easier to observe than the anomalous values of $A_{\text{opt}}(-1, +1) < -1$. Specifically, the small probabilities of the result $(-1, +1)$ are significantly enlarged by the noise background associated with limited visibilities. As the measurement strength drops, the initial bias in favor of P polarization in the input state ψ begins to outweigh the effect of the measurement result of $m_1 = -1$ that would indicate M polarization. Of particular interest is the crossing point around $\theta = 12.3^\circ$, where the initial information provided by ψ and the measurement information m_1 become equivalent and the estimate is $A_{\text{opt}}(-1, m_2) = 0$ for both $m_2 = +1$ and $m_2 = -1$. For measurement strengths below this crossing point, the initial bias provided by the initial state towards P polarization clearly dominates the estimate, resulting in positive values of $A_{\text{opt}}(-1, m_2)$. Significantly, the increase of the estimate with reduction in measurement strength is much faster for $m_2 = +1$ than for $m_2 = -1$, since the lower probability of the outcome $m_2 = +1$ effectively enhances the statistical weight of the information. For $\theta \approx 11^\circ$, this enhancement of the estimate even results in a crossing between $A_{\text{opt}}(-1, +1)$ and $A_{\text{opt}}(+1, +1)$, so that the value estimated for an outcome of $m_1 = -1$ actually exceeds the

value estimated for an outcome of $m_1 = +1$ at measurement strengths of $\theta < 11^\circ$. This counterintuitive difference between the outcome of the PM measurement and the estimated value of PM polarization appears due to the effects of the measurement outcome m_1 on the quantum correlations between m_2 and the target observable \hat{S}_{HV} in the initial state. Specifically, low probability outcomes always enhance the correlations between measurement results and target observable. Therefore, the low probability outcome $m_1 = -1$ enhances the correlation between $m_2 = +1$ and \hat{S}_{HV} , which favors the P polarization. On the other hand, the much higher probability of $m_1 = +1$ does not result in a comparative enhancement of this correlation, so that the estimated value $A_{\text{opt}}(+1, +1)$ for an outcome of $m_1 = +1$ is actually lower than the estimated value $A_{\text{opt}}(-1, +1)$ for an outcome of $m_1 = -1$. These nonclassical aspects of correlations between measurement results and target observable highlight the importance of the relation between the two measurement outcomes: it is impossible to isolate the measurement result m_1 from the context established by both ψ and m_2 . Since the estimated values $A_{\text{opt}}(m_1, m_2)$ correspond to weak values, this observation may also provide a practical example of the relation between weak values and contextuality [20]. The present analysis evaluates \hat{A} in a measurement context (m_1, m_2) , where the partial specification of the context by m_1 is fully compatible with the context of precise measurements of \hat{A} represented by eigenstate projections. However, the subsequent measurement of m_2 modifies this context, making the sequence (m_1, m_2) incompatible with eigenstate projections. The dependence of the value of $A_{\text{opt}}(m_1, m_2)$ on the second outcome m_2 thus provides a practical example of how the physical meaning of a measurement result changes when the context is specified further.

In the limit of zero measurement strength ($\theta = 0$), the estimated values depend only on m_2 , with the unlikely measurement outcome of $m_2 = +1$ resulting in an anomalous weak value of $A_{\text{opt}}(m_1, +1) = \sqrt{2} + 1$ and the likely outcome of $m_2 = -1$ resulting in a weak value estimate of $A_{\text{opt}}(m_1, -1) = \sqrt{2} - 1$. Since these estimates are based only on the outcomes of precise measurements of HV polarization, they provide a direct illustration of the nonclassical correlation between \hat{S}_{PM} and \hat{S}_{HV} in ψ . Due to the specific choice of initial state, $A_{\text{opt}}(m_1, +1)$ is larger than $A_{\text{opt}}(m_1, -1)$, which means that the detection of H polarization makes P polarization more likely, while the detection of V polarization increases the likelihood of M polarization. If we disregard for a moment that the estimated values for $m_2 = +1$ lie outside the range of possible eigenvalues, we can give a fairly intuitive characterization of this nonclassical correlation. Clearly, the lowest likelihood is assigned to the combination of H polarization and M polarization, which are the least likely polarization results obtained in separate measurements of HV polarization and PM polarization for the input state ψ . We can therefore summarize the result by observing that quantum correlations between Bloch vector components strongly suppress the joint contributions of the least likely results, to the point where the correlation can exceed positive probability boundaries, corresponding to an implicit assignment of negative values to the combination of the two least likely outcomes [18].

The results presented in this section clearly show that the final HV measurement provides additional information about the target observable $\hat{A} = \hat{S}_{PM}$. We can therefore expect that the measurement error will be reduced significantly if we use $A_{m_1, m_2} = A_{\text{opt}}(m_1, m_2)$ as measurement result assigned to the joint outcome (m_1, m_2) . In the final section of our discussion, we will therefore take a look at the measurement errors obtained at different measurement strengths θ and identify the amount of PM information obtained from the measurement of HV polarization.

VI. EVALUATION OF MEASUREMENT ERRORS

According to Eq. (6), the measurement errors for optimized measurement outcomes $A_m = A_{\text{opt}}(m)$ can be evaluated directly by subtracting the statistical fluctuations of A_m from the initial fluctuations of the target observable \hat{A} in the initial state ψ . We can therefore use the results of the previous sections to obtain the measurement errors $\varepsilon^2(A)$ for the measurement outcomes m_1 and for the combined measurement outcomes (m_1, m_2) . The results are shown in Fig. 6, together with the measurement error given by Eq. (12), which is obtained by assigning values of $A_{m_1} = \pm 1$ to the measurement outcomes m_1 .

Not surprisingly, the suboptimal assignment of eigenvalues to the measurement outcomes results in much avoidable extra noise. In fact, the error for this assignment exceeds the uncertainty of $\Delta A^2 = 0.5$ for the initial state ψ at measurement strengths of $\theta < 13.5^\circ$, indicating that one can obtain a better estimate of PM polarization from the expectation

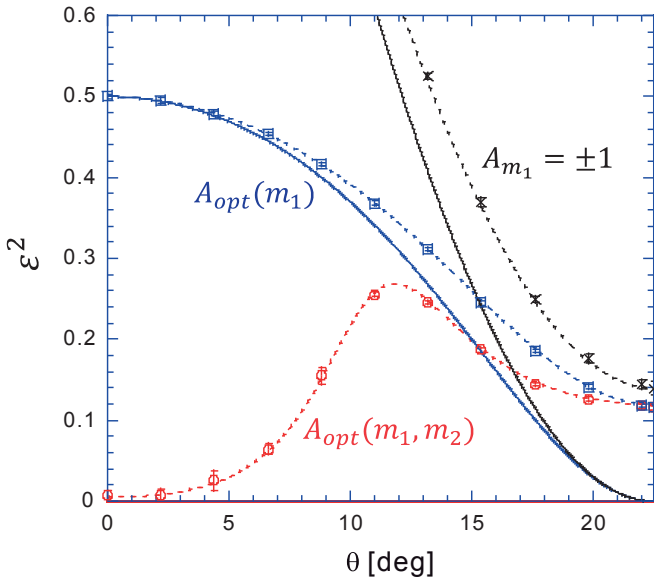


FIG. 6. Measurement errors for different measurement strategies. The highest errors are obtained by assigning eigenvalues of $A_{m_1} = \pm 1$ to the outcomes m_1 of the PM measurement. Optimization of the estimate based on m_1 results in an error that decreases with increasing measurement strength. By basing the estimate on the combined outcomes (m_1, m_2) , it is possible to achieve errors close to zero for low measurement strength θ , since the undisturbed HV measurement provides maximal information on the PM polarization through the nonclassical correlations between \hat{S}_{PM} and \hat{S}_{HV} in the initial state ψ .

value of the input state. This never happens in the case of the errors ε_{opt} associated with the optimal estimates of the target observable, since the optimized estimates based on the conditional averages for the different measurement outcomes include the information of the initial state. In the case of the classical estimate $A_{\text{opt}}(m_1)$ obtained from the variable strength PM measurement, the measurement error drops gradually from the variance of the initial state at $\theta = 0$ to a residual error caused by the limited visibility V_{PM} at $\theta = 22.5^\circ$. By including the information of the final HV measurement, the estimate can be improved to $A_{\text{opt}}(m_1, m_2)$, resulting in a reduction of the error that is particularly significant when the measurement strength approaches $\theta = 0$.

The most interesting experimental result might be the error obtained for the optimal estimate $A_{\text{opt}}(m_1, m_2)$, which summarizes all of the available information in the estimates shown in Fig. 5. Theoretically, the error of this estimate would be zero if the measurements could be performed without any experimental imperfections, as indicated by the red solid line in Fig. 6. The actual results are close to zero error in the limit of low measurement strength. In this limit, the high visibility of the final HV measurement for m_2 dominates the estimate, with a much lower impact of the less reliable PM measurement for m_1 . The errors then start to rise as the experimental values of $A_{\text{opt}}(-1, +1)$ in Fig. 5 reach their maximal values near $\theta = 8^\circ$. The value of the error continues to rise beyond the maximum of $A_{\text{opt}}(-1, +1)$ and reaches its maximal value near the $\theta = 12.3^\circ$ crossing point where $A_{\text{opt}}(-1, +1) = A_{\text{opt}}(-1, -1) = 0$. At this point, the estimate is particularly sensitive to measurement noise, since the extremely low probabilities of an outcome of $(-1, +1)$ are strongly affected by experimental noise backgrounds. For measurement strengths greater than this crossing point ($\theta > 12.3^\circ$), the error of $A_{\text{opt}}(m_1, m_2)$ is not much lower than the error of $A_{\text{opt}}(m_1)$, indicating that the final measurement result m_2 provides only very little additional measurement information on \hat{S}_{PM} . This appears to be a result of the experimental noise in the PM measurement, which limits the error to $\varepsilon^2 = 0.12$ at a maximal measurement strength of $\theta = 22.5^\circ$.

In summary, the analysis of the measurement errors shows that the nonclassical correlation between m_2 and \hat{S}_{PM} used to obtain the estimate $A_{\text{opt}}(m_1, m_2)$ in the limit of weak measurement interactions results in much lower errors than the use of the classical correlations between m_1 and \hat{S}_{PM} that dominate in the strong measurement regime. This is a result of the fact that the errors in the limit of weak measurement are dominated by the HV visibility of the setup, while the errors in the strong measurement regime mostly originate from the PM visibility, which happens to be much lower than the HV visibility in the present setup. Our setup is therefore ideally suited to illustrate the importance of nonclassical correlations in the evaluation of measurement errors when the initial state is taken into account. The optimal estimate $A_{\text{opt}}(m_1, m_2)$ is obtained by considering the specific relation between the measurement outcomes and the target observable in the specific input state, which may result in counterintuitive assignments of values to the different measurement outcomes. In the present case, the lowest errors are obtained as a consequence of this counterintuitive assignment, since the experimental setup is

particularly robust against experimental imperfections in the regime of low measurement strength which is most sensitive to the effects of nonclassical correlations. Our results thus provide a particularly clear experimental demonstration of the reduction of measurement errors by nonclassical correlations between measurement result and target observable in the initial quantum state.

VII. CONCLUSIONS

We have investigated the nonclassical correlations between the outcomes of a quantum measurement and the target observable of the measurement by studying the statistics of measurement errors in a sequential measurement. In the initial measurement, the measurement operator commutes with the target observable and the measurement outcome m_1 relates directly to the target observable, while the final measurement of a complementary observable introduces the effect of nonclassical correlations between the outcome m_2 and the target observable. To evaluate the errors, we applied the operator formalism introduced by Ozawa and show that the evaluation of two-level statistics can be performed by combining the measurement statistics of the input state ψ with the statistics obtained from eigenstate inputs of the target observable. By combining the statistics of separate measurements according to the rules obtained from the operator formalism, it is possible to identify the optimal estimate of the target observable using only the available experimental data. Due to the specific combination of the statistical results, this estimate can exceed the limits of classical statistics by obtaining values that lie outside the range of possible eigenvalues. Typically, the least likely outcomes are associated with extreme values of the target observable. In the present experiment, we find extremely high estimates of the target observable when the strength of the initial measurement is weak and the measurement result

is dominated by the nonclassical correlations between the target observable and the complementary observable detected in the final measurement. In this limit, the initial measurement outcome that refers directly to the target observable mainly enhances or reduces the effects of the nonclassical correlations, which results in the counterintuitive anticorrelation between the actual measurement result and the associated estimate of the target observable for a final outcome of $m_2 = +1$.

Our discussion provides a more detailed insight into the experimental analysis of measurement errors that has recently been used to evaluate the uncertainty limits of quantum measurements derived by Ozawa [1–5,7,8]. It is important to note that the estimation procedure associated with this kind of error analysis also reveals important details of the nonclassical statistics originating from the correlations between physical properties in the initial state. In the present work, we have taken a closer look at the experimental analysis of measurement errors and clarified its nonclassical features. The results show that some of the effects involved in the optimal evaluation of the experimental data are rather counterintuitive and exhibit features that exceed the possibilities of classical statistics in significant ways. For a complete understanding of measurement statistics in quantum mechanics, it is therefore necessary to explore the effects of nonclassical correlations in more detail, and the present study may be a helpful starting point for a deeper understanding of the role such correlations can play in various measurement contexts.

ACKNOWLEDGMENTS

This work was supported by JSPS KAKENHI Grant No. 24540428. One of authors (Y.S.) is supported by Grant-in-Aid for JSPS Fellows 265259.

-
- [1] M. Ozawa, *Phys. Rev. A* **67**, 042105 (2003).
 - [2] J. Erhart, S. Sponar, G. Sulyok, G. Badurek, M. Ozawa, and Y. Hasegawa, *Nat. Phys.* **8**, 185 (2012).
 - [3] S.-Y. Baek, F. Kaneda, M. Ozawa, and K. Edamatsu, *Sci. Rep.* **3**, 022221 (2013).
 - [4] L. A. Rozema, A. Darabi, D. H. Mahler, A. Hayat, Y. Soudagar, and A. M. Steinberg, *Phys. Rev. Lett.* **109**, 100404 (2012).
 - [5] M. M. Weston, M. J. W. Hall, M. S. Palsson, H. M. Wiseman, and G. J. Pryde, *Phys. Rev. Lett.* **110**, 220402 (2013).
 - [6] C. Branciard, *Proc. Natl. Acad. Sci. USA* **110**, 6742 (2013).
 - [7] M. Ringbauer, D. N. Biggerstaff, M. A. Broome, A. Fedrizzi, C. Branciard, and A. G. White, *Phys. Rev. Lett.* **112**, 020401 (2014).
 - [8] F. Kaneda, S.-Y. Baek, M. Ozawa, and K. Edamatsu, *Phys. Rev. Lett.* **112**, 020402 (2014).
 - [9] Y. Watanabe, T. Sagawa, and M. Ueda, *Phys. Rev. A* **84**, 042121 (2011).
 - [10] P. Busch, P. Lahti, and R. F. Werner, *Phys. Rev. Lett.* **111**, 160405 (2013).
 - [11] J. Dressel and F. Nori, *Phys. Rev. A* **89**, 022106 (2014).
 - [12] A. P. Lund and H. M. Wiseman, *New J. Phys.* **12**, 093011 (2010).
 - [13] M. Ozawa, *Ann. Phys.* **311**, 350 (2004).
 - [14] H. F. Hofmann, *Phys. Rev. A* **81**, 012103 (2010).
 - [15] M. J. W. Hall, *Phys. Rev. A* **69**, 052113 (2004).
 - [16] A. J. Leggett and A. Garg, *Phys. Rev. Lett.* **54**, 857 (1985).
 - [17] G. C. Knee, S. Simmons, E. M. Gauger, J. J. L. Morton, H. Riemann, N. V. Abrosimov, P. Becker, H.-J. Pohl, K. M. Itoh, M. L. W. Thewalt, G. A. D. Briggs, and S. C. Benjamin, *Nat. Commun.* **3**, 606 (2012).
 - [18] Y. Suzuki, M. Iinuma, and H. F. Hofmann, *New J. Phys.* **14**, 103022 (2012).
 - [19] M. Iinuma, Y. Suzuki, G. Taguchi, Y. Kadoya, and H. F. Hofmann, *New J. Phys.* **13**, 033041 (2011).
 - [20] M. F. Pusey, *Phys. Rev. Lett.* **113**, 200401 (2014).

Weak measurement of photon polarization by back-action-induced path interference

Masataka Iinuma^{1,3}, Yutaro Suzuki¹, Gen Taguchi¹,
Yutaka Kadoya¹ and Holger F Hofmann^{1,2}

¹ Graduate School of Advanced Sciences of Matter, Hiroshima University,
1-3-1 Kagamiyama, Higashi-Hiroshima 739-8530, Japan

² JST, Crest, Sanbancho 5, Chiyoda-ku, Tokyo 102-0075, Japan

E-mail: iinuma@hiroshima-u.ac.jp

New Journal of Physics **13** (2011) 033041 (11pp)

Received 1 December 2010

Published 31 March 2011

Online at <http://www.njp.org/>

doi:10.1088/1367-2630/13/3/033041

Abstract. An essential feature of weak measurements on quantum systems is the reduction of measurement back-action to negligible levels. To observe the non-classical features of weak measurements, it is therefore more important to avoid additional back-action errors than it is to avoid errors in the actual measurement outcome. In this paper, it is shown how an optical weak measurement of diagonal (PM) polarization can be realized by path interference between the horizontal (H) and vertical (V) polarization components of the input beam. The measurement strength can then be controlled by rotating the H and V polarizations towards each other. This well-controlled operation effectively generates the back-action without additional decoherence, while the visibility of the interference between the two beams only limits the measurement resolution. As the experimental results confirm, we can obtain extremely high weak values, even at rather low visibilities. Our method therefore provides a realization of weak measurements that is extremely robust against experimental imperfections.

³ Author to whom any correspondence should be addressed.

Contents

1. Introduction	2
2. Quantum measurement by back-action-induced interference	3
3. Experimental demonstration of the weak measurement	6
4. Relation between measurement resolution and back-action	8
5. Conclusions	10
Acknowledgment	10
References	10

1. Introduction

In ideal quantum measurements, there is a trade-off between the information obtained about the measured observable and the back-action suffered by observables that do not share any eigenstates with the measured observable. A fully resolved strong measurement has a maximal back-action since it completely removes any coherences between the eigenstates of the measured observable. On the other hand, a weak measurement with low resolution can have negligible back-action, leaving the coherences of the initial state almost completely intact. As first pointed out by Aharonov *et al* [1], it is then possible to obtain measurement results far outside the spectrum of the eigenvalues of the measured observable by post-selecting a specific final measurement outcome. In the limit of negligible back-action, these post-selected results only depend on the initial state the final state, and the operator of the measured observable. It is therefore possible to define the measurement result as the weak value of the measured observable for the specific combination of initial and final states defined by state preparation and post-selection.

It was soon realized that photon polarization was an ideal system for the experimental realization of weak measurements, since optics provide optimal control of coherence using well-established technologies [2, 3]. At first, the implications and usefulness of weak values were unclear. However, recent advances in quantum technologies have revived the interest in the unusual properties of weak values, with possible applications in precision measurements [4]–[7], realizations using quantum logic gates [8, 9], resolution of quantum paradoxes [10]–[14] and more fundamental implications for quantum statistics and quantum physics [15]–[17]. Because of the wide range of problems that can be addressed by weak measurements, it seems to be desirable to develop simple and efficient technological implementations that are not too sensitive to experimental errors. In the following, we therefore present an experimental setup for the weak measurement of photon polarization that uses a basic two-path interferometer as the meter system.

The magnitude of weak values observed in the experiments is generally limited by the actual back-action, which is unavoidable in the implementation of weak measurements. In an interferometric setup, the limited visibility of the interferences between two paths may cause an additional back-action on coherent superpositions of the eigenstates of the measured observable. To avoid this effect, we propose a realization of weak measurements where the interference occurs instead between eigenstates of the back-action observable defined by the post-selection. The measurement effect is then obtained by the phase dependence between eigenstates of the back-action observable corresponding to the different values of the measured observable.

To enable this interference, the distinguishability between the eigenstates of the back-action observable must be reduced by a finite back-action. However, as we discuss in more detail below, it is possible to control this unavoidable back-action precisely by implementing it separately in each path. The result is a conventional weak measurement (or variable strength measurement), but now the errors caused by finite visibility of the interference only reduce the measurement resolution, without increasing the back-action. Our setup is therefore ideally suited to weak measurements in the presence of experimental imperfections.

The rest of the paper is organized as follows. In section 2, we describe the principle of back-action-induced interference and the experimental setup used to realize it. In section 3, we present the experimental results obtained for the weak values of photon polarization and show that the errors are close to the theoretical limit for the measurement strength used in the experiment. In section 4, we present experimental results for the trade-off between resolution and back-action in our setup. The results show that the visibility only limits measurement resolution, without contributing to the back-action. Section 5 summarizes the results and concludes the paper.

2. Quantum measurement by back-action-induced interference

In our experiment, we realize a measurement of photon polarization with variable measurement strength by making use of the fact that the diagonal polarization is determined by the phase coherence between the horizontal (H) and vertical (V) polarizations. The positive (P) and the negative (M) superpositions can therefore be distinguished by interference between the H and V components of the photon state. Although path interference between these two components cannot occur if the beams corresponding to the H and V polarizations can still be distinguished by their orthogonal polarization states, it is possible to induce a well-controlled amount of interference by erasing the HV information in the beams using a coherent rotation of polarization towards a common diagonal polarization. The increase in interference as the polarizations become less and less distinguishable corresponds to the trade-off between measurement information and back-action in the quantum measurement. Significantly, the final interference that results in a correlation between the output path and the PM polarization of the input state does not change the HV polarization at all, regardless of the visibility of the interference. The flips of HV polarization caused by the measurement back-action are therefore limited to the flips caused by the rotation of the polarization in the two arms of the interferometer. This method thus ensures optimal control of the back-action, permitting arbitrarily low back-action even in the presence of significant experimental errors.

Figure 1 shows our setup in more detail. The photon path is split by a polarizing beam splitter (PBS) into a V-polarized path $a1$ and an H-polarized path $a2$. The polarizations are then rotated in opposite directions by half-wave plates (HWP) mounted in each path. Specifically, the HWP in path $a1$ is rotated by an angle of $-\theta$ from the horizontal/vertical alignment, whereas the HWP in path $a2$ is rotated by an angle of $+\theta$. Finally, the two polarization components interfere at a beam splitter (BS) with 50% reflectivity for all polarizations, resulting in the output beams $b1$ and $b2$. A glass plate is used to compensate for path length differences between path $a1$ and path $a2$, and an HWP is inserted in $b2$ to compensate for the phase shift caused by the difference in the number of reflections between the H and V components.

The input photons were generated by using a CW titanium-sapphire laser (wavelength 830 nm, output power 300 mW) and passed through a Glan-Thompson prism to select photons

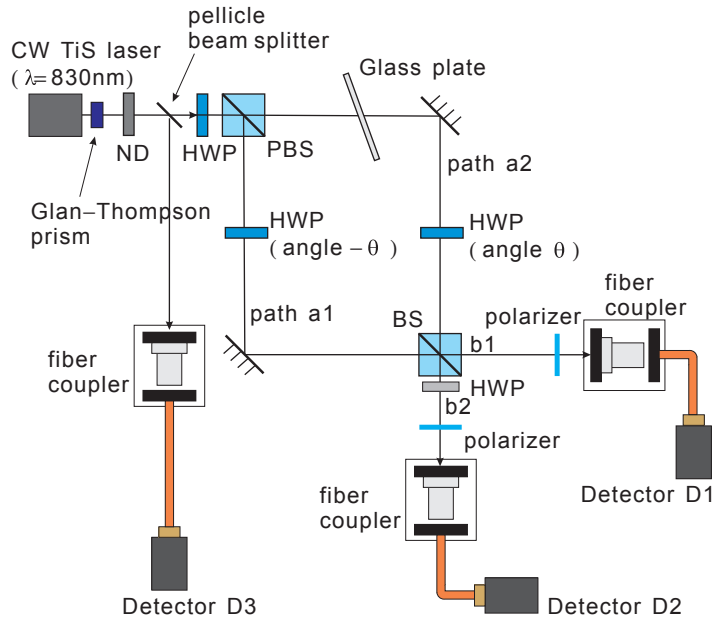


Figure 1. Setup of the polarization measurement using back-action induced interference. Interferences between the V-polarized path $a1$ and the H-polarized path $a2$ is induced using oppositely rotated HWP to reduce the angle between the polarization and therefore the distinguishability of the paths in terms of polarization. The output beams then distinguish positive and negative superpositions of H and V, corresponding to diagonal P and M polarizations.

with horizontal polarization. Neutral density (ND) filters were used to obtain intensities suitable for single photon counting with typical count rates around 100 kHz. The initial state of photon polarization was prepared by rotating the HWP upstream of the PBS. The numbers of output photons in paths $b1$ and $b2$ were counted using the single photon counting modules (SPCM-AQR-14) D1 and D2, which were optically coupled to paths $b1$ and $b2$ through fiber couplers and optical fibers. To keep track of fluctuations in the input light, the input intensity was monitored by detecting photons reflected by a pellicle BS (reflectivity = 8%) with another single photon counting module D3. Experimentally, the ratio of counts in D3 to total counts in D1 and D2 was found to be 0.020. Post-selection was realized by inserting polarizers in the output beams to select only the desired output polarization in both paths.

The weak measurement is realized by the interferometer setup between the PBS and the BS. If the polarizations in paths $a1$ and $a2$ are orthogonal at the final BS, no interference will be observed in the output probabilities of $b1$ and $b2$. The interference at the final beam splitter BS will simply restore the original superposition of H and V polarizations of the input state. By rotating the polarization in both arms towards the same diagonal polarization P, the distinguishability of the two paths is reduced and the phase coherence between the HV components is converted into interferences between the paths. As a result, the probability of finding the photon in path $b1$ increases for positive superpositions of H and V (P polarization), and decreases for negative superpositions (M polarization). In the absence of experimental imperfections, the interference at the final BS can be expressed in terms of the polarization

vectors in paths $a1$ and $a2$ given in the HV -basis,

$$\begin{aligned} |b1\rangle &= \frac{1}{\sqrt{2}} C_H \begin{bmatrix} \cos 2\theta \\ \sin 2\theta \end{bmatrix} + \frac{1}{\sqrt{2}} C_V \begin{bmatrix} \sin 2\theta \\ \cos 2\theta \end{bmatrix}, \\ |b2'\rangle &= \frac{1}{\sqrt{2}} C_H \begin{bmatrix} \cos 2\theta \\ \sin 2\theta \end{bmatrix} - \frac{1}{\sqrt{2}} C_V \begin{bmatrix} \sin 2\theta \\ \cos 2\theta \end{bmatrix}, \end{aligned} \quad (1)$$

where C_H and C_V are the probability amplitudes of the H and V polarized components of the input state. For $\theta = 0$, $|b1\rangle$ reproduces the input polarization, while the polarization in $|b2'\rangle$ is changed by a phase flip between the H and V components. The HWP in $b2$ compensates for this phase flip, resulting in the non-normalized output states $|b1\rangle$ and $|b2\rangle$ in the output beams of the measurement setup,

$$\begin{aligned} |b1\rangle &= \frac{1}{\sqrt{2}} \begin{bmatrix} \cos 2\theta & \sin 2\theta \\ \sin 2\theta & \cos 2\theta \end{bmatrix} \begin{bmatrix} C_H \\ C_V \end{bmatrix} = \hat{M}_{b1} |\psi_i\rangle, \\ |b2\rangle &= \frac{1}{\sqrt{2}} \begin{bmatrix} \cos 2\theta & -\sin 2\theta \\ -\sin 2\theta & \cos 2\theta \end{bmatrix} \begin{bmatrix} C_H \\ C_V \end{bmatrix} = \hat{M}_{b2} |\psi_i\rangle, \end{aligned} \quad (2)$$

where $|\psi_i\rangle$ is the input state defined by C_H and C_V and the measurement operators \hat{M}_{b1} and \hat{M}_{b2} represent the effects of the measurement described by their matrix representation in the HV -basis.

It is easy to see that the eigenstates of the measurement operators are the positive and negative superpositions of $|H\rangle$ and $|V\rangle$, corresponding to the diagonal polarization states, $|P\rangle$ and $|M\rangle$. In terms of the Stokes parameter $\hat{S}_{PM} = |P\rangle\langle P| - |M\rangle\langle M|$, the positive operator measure defining the probabilities of finding the photon in $b1$ or $b2$ is therefore given by

$$\begin{aligned} \hat{M}_{b1}^\dagger \hat{M}_{b1} &= \frac{1}{2} \left(\hat{1} + \epsilon_{PM} \hat{S}_{PM} \right), \\ \hat{M}_{b2}^\dagger \hat{M}_{b2} &= \frac{1}{2} \left(\hat{1} - \epsilon_{PM} \hat{S}_{PM} \right), \end{aligned} \quad (3)$$

where $\epsilon_{PM} = \sin 4\theta$ determines the measurement resolution. Without post-selection, the difference between the output probabilities in $b1$ and $b2$ is directly related to the PM polarization of the input state,

$$\begin{aligned} P(b1) - P(b2) &= \langle \psi_i | \hat{M}_{b1}^\dagger \hat{M}_{b1} | \psi_i \rangle - \langle \psi_i | \hat{M}_{b2}^\dagger \hat{M}_{b2} | \psi_i \rangle \\ &= \epsilon_{PM} \langle \psi_i | \hat{S}_{PM} | \psi_i \rangle. \end{aligned} \quad (4)$$

Experimentally, it is therefore possible to determine the polarization of the input light by dividing the difference in output probability by a constant value ϵ_{PM} , where the proper value of ϵ_{PM} can be determined from the visibility obtained for maximally polarized inputs.

In the case of output post-selection, the difference in the conditional output probabilities can now be interpreted as a conditional measurement of PM polarization. Experimentally, the conditional value $\langle \hat{S}_{PM} \rangle_{\text{exp}}(m_f)$ obtained by post-selecting an output polarization state $|m_f\rangle$ is determined from the output probabilities by

$$\langle \hat{S}_{PM} \rangle_{\text{exp}}(m_f) = \frac{1}{\epsilon_{PM}} (P(b1|m_f) - P(b2|m_f)). \quad (5)$$

In the limit of negligible back-action ($\epsilon_{\text{PM}} \rightarrow 0$), this experimental value is equal to the theoretically predicted weak value,

$$\langle \hat{S}_{\text{PM}} \rangle_{\text{weak}} = \text{Re} \left[\frac{\langle m_f | \hat{S}_{\text{PM}} | \psi_i \rangle}{\langle m_f | \psi_i \rangle} \right]. \quad (6)$$

However, the finite measurement back-action for non-zero measurement resolutions ϵ_{PM} modifies this result even in the case of an ideal measurement. Using equation (5) to determine the conditional probabilities, the experimental value expected at finite back-action is

$$\begin{aligned} \langle \hat{S}_{\text{PM}} \rangle_{\text{exp}}(m_f) &= \frac{1}{\epsilon_{\text{PM}}} \frac{|\langle m_f | \hat{M}_{b1} | \psi_i \rangle|^2 - |\langle m_f | \hat{M}_{b2} | \psi_i \rangle|^2}{|\langle m_f | \hat{M}_{b1} | \psi_i \rangle|^2 + |\langle m_f | \hat{M}_{b2} | \psi_i \rangle|^2} \\ &= \frac{|\langle m_f | \psi_i \rangle|^2}{|\langle m_f | \psi_i \rangle|^2 + \eta_{\text{HV}} \Delta_{\text{flip}}} \langle \hat{S}_{\text{PM}} \rangle_{\text{weak}}, \end{aligned} \quad (7)$$

where $\eta_{\text{HV}} = \sin^2(2\theta)$ is equal to the transition probability between H and V polarizations given by the measurement operators \hat{M}_{b1} and \hat{M}_{b2} , and Δ_{flip} is the change in the post-selection probability caused by a polarization flip described by the operator \hat{S}_{PM} , given by

$$\Delta_{\text{flip}} = |\langle m_f | \hat{S}_{\text{PM}} | \psi_i \rangle|^2 - |\langle m_f | \psi_i \rangle|^2. \quad (8)$$

As shown in equation (7), the experimental value is approximately equal to the weak value if the back-action-induced change in the post-selection probability given by $\eta_{\text{HV}} \Delta_{\text{flip}}$ is sufficiently smaller than the original post-selection probability of $|\langle m_f | \psi_i \rangle|^2$. However, extremely large weak values can only be obtained when the original post-selection probability goes to zero. To achieve extremely enhanced experimental weak values, it is therefore essential to keep the transition probability η_{HV} as small as possible. In particular, it is necessary to avoid additional errors from dephasing between the P and M polarized components. In our setup, we achieve extremely small values of η_{HV} by limiting the use of path interferences to an interference between a path associated with the initial H polarization and a path associated with the initial V polarization, therefore avoiding the HV transitions that would be caused by finite visibility interferences between the P and M polarized eigenstates of the measurement operators. As a result, our setup enables us to measure extremely high weak values, even at low visibilities of the path interference.

3. Experimental demonstration of the weak measurement

For the experimental demonstration of the weak measurement, we chose a variable input state given by $C_{\text{H}} = \sin \phi$ and $C_{\text{V}} = \cos \phi$. Post-selection was implemented by inserting polarization filters selecting only the H-polarized output components between the output ports and the detectors. Ideally, we should then be able to observe a theoretical weak value of $\langle \hat{S}_{\text{PM}} \rangle_{\text{weak}} = 1/\tan \phi$. However, the measurement back-action modifies the directly determined experimental values to

$$\langle \hat{S}_{\text{PM}} \rangle_{\text{exp}} = \frac{\sin \phi \cos \phi}{\sin^2 \phi + \eta_{\text{HV}}(\cos^2 \phi - \sin^2 \phi)}, \quad (9)$$

where η_{HV} is the transition probability between H and V polarizations, including both the uncertainty-limited back-action and additional effects of experimental imperfections in the

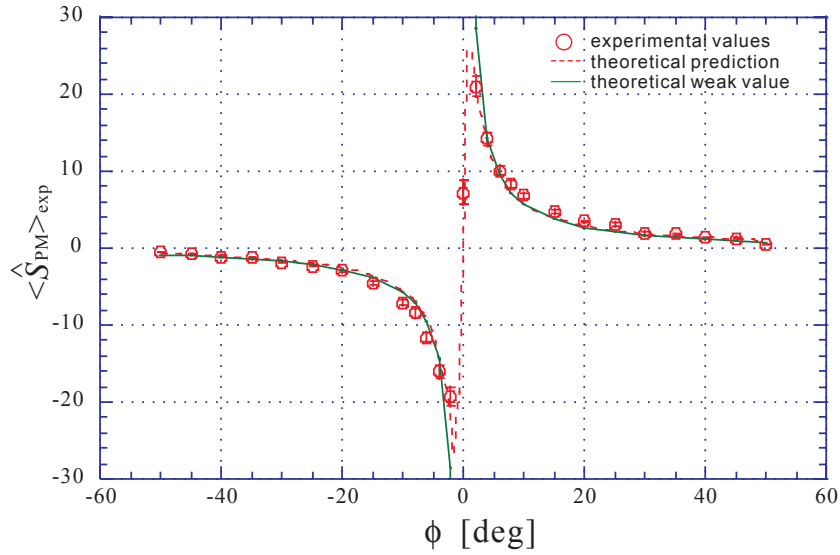


Figure 2. Experimental results of the weak measurement. The experimental weak values $\langle \hat{S}_{PM} \rangle_{\text{exp}}$ are shown as a function of initial polarization angle ϕ . The open circles indicate the experimental data obtained from the conditional probabilities of the post-selected results, the broken line shows the expected effects of back-action given by equation (9) and the solid line shows the theoretical weak value.

setup. As discussed in the previous section, the back-action effects summarized by η_{HV} limit the magnitude of the experimental weak values that can be observed experimentally. For small η_{HV} , the maximal value is $\langle \hat{S}_{PM} \rangle_{\text{exp}} = 1/\sqrt{4\eta_{\text{HV}}}$, obtained at an input polarization angle of $\phi = \sqrt{\eta_{\text{HV}}}$.

Figure 2 shows the experimental results for the weak values obtained with the measurement resolution obtained by setting the HWPs to $\theta = 0.5^\circ$. Theoretically, this corresponds to a measurement resolution of $\epsilon_{\text{PM}} = 0.035$ and a back-action-related transition probability of $\eta_{\text{HV}} = 0.0003$. The experimental results are in good agreement with the theoretical weak values up to and including the measurement values obtained at $\phi = \pm 4^\circ$. The three measurement values obtained close to $\phi = 0$ are consistent with the theoretical prediction for the back-action effects given by equation (9) for $\eta_{\text{HV}} = 0.0003$. This correspondence suggests that almost all of the flips in HV polarization are caused by the rotation of the HWPs in the measurement setup, with only negligible contributions from additional error sources.

The extremal weak values observed in the experiment were found at ± 20 . Since the input angles for these values are at $\phi = \pm 2^\circ$, this is lower than the maximal value of ± 28.6 theoretically predicted for angles of about $\phi = \pm 1^\circ$. However, even the achievement of a 20-fold enhancement of the weak value requires a transition probability below 0.0006. If the weak measurement was realized by a separation of the P and M polarizations followed by an interference between the paths to partially erase the measurement information, the visibility of the interference needed to obtain a 20-fold enhancement of the weak value would have to be as high as $V_{\text{PM}} = 1 - 2\eta_{\text{HV}} = 0.9988$. It is therefore essential that our setup only uses interferences between the H and V polarized paths, avoiding the errors that would be introduced by limited visibilities in path interferences between P and M polarizations.

In our setup, the visibility of the path interference between the H and V polarized components was found to be $V_{HV} = 0.71$. The effects of this error reduce the measurement resolution by introducing transitions between the P and M polarizations. As a result, the measurement resolution is $\epsilon_{PM} = 0.025$ instead of the ideal value of 0.035 predicted from θ . However, this reduced resolution has no effects on the observation of weak values at low θ , since weak values are always obtained from averages over a sufficiently high number of low-resolution measurements. The experimental results thus confirm the main merit of our method for the realization of weak measurements. In contrast, the method is not as suitable for strong measurements, where back-action is always maximal and an optimization of measurement resolution is desirable. Since we can vary the measurement strength of our setup continuously between weak and strong measurements, we can illustrate the performance of our setup in these very different operating regimes in terms of the experimental errors observed in measurement resolution and back-action as the measurement strength is varied by rotation of the HWPs from $\theta = 0^\circ$ to $\theta = 22.5^\circ$.

4. Relation between measurement resolution and back-action

In principle, the measurement resolution ϵ_{PM} and the measurement back-action given by η_{HV} should be defined in terms of the experimental input–output relations of the measurement setup. For a specific input state with a PM polarization of $\langle \hat{S}_{PM} \rangle = 2\text{Re}[C_H^* C_V^*]$, the measurement resolution is given by the ratio between the output probability difference and the expectation value of the Stokes parameter in the input,

$$\epsilon_{PM} = \frac{P(b1) - P(b2)}{2\text{Re}[C_H^* C_V^*]}, \quad (10)$$

where $P(b1)$ and $P(b2)$ are obtained from the total number of counts in $b1$ and $b2$. Likewise, the measurement back-action flips H and V polarizations, reducing the input HV polarization of $\langle \hat{S}_{HV} \rangle = |C_H|^2 - |C_V|^2$ by a factor of $1 - 2\eta_{HV}$. If a measurement of HV polarization is performed in the output, the experimental measurement back-action is obtained from

$$1 - 2\eta_{HV} = \frac{P(H) - P(V)}{|C_H|^2 - |C_V|^2}, \quad (11)$$

where $P(H)$ and $P(V)$ are the total H and V polarized counts summed over both $b1$ and $b2$. For consistency, it is convenient to define the measurement back-action as $2\eta_{HV}$, since a complete randomization of HV polarization ($P(H) = P(V)$) then corresponds to a back-action of 1.

In the absence of experimental errors, our measurement setup would have a measurement resolution of $\epsilon_{PM} = \sin 4\theta$ and a back-action given by $1 - 2\eta_{HV} = \cos 4\theta$, depending on the angles θ of the HWPs. This result achieves the uncertainty limit for resolution and measurement back-action in two-level systems [18], as given by the uncertainty relation

$$\epsilon_{PM}^2 + (1 - 2\eta_{HV})^2 \leq 1. \quad (12)$$

In the actual experiment, linear decoherence effects reduce the values of ϵ_{PM} and $1 - 2\eta_{HV}$ from their ideal values to values below the uncertainty limit. If these reductions are expressed in terms of experimental visibilities, $\epsilon_{PM} = V_{HV} \sin 4\theta$ and $1 - 2\eta_{HV} = V_{PM} \cos 4\theta$, the actual

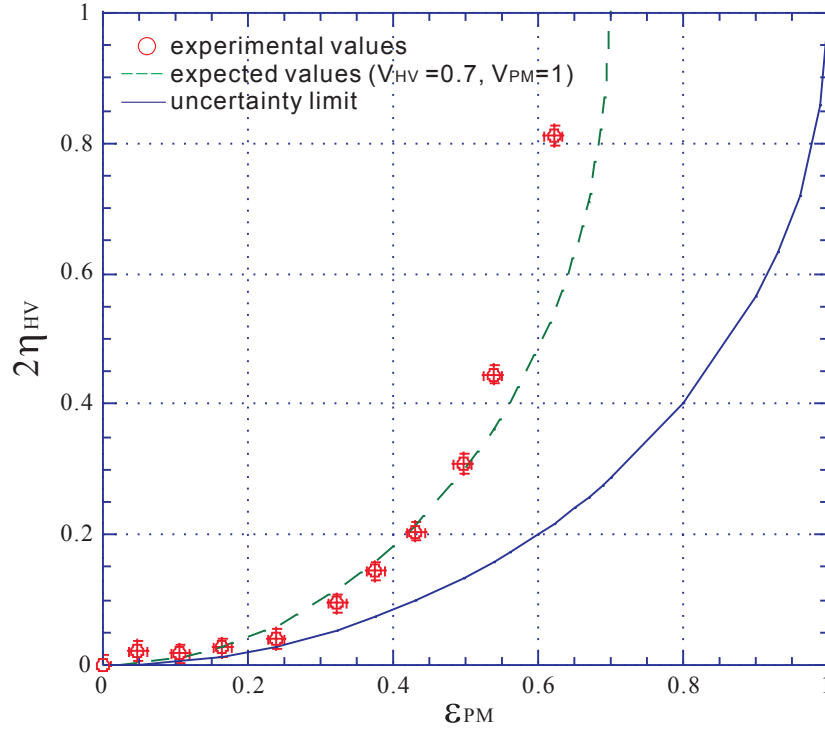


Figure 3. Relation between measurement back-action η_{HV} and measurement resolution ϵ_{PM} . Open circles indicate experimental values obtained for different measurement strengths θ . The broken line shows the relation expected for a visibility of 0.7 in our setup. The solid line indicates the uncertainty limit given by equation (12).

relation between back-action and resolution can be described by

$$\frac{\epsilon_{PM}^2}{V_{HV}^2} + \frac{(1 - 2\eta_{HV})^2}{V_{PM}^2} = 1. \quad (13)$$

If the values obtained for ϵ_{PM} and $2\eta_{HV}$ are shown for different measurement strengths θ , they should therefore lie on an ellipse around $(\epsilon_{PM} = 0, 2\eta_{HV} = 1)$, where V_{HV} determines the resolution in the strong measurement limit at $\theta = 22.5^\circ$, and V_{PM} determines the back-action in the weak measurement limit at $\theta = 0^\circ$.

Figure 3 shows the experimental results obtained with an input state at $\phi = 25^\circ$. The results reproduce the relation between resolution and back-action expected for $V_{HV} = 0.7$ and $V_{PM} = 1$ as shown by the broken line in the graph, except for some discrepancy in the values obtained in the strong measurement limit. Since the strong measurement limit is very sensitive to the visibilities of our interferometer, it is possible that these discrepancies may have been caused by instabilities in the interferometer.

In general, the result is consistent with the values of $V_{HV} = 0.71$ and $V_{PM} > 0.9988$ estimated from the weak measurement results. Since there is no experimentally resolvable limitation to the reduction of measurement back-action at low θ , the experimentally obtained relation between resolution and back-action confirms that our setup is particularly suited to weak measurements. Figure 3 thus illustrates the specific feature of our measurement setup in terms of the noise characteristics at different measurement strengths.

5. Conclusions

We have realized a weak measurement of diagonal (PM) photon polarization by path interference between the H- and V polarized components. In this case, the visibility of the path interference depends on the amount of back-action induced by gradually rotating the orthogonal polarizations of the paths towards each other. It is therefore possible to control the amount of back-action precisely, while errors caused by the limited visibility of the path interference only affect the measurement resolution. This situation is ideal for the realization of weak measurements, since the achievement of extremely high weak values depends critically on the limitation of the total back-action to error rates below the post-selection probability.

Our results show that we can achieve 20-fold enhancement of the weak values, even though the visibility of the path interference was only 0.71. This robustness against experimental errors can be achieved because the measurement resolution is not relevant for the measurement of weak values. The requirements for operating in the weak measurement regime are therefore quite different from the requirements for operating in the strong measurement regime. We have characterized this difference in the experimental requirements by measuring the resolution and back-action of our setup at different measurement strengths. The present setup achieves the uncertainty limit in the weak measurement regime, but not in the strong measurement regime, where its measurement resolution is limited by the visibility of path interference. The characterization of errors for different measurement strengths thus confirms the specific usefulness of our approach for weak measurements.

It should be noted that the robustness against experimental imperfections is obtained with respect to a specific post-selection measurement. To integrate this kind of weak measurement circuit into a larger network, it is therefore essential that the post-selection condition is well defined at the output. However, it is not necessary to fix the measured observable, so that a cascade of diagonal (PM) polarization and circular polarization measurements with subsequent post-selection of the H or V polarized components would share the same robustness properties. In general, the setup presented here is easy to realize and permits the observation of extreme weak values even in the presence of significant experimental imperfections. It may therefore greatly simplify the implementation of weak measurements on the outputs of optical quantum circuits, or as the last stages in cascaded systems. We hope that these simplifications will help us to establish weak measurements as part of the quantum information toolbox, leading to better insights into the fundamental properties of emerging quantum technologies.

Acknowledgment

Part of this work was supported by the Grant-in-Aid program of the Japanese Society for the Promotion of Science.

References

- [1] Aharonov Y, Albert D Z and Vaidman L 1988 *Phys. Rev. Lett.* **60** 1351–4
- [2] Duck I M, Stevenson P M and Sudarshan E C G 1989 *Phys. Rev. D* **40** 2112–7
- [3] Ritchie N W, Story J G and Hulet R G 1991 *Phys. Rev. Lett.* **66** 1107
- [4] Hosten O and Kwiat P 2008 *Science* **319** 787
- [5] Dixon P B, Starling D J, Jordan A N and Howell J C 2009 *Phys. Rev. Lett.* **102** 173601

- [6] Brunner N and Simon C 2010 *Phys. Rev. Lett.* **105** 010405
- [7] Hofmann H F 2010 arXiv:[quant-ph/1005.0654](https://arxiv.org/abs/quant-ph/1005.0654)V1
- [8] Pryde G J, O'Brien J L, White A G, Ralph T C and Wiseman H M 2005 *Phys. Rev. Lett.* **94** 220405
- [9] Ralph T C, Bartlett S D, O'Brien J L, Pryde G J and Wiseman H M 2006 *Phys. Rev. A* **73** 012113
- [10] Resch K J, Lundeen J S and Steinberg A M 2004 *Phys. Lett. A* **324** 125
- [11] Williams N S and Jordan A N 2008 *Phys. Rev. Lett.* **100** 026804
- [12] Lundeen J S and Steinberg A M 2009 *Phys. Rev. Lett.* **102** 020404
- [13] Yokota K, Yamamoto T, Koashi M and Imoto N 2009 *New J. Phys.* **11** 033011
- [14] Goggin M E, Almeida M P, Barbieri M, Lanyon B P, O'Brien J L, White A G and Pryde G J 2009 arXiv:[quant-ph/0907.1679](https://arxiv.org/abs/quant-ph/0907.1679)V1
- [15] Tamate S, Kobayashi H, Nakanishi T, Sugiyama K and Kitano M 2009 *New J. Phys.* **11** 093025
- [16] Hofmann H F 2010 *Phys. Rev. A* **81** 012103
- [17] Hosoya A and Shikano Y 2010 *J. Phys. A: Math. Theor.* **43** 385307
- [18] Englert E-G 1996 *Phys. Rev. Lett.* **77** 2154–7